

School of Applied Science

A Study of Cyclogenesis in the North of Western Australia

Gregory Stuart Hamilton

This thesis is presented as part of the requirements for
the award of the Degree of Master of Science
of the
Curtin University of Technology

August 2002

ABSTRACT

The region of interest in this study is the ocean area to the north of the Western Australian coast; that is, the Timor Sea. It is the tropical cyclones (TC) that generate in this area that most often affect the people and industries located in this region of Western Australia. Accordingly, it is the case that there is a continuing need to improve our understanding of these systems using both observations and numerical models.

After an introduction to the problems caused by TCs in the north of Western Australia, a description is made of the study area. A review of the various meteorological systems that can be identified in the tropics is provided. This is followed by a history of research on cyclogenesis. A detailed discussion is undertaken on the current state of knowledge of tropical cyclogenesis. This theoretical understanding subsequently is applied to three case studies. Following a description of the data used and the analysis techniques, the three case studies are presented. In each case study, a system, which later becomes a tropical cyclone, is analysed during the genesis period.

The three case studies examined in this thesis are, case 1 (TC Tim, 1994), case 2 (TC Elaine, 1999) and case 3 (TC Isobel, 1996). In each case, the system was studied for at least 10 days prior to it being named. This approach was adopted to ensure that any potential development was not overlooked. A system is named when it reaches sufficient intensity for gale force winds to exist in all quadrants around the centre of that system. For each case, the environment in the vicinity of the location where the system was initially identified was studied until an evolving system was identified. Monitoring of the system continued until it was named.

Observations from the Geostationary Meteorological Satellite and the Defense Meteorological Satellite Program comprised the physical data set. In parallel with this data collection activity, meteorological products from a numerical model were catalogued over the same time interval. The thesis presents comparisons of the satellite products and the model output over the study period. In part, motivated by the outcomes of this comparison, it was determined to investigate further prospects for using the array

of satellite-derived products that might be more appropriate for use as a forecasting support tool.

Finally, as an example, a prototype index is proposed which has potential to demonstrate the degree of development of a system. In this work, for want of a name, this index is termed the Hamilton Index (HI). It uses meteorological products derived from the microwave DMSP series of satellites and provides a temporal sequence of values of the index that are applied to monitor the developing of the TC systems in the three case studies. The meteorological variables used in the index were selected because they were accepted indicators of tropical cyclogenesis identified in the research literature. When applied to the three case studies, the HI showed a significant improvement in sensitivity to the state of development of the systems, especially when compared to the computer model data examined for the case studies.

The index is shown below,

$$HI = ((a * wv) * ((b * lw) + (c * ra) + (d * sst)) * (e * ws))$$

where wv is water vapour, lw is liquid water content, ra is rainfall, ws is surface wind speed, and a, b, c, d, and e are dimensional weighting factors.

ACKNOWLEDGMENTS

Many people have given advise and comments during the course of this study. To each one of them I give my thanks. My fellow staff members at the Perth Regional Office of the Bureau of Meteorology have been untiring in their support of this project. From our Head Office in Melbourne, Dr Beth Ebert supplied some of the early SSM/I data used in the project and Dr Noel Davidson supplied the computer model data. Graham Warren supplied some of the SST data, the rest coming from the Bureau of Meteorology Regional Office in Darwin.

Many of the references used in this document were supplied by Andrew Hollis and his group in the Research Library of the Bureau of Meteorology in Melbourne. To him and his team I am truly grateful for their untiring efforts to track articles down for me.

Some of the data used in this study was downloaded via the internet from a site in the U.S.A., Remote Sensing Systems, <http://ssmi.com>. They have quite rightly asked that their source be recognised with the following statement;

Data and images are produced by Remote Sensing Systems and sponsored, in part, by NASA's Earth Science Information Partnerships (ESIP): a federation of information sites for Earth science; and by the NOAA/NASA Pathfinder Program for early EOS products; principal investigator: Frank Wentz.

My associate supervisor, Dr Mark Williams provided many useful and helpful comments as the project progressed.

In particular I would like to thank my program supervisor, Dr Mervyn Lynch who kept me on track through many potential (and real) diversions.

TABLE OF CONTENTS

ABSTRACT	i
ACKNOWLEDGMENTS	iii
TABLE OF CONTENTS	iv
LIST OF FIGURES	viii
LIST OF TABLES	xi
1.0 INTRODUCTION	1
1.1 The Problem	1
1.2 Interest in the Problem	1
1.3 Other Aspects	2
2.0 STUDY AREA	3
2.1 Geography	3
2.2 Oceanography	4
2.3 Regional Climatology	7
2.3.1 Rainfall	7
2.3.2 Humidity	8
2.3.3 Air Temperatures	9
2.3.4 Evaporation	9
2.3.5 Cyclogenesis	9
2.4 Conclusions	11
3.0 ATMOSPHERIC STATES IN THE TROPICS	12
3.1 The “fair weather” state.	12
3.2 Tropical Circulations	13
3.3 Conclusions	17

4.0	HISTORY OF RESEARCH IN TROPICAL CYCLOGENESIS	18
4.1	General	18
4.2	Australian Region	18
4.3	In the north of Western Australia	19
4.4	Conclusions	21
5.0	DESCRIPTION OF TROPICAL CYCLOGENESIS	22
5.1	Definitions of cyclogenesis	22
	5.1.1 General	22
	5.1.2 Genesis and Intensification	23
	5.1.3 Development and non-development	26
5.2	Synoptic	27
	5.2.1 General	27
	5.2.2 Pre-existing Disturbance	27
	5.2.3 Lower tropospheric warm core	31
	5.2.4 Large Scale spin up	31
	5.2.5 Small vertical wind shear	32
	5.2.6 Curved cloud features	33
	5.2.7 Mid -level mesoscale vortex	34
5.3	Seasonal Factors	34
5.4	Dynamics	37
5.5	MCC's	38
5.6	Conclusions	39
6.0	CURRENT RESEARCH INTO TROPICAL CYCLOGENESIS	41
6.1	Observations	41
	6.1.1 In situ observations	41
	6.1.2 Radar observations	42
	6.1.3 Satellite observations	42
6.2	Computer Modeling	43
6.3	Status and Problems	44

6.4	Conclusions	45
7.0	CASE STUDIES, OBSERVATIONS AND ANALYSIS	46
7.1	Satellite Observations	46
7.1.1	DMSP Observations	46
7.1.2	GMS observations	48
7.1.3	NOAA Series of Satellites	49
7.2	Numerical models	49
7.2.1	Global Models	49
7.2.2	Regional Models	50
7.3	In-situ Observations	50
7.4	Classification of case studies	51
7.5	Conclusions	51
8.0	REVIEW OF CASE STUDIES	52
8.1	Case 1. - TC “Tim”	58
8.1.1	Antecedent Conditions	59
8.1.1.1	GMS Satellite imagery	59
8.1.1.2	Sea Surface temperatures	60
8.1.1.3	DMSP Satellite imagery	60
8.1.1.4	Model data	63
8.1.1.5	Gray’s Parameters	66
8.1.2	Discussion	69
8.2	Case 2. - TC “Elaine”	81
8.2.1	Antecedent Conditions	82
8.2.1.1	GMS Satellite imagery	82
8.2.1.2	Sea Surface temperatures	83
8.2.1.3	DMSP Satellite imagery	83
8.2.1.4	Model data	85
8.2.1.5	Gray’s Parameters	88
8.2.2	Discussion	90
8.3	Case 3. - TC “Isobel”	103

8.3.1	Antecedent Conditions	104
8.3.1.1	GMS Satellite imagery.	104
8.3.1.2	Sea Surface temperatures	105
8.3.1.3	DMSP Satellite imagery	105
8.3.1.4	Model data	107
8.3.1.5	Gray's Parameters	112
8.3.2	Discussion	114
8.4	Discussion of the case studies	125
8.4.1	Comparison of the three case studies	125
8.5	A Proposed Index for using satellite imagery to monitor cyclone development.	130
8.5.1	Background	130
8.5.2	The Index	131
8.5.2.1	Implementation of the index	131
8.5.2.2	Rules for use with the formula	135
8.5.3	Potential usage	136
8.5.4	Example using the case studies	137
8.5.5	Comparison between Hamilton Index (HI) and GASP model data	138
8.5.6	A review of amplitude and the temporal development of the index	140
8.5.7	Future development of the Hamilton Index (HI)	141
9.0	CONCLUSIONS AND RECOMMENDATIONS	142
9.1	Conclusions	142
9.2	Recommendations	149
10.0	REFERENCES	150
11.0	APPENDICES	164
11.1	Meteorological terms used in this document	164
11.2	Comparison of terms used in different cyclone basins	167

11.3 Contents of the Computer Data disk attached to this thesis. 168

LIST OF FIGURES

Figure 2.1: Map showing the Timor Sea and the study area	3
Figure 2.2: Map showing the point at which a cyclone was named. Taken from a Database held by the Bureau of Meteorology (Perth Regional Office). There is no particular significance in the different indicators used apart from the fact that this is scanned in from a colour map where the colour indicated year of genesis.	11
Figure 3.1: Diagram showing the northern and southern limits of the Asian Monsoon. Taken from Ramage (1971).	14
Figure 5.1 Model of tropical cyclone development used in intensity analysis (curved band pattern type). Taken from Dvorak (1984).	24
Figure 8.1: Map showing the point at which each of the tropical cyclones used in this study were named and the subsequent track.	53
Figure 8.2a: Example DMSP image of the study area. In this case showing water vapour (mm) over the Timor Sea on the morning of 20 March 1994 with a scale giving the grey scale shading.	56
Figure 8.2b: Example DMSP image of the study area. In this case showing liquid water content (mm) over the Timor Sea on the morning of 20 March 1994 with a scale giving the grey scale shading.	56
Figure 8.2c: Example DMSP image of the study area. In this case showing rainfall (mm/hr) over the Timor Sea on the morning of 20 March 1994 with a scale giving the grey scale shading.	56
Figure 8.2d: Example DMSP image of the study area. In this case showing surface wind speed (m/s) over the Timor Sea on the morning of 20 March 1994 with a scale giving the grey scale shading.	56
Figure 8.3a: GMS IR image of the Timor Sea showing the latitude and longitude markings. In this case the image was at 00Z on March 20, 1994.	57
Figure 8.3b: Navigation for the DMSP images of the Timor Sea showing the latitude and longitude markings. For this study the corner pixels were defined as 5.625°S, 95.125°E and 21.5°S, 130.125°E.	57

Figure 8.4: Map showing the location of the area where the system that became TC Tim was first identified (marked F) and where it was eventually named (marked N).	58
Figure 8.5a-c: Sea Surface Temperature for the week ending 13 Mar 1994. Taken from a product issued by the Darwin RSMC (Australian Bureau of Meteorology).	71
Figure 8.6a-v: GMS4 image of the Timor Sea starting 00Z 20 Mar 1994.	72
Figure 8.7a-j: Water vapour image of the Timor Sea starting am 20 Mar 1994. . .	75
Figure 8.8a-j: Liquid water content over the Timor Sea starting am 20 Mar 1994. .	76
Figure 8.9a-k: Rainfall over the Timor Sea starting am 20 Mar 1994.	77
Figure 8.10a-k: Surface wind speed over the Timor Sea starting am 20 Mar 1994. .	79
Figure 8.11: Map showing the location of the area where the system that became TC Elaine was first identified (marked F) and where it was eventually named (marked N).	81
Figure 8.12a-c: Sea Surface Temperature starting 28 Feb 1999.	91
Figure 8.13a-v: GMS image of the Timor Sea starting 00Z 06 Mar 1999.	92
Figure 8.14a-l: Water vapour image of the Timor Sea starting 00Z 06 Mar 1999. .	95
Figure 8.15a-l: liquid water image of the Timor Sea starting am 06 Mar 1999. . . .	97
Figure 8.16a-l: Rainfall over the Timor Sea starting am 06 Mar 1999.	99
Figure 8.17a-l: Surface wind speed over the Timor Sea starting am 06 Mar 1999. .	101
Figure 8.18: Map showing the location of the area where the system that became TC Isobel was first identified (marked F) and where it was eventually named (marked N).	103
Figure 8.19a-c: Sea Surface Temperature starting 14 Jan 1996. Taken from a product issued by the Darwin RSMC (Australian Bureau of Meteorology).	117
Figure 8.20a-v: GMS4 image of the Timor Sea starting 00Z 19 Jan 1996.	118
Figure 8.21a-j: Water Vapour image of the Timor Sea starting am 20 Jan 1996. .	121
Figure 8.22a-j: Liquid Water content over the Timor Sea starting am 20 Jan 1996.	122
Figure 8.23a-j: Rainfall over the Timor Sea starting am 20 Jan 1996.	123
Figure 8.24a-j: Surface wind speed over the Timor Sea starting am 20 Jan 1996. .	124

Figure 8.25: Relationship between sea surface temperature and precipitable water. Note the linear relationship above 25°C	133
Figure 8.26: The Hamilton Index as applied to the daily data from each of the case studies used in this thesis	139
Figure 8.27: The Zehr Index as applied to the daily data from each of the case studies used in this thesis	139

LIST OF TABLES

Table 2.1.	Mean and standard deviation (°C) of Sea Surface temperature in January and July. Values extracted from a table in Hasternath and Lamb 1979.	5
Table 2.2:	Table showing number of cyclones developing within the study area for each decade available in the database.	10
Table 5.1	A comparison of tropical cyclone intensity, the mean maximum wind speed and the minimum sea level pressure (MSLP) in tropical cyclones.	25
Table 8.1:	A comparison of maximum values of surface wind speed, columnar water vapour, cloud liquid water, and precipitation rate (rainfall) taken from DMSP 11 orbits over the study area between the 20 th and 30 th 1994.	62
Table 8.2:	Table showing information taken from the daily computer model (GASP) runs and giving some of the key data which should show any changes in the environment. Unfortunately relative humidity data were not able to be retrieved for this event. The convention with winds is that Westerly and Southerly winds are positive.	65
Table 8.3:	Table showing 850hPa vorticity value at the computer grid point nearest to the development of the tropical system during March 1994. The value shown is in units of s ⁻¹	67
Table 8.4:	Table showing vertical shear between 850hPa and 200hPa at the grid point nearest to the development of the tropical system. The values shown are in knots. The data were extracted from the GASP model runs by the Bureau of Meteorology and are for the dates in March 1994 as indicated.	67
Table 8.5:	A comparison of maximum values of surface wind speed, columnar water vapour, cloud liquid water, and precipitation rate (rainfall) taken from DMSP 13 orbits over the study area between the 07 th and 17 th March 1999 for TC Elaine.	84

Table 8.6:	Information taken from the daily computer model (GASP) runs for TC Elaine and giving some of the key data which should show any changes in the environment.	87
Table 8.7	Table showing 850 hPa vorticity at the computer grid point nearest to the development of TC Elaine for a sequence of days in March 1999. The value shown are in units of s^{-1}	88
Table 8.8	Table showing vertical shear between 850hPa and 200hPa at the computer grid point nearest to the development of TC Elaine for a sequence of days in March 1999. The values shown are in knots . .	89
Table 8.9:	A comparison of maximum values of surface wind speed, columnar water vapour, cloud liquid water, and precipitation rate (rainfall) taken from DMSP 14 orbits over the study area between the 19 th and 29 th January 1996.	107
Table 8.10:	Table showing information taken from the daily computer model (GASP) runs for TC Isobel and giving some of the key data which should show any changes in the environment.	111
Table 8.11	Table showing vorticity at the computer grid point nearest to the development of TC Isobel. The value shown is in s^{-1}	112
Table 8.12	Table showing vertical shear between 850hPa and 200hPa at the computer grid point nearest to the development of TC Isobel. The values shown are in knots.	113
Table 8.13:	Table comparing surface winds between the three case studies. . .	126
Table 8.14:	Table comparing water vapour content between the three case studies.	126
Table 8.15:	Table comparing Liquid water content between the three case studies.	127
Table 8.16:	Table comparing rainfall between the three case studies.	127
Table 8.17:	Table comparing 850 hPa winds from the GASP model for the three case studies. The hyphens in day -10 represent missing data.	128
Table 8.18:	Table comparing 200 hPa winds from the GASP model for the three case studies. The hyphens on day -10 are missing data.	129

Table 8.19:	The look-up table to obtain the score values for inserting into the formula used to derive the Hamilton Index.	135
Table 8.20:	Example showing how to use table 8.19 to obtain a score for each parameter. These scores are then inserted into equation 8.1 to derive the Hamilton Index (HI).	136

Now it happened on the day that such a gale was blowing from the north that the troops declared that if they did not get away, all their ships would be wrecked.

Marco Polo (Latham 1958, English translation of Polo 1289)

1.0 INTRODUCTION

1.1 The Problem

The earliest description known to this author, of the devastating affects of a tropical cyclone given by a Caucasian was that of Marco Polo (quoted above) in describing Genghis Khan's disastrous attempt to invade Japan in 1268.

The effects of tropical storms on economic and social structures in tropical parts of the world is growing in severity as utilisation of natural resources and population increases in those areas. A clear understanding of the mechanisms that cause tropical storms to form will lead to longer lead times by warning services providers. This will enable better protection against the damage caused by cyclones.

Tropical cyclogenesis has been studied in many parts of the world, but not in much detail in the area off the Western Australian coast. The general principles of cyclogenesis are reasonably well understood for other cyclonic "basins". The mechanisms associated with the very early stages of cyclonic development are not all that well known. The dominant mechanisms associated with cyclogenesis off the Western Australian coast have not been studied at all.

1.2 Interest in the Problem

The question of how early in the life of a tropical depression, signals can be reliably identified which indicate the presence of a disturbance in the area to the north of Western Australia is of considerable importance. This study aims to investigate the very early development of several tropical systems to ascertain what evidence becomes

available at each stage and to see how reliably the evidence points to continued development or to an early demise of the system.

The use of remote sensed data to recognise the presence of tropical systems is essential in the study area due to the paucity of consistent data. The routine use of remotely sensed data should help provide a systematic approach to the recognition and fore-warning of such disturbances.

This study has several purposes. Personal development of this student in firstly enhancing this student's skills in interpreting remote sensed data, and secondly as an 'operational' officer to develop a more rigorous approach in research technique. The practical application of this research is to examine specifically the North of Western Australian region to study the very early processes involved in the initiation and development of tropical disturbances.

1.3 Other Aspects

One of the continuing problems in studies of tropical meteorology has been that of terminology. In this study the terminology as used in the Australian basins will be applied consistently. A brief definition of some of the terms used in this study is also included in the appendices. For interest, a comparison of terminology in the various cyclone basins also is included in the appendices.

2.0 STUDY AREA

In this chapter I will describe the attributes of the study area. In particular discussion will take place about the following

- Geography
- Oceanography, and
- Regional Climatology of the area

This will give an overview of the study area in general terms. Hence the reader will gain a background understanding of the region and the processes that take place there.

2.1 Geography

The study area is displayed in the map provided in Figure 2.1. This area falls within the western part of the area described in Gray (1979) as ‘North west Australia’.

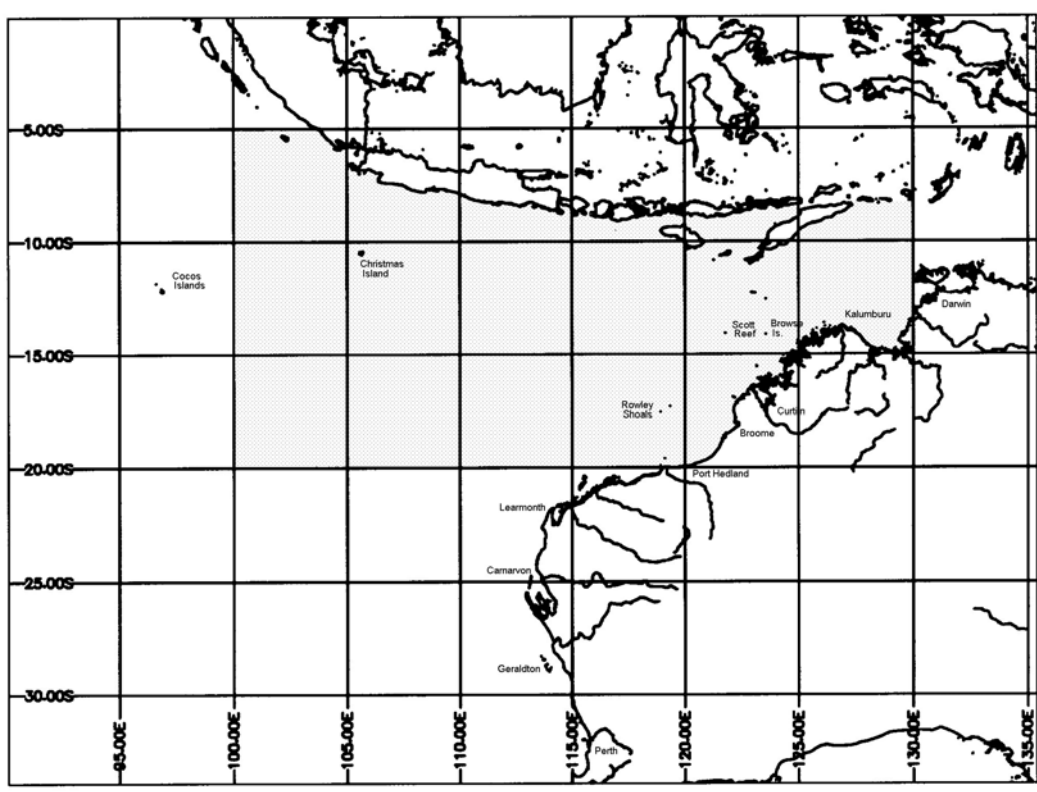


Figure 2.1: Map showing the Timor Sea and the study area

The area to the north of Western Australia is the focus of this study. Geographically, the area is bounded by the Indonesian archipelago to the north. This group of islands is

topographically zonally orientated and averages 1000m high with peaks to 3000m (Holland 1983). The eastern and part of the southern boundaries are flanked by the Australian continent, much of which is low lying and relatively featureless. The only islands of any significance within the study area are Christmas Island (10°S, 105°E) and near the western boundary, Cocos Island (12°S, 097°E). Near the Australian coast there are many small coral islands, some of which have Automatic Weather Stations located on them. To the north and the east of the Indonesian islands is the area known as the ‘Maritime Continent’ (Ramage 1968).

2.2 Oceanography

The study area consists of two primary areas in terms of ocean floor. Around the edges there are the continental shelves. Near Australia the shelf is quite large, extending several hundred kilometres off the coast. Near Indonesia however, the shelf is very narrow. The intervening area and the western part of the study area is open ocean with abyssal plains as deep as 2000m (Baines 1989).

Wind driven currents are weak within the study area (Baines 1989) but tidal activity is significant. Until recently, little work has been done on the oceanography of the area apart from at specific sites such as at offshore oil and gas platforms. The main current through the area is the South Equatorial Current. This is fed partly by the main South Indian Ocean gyre and from some flow through from the Indonesian Islands.

The eastern part of the area is significant in that it is the source of the Leeuwin Current; a narrow southward flowing current which is located over the continental slope. It is predominantly an autumn and winter event. Part of the source water for the current comes from flow through from the Indonesian archipelago. The Leeuwin Current shows a significant correlation with the El Niño/Southern Oscillation (ENSO) (Pearce 1988). In normal, that is, non-ENSO years, coastal water levels are high leading to a relatively strong Leeuwin Current. During ENSO years coastal water levels are lower leading to weaker flows in the Leeuwin Current.

The question of interbasin flow is addressed by Toole (1987). The Indonesian straits between the Pacific and Indian Oceans is unique in that it is the only tropical interconnection between oceans.

Sea surface temperatures (SST) show some variation between summer and winter temperatures. The coolest month being August when SST near the southern boundary are about 22°C increasing northwards to be about 26°C in the north and east and as much as 28°C near the Sunda Strait. SST in the warmest month, which is February, are about 26°C near the southern boundary increasing to 29°C near the Indonesian Island and in the north east. Most of the northern half of the study area is above 28°C. Hasternath and Lamb (1979) give charts showing SST which includes the study area. In Table 2.1, the mean SST for January and July are shown. The values given in the table are for 5°S and 15°S respectively. Hasternath and Lamb (1979) also give a table of the standard deviation of temperatures in the Indian Ocean which is reproduced in part below in Table 2.1

	80°E-90°E	90°E-100°E	100°E-110°E	110°E-120°E
January 0°S-10°S	28.0 0.5	28.0 0.5	28.5 0.5	28.5 0.6
January 10°S-20°S	27.0 0.8	27.0 0.8	27.5 0.9	28.5 1.0
July 0°S-10°S	28.0 0.9	28.0 0.6	28.0 0.6	28.5 0.8
July 10°S-20°S	24.5 1.2	25.0 1.2	25.0 1.0	25.5 0.8

Table 2.1. Mean and standard deviation (°C) of Sea Surface temperature in January and July. Values extracted from a table in Hasternath and Lamb 1979.

Nicholls (1984,1989) in a statistical study found that there was a significant correlation between the sea surface temperature anomalies and ENSO He found that the SST anomalies lead ENSO events by about one season.

The significance of these currents is in the transport of heat, salt and fresh water into and within the study area. Obviously the only two sources of heat can be from insolation and from transport. The availability of sufficient heat flux from the ocean to the atmosphere is considered to be one of the basic requirements for tropical cyclogenesis.

An interesting feature that has only relatively recently been described is the Indian Ocean Dipole (IOD) (Saji, et al, 1999. Feng et al, 2001. Rao, et al, 2002) The extremes of this feature are firstly when there is a warm anomaly to the north of Australia. It is this phase that produces enhanced rainfall over Australia. The other extreme is when there is a warm anomaly over western and southern Indian Ocean with a negative anomaly over the Timor Sea. It is this second extreme that produces reduced rainfall over Australia and particularly southeast Australia.

The depth of the thermocline is also affected between phases of the dipole. Meyers (1996) and Matsumoto and Meyers (1998) showed that the thermocline depth along the coast of Java is closely related to the phase of the IOD while the thermocline depth along the coast of Australia is forced by the ENSO wind field over the Pacific Ocean. The IOD is now sufficiently well understood for Saji et al (1999) to be able to develop an index of the event. They identified a time series they called the Dipole Mode Index (DMI) to represent SST anomalies over the Indian Ocean. The DMI is the difference between the anomaly in the western Indian Ocean (50°E - 70°E, 10°S - 10°N) and the anomaly in the southeastern Indian Ocean (90°E - 110°E, 10°S - Equator). This eastern part of the index overlaps the study area for this document.

Nicholls (1989) discussed the IOD and its relationship to rainfall over the Australian continent. He found there was even a correlation between the IOD and rainfall in eastern Australia. Drosowsky and Chambers (1998) used an index based on the IOD and ENSO to develop a predictor of rainfall over the Australian continent.

2.3 Regional Climatology

The tropical cyclone season in the Australian region is generally considered to start in October or November and continue until about May, although tropical cyclones in June are not unknown (Bur Met., 1978; Reville,1981).

By January, the monsoonal trough extends along the north of the Australian continent and northwestwards to the Indonesian Islands. Usually by March the monsoonal trough has contracted to the north of Australia. North of this trough, monsoonal westerlies are prevalent and to the south, the south east trade winds are the dominant feature.

For the remainder of the year the area is entirely within the southeasterly trade wind regime.

2.3.1 Rainfall

Rainfall is primarily associated with the north west monsoon, that is it occurs mainly between November and March. This is colloquially called the 'wet season' in northern parts of Australia. Early and late in the season rainfall comes mainly from thunderstorm activity. In the middle of the season with the monsoon trough over northern Australia, much rainfall is derived as rain (as distinct from showers) from depressions within or from convergence along the trough.

The Precipitation Frequency charts in Hasternath and Lamb (1979, Part I) show that the southern boundary is something of a desert with only 10% for all year round. A few winter fronts would extend into the area in the Austral winter. In the summer, isolated thunderstorm activity would be the main source of precipitation.

In the north east the frequency increases from 10% in the dry season (winter) to 20% in the wet season. This is consistent with dry continental air flowing over the area in the dry season. In the wet season, mainly isolated thunderstorm activity is present. On relatively rare occasions a TC would cause heavy rainfall although this would rarely be recorded as any ship near a cyclone would deliberately steer away from it. A complaint

by this author (in his capacity as a duty forecaster) to a ships captain that I thought it inconsiderate of ships to avoid TC's and hence rob us of vital observations was met with what could only be politely described as a loud raspberry!

The Indonesian Islands have a fairly steady 30% in the west but the east varies between 10% in the dry season and 30% in the wet season. The western part of the study area appears to have a reasonably steady 20% or there about. This would come from Trade wind showers in the dry season and monsoonal activity in the wet season. This is consistent with satellite observations which show persistent thunderstorm activity in the vicinity of the Sunda Strait, probably due to the warm flow through in the Strait. In the east the flow through seems not to affect the weather so much and precipitation is more seasonal.

A recent discovery has been that the study area is also a source area for rain for the Australian continent. Tapp and Barrel (1984) showed that a cloud feature known as the north-west cloud band originated in the study area but brought rain to parts of the Australian continent as far away as Victoria (in the south-east corner of the continent). Drosdowsky and Chambers (1998) used a statistical scheme based on the IOD and ENSO to produce an enhanced technique for prediction of rain throughout Australia.

2.3.2 Humidity

As would be expected of an oceanic area, humidity is reasonably constant. Hasternath and Lamb (1979, Part I) show charts of specific Humidity. In July the trend is latitudinal with increasing humidity to the north. Along the southern border humidity is about 11 g/kg while in the north it is 18 g/kg. In January humidity increases to 16 g/kg along the southern border. Off the North West Shelf and near the Indonesian Islands the humidity is as high as 19 g/kg.

2.3.3 Air Temperatures

Tables in Hasternath and Lamb (1979, Part I) show that in January air temperatures are generally within 1°C of the SST with SST generally slightly warmer.

In July, SST are generally ½°C to 1°C warmer than the air temperatures. A maximum of 1.5°C warmer was observed over the North West Shelf.

2.3.4 Evaporation

Somewhat surprisingly maximum evaporation occurs in July at about 20°S where 6mm H₂O day⁻¹ is calculated (Hasternath and Lamb, 1979, Part I). Near the southern boundary 5mm H₂O day⁻¹ occurs while near the Indonesian archipelago around 3mm H₂O day⁻¹ is reported. This would be consistent with the persistent South Easterly trade winds that blow over the area. Evaporation as high as 7mm H₂O day⁻¹ occurs along the North West Coast of Western Australia with the dry offshore winds that are prevalent at this time of year.

In January most of the area has between three and four mm H₂O day⁻¹ evaporation. Along the North West Coast evaporation is five mm H₂O day⁻¹.

2.3.5 Cyclogenesis

The area is described as ‘North West Australia’ by Gray (1979) and the ‘South East Indian Ocean/ Australian Basin’ by McBride (1995). In both cases the western boundary actually becomes fairly nebulous and loosely joins the South West Indian Ocean basin.

A restricted search of a cyclone data base held by the Bureau of Meteorology (Australia) was undertaken. The limiting parameters set to between 5°S and 20°S, and between 100°E and 125°E (the primary focus of the study). The search showed that there were 250 cyclones formed within the area. As an interesting side comment, cyclones formed on all the boundaries as well as within the study area. The earliest cyclone in the

data base was in 1910 and the last was in 2000. This represents an average of 2.8 cyclones per year in the study area. Map 2.2 shows the location of the position at which a developing cyclone was named within the study area..

Years	1911- 1920	1921- 1930	1931- 1940	1941- 1950	1951- 1960	1961- 1970	1971- 1980	1981- 1990	1991- 2000
Total	13	14	12	29	31	41	40	41	29

Table 2.2: Table showing number of cyclones developing within the study area for each decade available in the database.

It should be mentioned that some caution would be required in assessing the database. In pre-satellite days, verification of the existence of a cyclone was somewhat hit and miss, particularly in mid oceanic areas. Verification was often dependent on the misfortune of a ship passing near (or even worse for the ship) through the system. This is particularly evident in the sudden jump in cyclones after the 1930's. The Second World War with the consequent increase in shipping and aircraft traffic through the area would explain the jump in that period. After the war there was an increase in commercial traffic through the area which increased observations. Then in the 1960's one of the most useful tools for regular observations of oceanic areas was the polar orbiting satellite. Since then geostationary and polar orbiting satellites have been used as a primary tool for routine observation of the ocean.

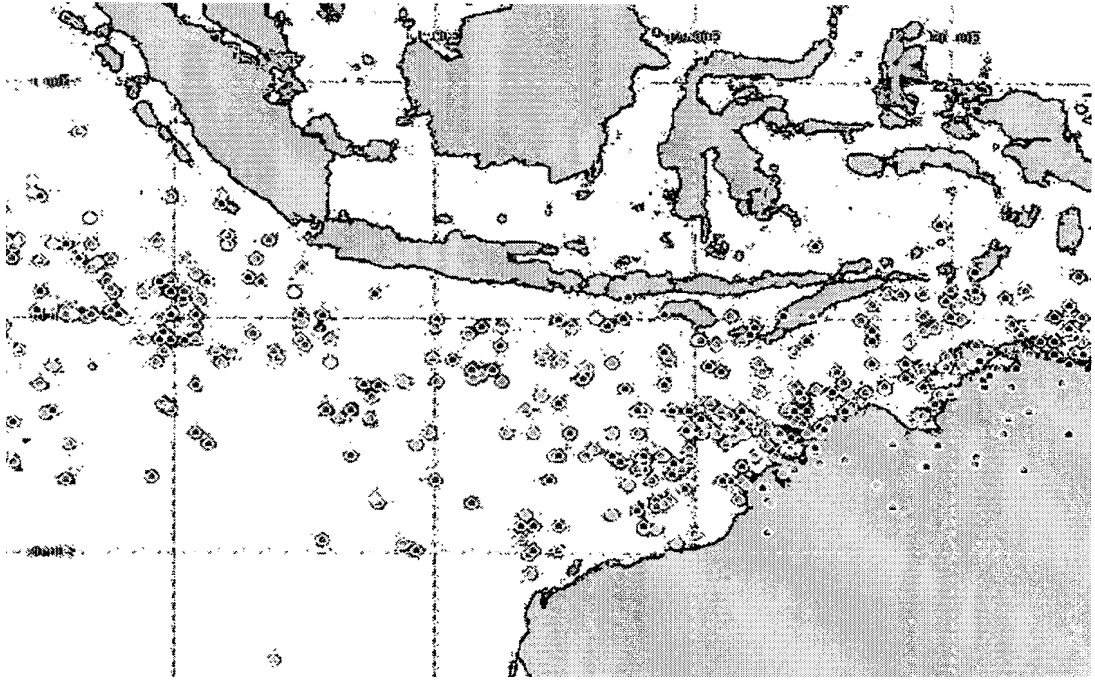


Figure 2.2: Map showing the point at which a cyclone was named. Taken from a database held by the Bureau of Meteorology (Perth Regional Office). There is no particular significance in the different indicators apart from the fact that it was scanned from a colour map where the colour indicated the year of genesis.

2.4 Conclusions

The study area was selected as the Timor Sea. It is primarily open ocean with islands to the north and the Australian continent in the south east. The area is subject to ocean movement from the Indonesian flowthrough. The area is known to be affected by the ENSO and recently an IOD has been identified. Climatological parameters have been described. Briefly, the area is a monsoonal regime with a north west monsoon in the wet season and a south easterly monsoon in the dry season. Rainfall, humidity and temperatures reflect this pattern. Significantly, this is an important genesis area for TCs that later affect the Western Australian coast.

3.0 ATMOSPHERIC STATES IN THE TROPICS

Circulations are well described in many of the well known texts on tropical meteorology. Below is a brief summary of some of the more significant circulations. Given that TC's form from pre-existing disturbances, these are some possibilities as to the genesis of a storm.

There are two basic states in which the atmosphere prevails in the tropics and these are described as follows

- The fair weather state, ie how the situation looks in fine weather, and
- Tropical circulations. Some of the features that cause interesting weather in the tropics.

Having previously looked at the climatology of the area we now look at the meteorology of systems that can be observed in the study area.

3.1 The “fair weather” state.

The atmosphere over the Timor Sea is for most of the year within the South-East Trade wind regime between the sub tropical ridge and the Equatorial trough. In the east of the study area these winds are actually off the continent of Australia and hence quite dry. In the western parts the much longer over sea trajectory means that there is some cloud.

The strength of the trade winds depends largely on the location and intensity of the centre of the high pressure system to the south. As a new high moves through to the south of the study area there is a surge in the South Easterlies usually lasting a few days before returning to more typical speeds.

There is rarely little rainfall in the trade winds although during a surge there is often shower activity.

3.2 Tropical Circulations

Tropical circulations vary in scale from several years to a few minutes. Not only do the different scales exist but they also interact to complicate the various signals.

By far the most important feature and in fact, dominant feature of weather in the tropics is the Equatorial trough. During the Australian dry season the Equatorial trough is located in the northern hemisphere. As the wet season approaches the Equatorial trough moves south to be over Indonesia by November and over Australia by December where it remains until about February. The weather associated with the trough is often deep moisture with associated cloud and heavy rainfall. The size of this system is such that when it is present, it extends laterally across the entire study area. This weather associated with the Equatorial trough is often known as the monsoon. In the case of Australia it is the North West monsoon that brings the wet weather. In the north of Australia the season is simply called “the wet”. The extent of the monsoon, and hence the Equatorial troughs movement is shown below in figure 3.1. Asnani (1993) gives a long and full explanation of the Australian monsoon including four possible triggers for initiation. These are:

1. Cold surges in the south China Sea,
2. Surge of low level southerlies along the west coast of Australia,
3. Formation of tropical depressions, and,
4. Seasonal build up of planetary scale temperature gradients augmented by the Australian continent land-sea contrast (Davidson et al 1983)

It is interesting to note that both triggers two and four are affected by the semi-permanent anti-cyclone in the Indian Ocean. When westerly waves strengthen the Indian Ocean anti-cyclone there is a surge in the southerlies along the west coast.

McBride and Keenan (1982) and Holland (1984a, b, c) demonstrated that the vast majority of TC's actually form in the monsoon trough.

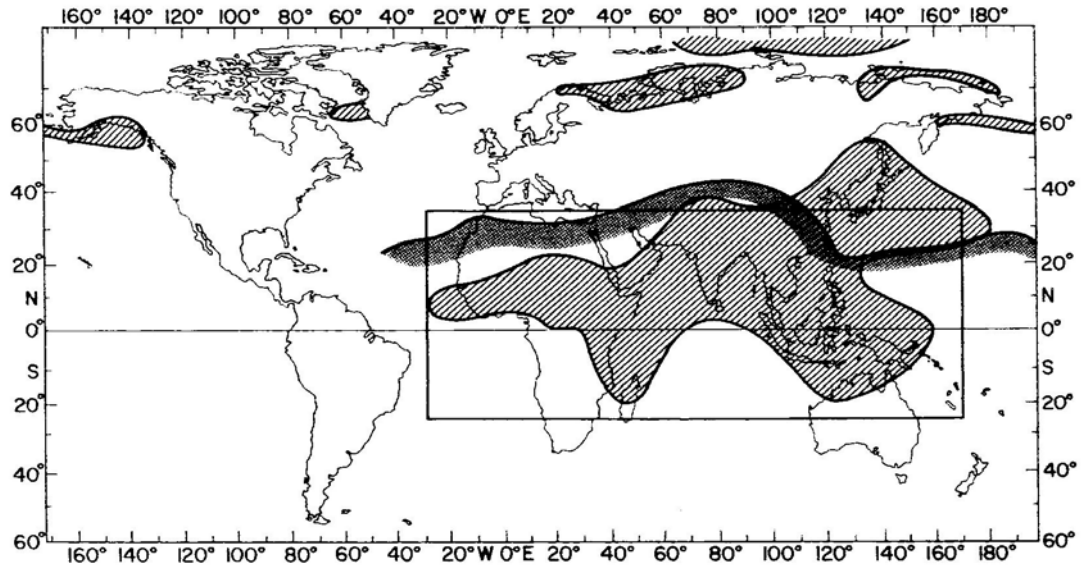


Figure 3.1: Diagram showing the northern and southern limits of the Asian Monsoon. Taken from Ramage (1971).

McBride (1986) proposed that there were in fact two modes of the active phase of the monsoon, which he described as active type 1 and active type 2.

In active type 1, convection was arranged in a 30 degree long super cluster (McBride 1983, Keenan and Brody 1988) . This 30 degrees translates to almost the whole of tropical Australia being covered by a more or less coherent mass of cloud when everything is in phase.

In active type 2, the monsoon trough was broken into and number of discrete elements such as TC's or monsoon depressions. Davidson and Hendon (1989) suggested that a possible mechanism for this type was eastwards energy dispersion.

An interesting feature of the tropics is an oscillation known as the 40 - 50 day oscillation, the Madden - Julian Oscillation (MJO), the 30 - 60 day oscillation and various other names. This is a large scale area of cloud and convection that travels slowly eastwards around the equator. It was first quantified by Madden and Julian (1971, 1972) in two land mark papers. Madden (1986) further found that the feature exhibited marked seasonality being strong over the Australian region during the Austral

summer months. He further found that the MJO was very weak in the Australian region in the Australian winter months. The interaction between the MJO and the Equatorial Trough is keenly watched in Cyclone Warning Centres, and particularly in the Perth Cyclone Warning Centre (personal communication with Len Van Burgel (Senior forecaster) and Andrew Burton (Manager, Severe Weather Services) of the Perth Cyclone Warning Centre).

The significance of the MJO is that it modulates the intensity of the Equatorial trough at intra-seasonal levels. The active phase and the quiet phase are closely related to the presence or not of the MJO in the area.

If the MJO is a major modulator of Equatorial trough activity at intra-seasonal periods, then a major feature of Equatorial activity at inter-seasonal time scales is the El Niño/Southern Oscillation (ENSO). There are two major signals for this feature, the SST in the Pacific Ocean and the atmospheric pressure in the same area.. During an El Niño event, the warmest parts of the Pacific Ocean migrate from the western edge to the central or eastern parts of the ocean. Several authors have looked at the consequences of this change and found that during an El Niño event, the frequency cyclone generation east of 170 degrees East increases (Revell and Goulter 1986a, b, Hastings 1990, Evans and Allen 1992). During an El Niño warm event atmospheric pressure over Australia is relatively high. This contributes to relatively stable conditions and reduced cyclogenesis.

Hendon and Liebmann (1990) found that there was a pronounced 30-50 day oscillation in the Australian summer monsoon, finding a signal in the westerly winds, rainfall and outgoing long wave radiation (OLR) over north Australia. After studying 30 years of data and identifying 91 events they were able to make the following conclusions;

1. The oscillation is deep (up to 300hPa) and baroclinic in nature.
2. The amplitude of the oscillation at Darwin is about 5 ms^{-1} in zonal wind, 1 ms^{-1} in meridional wind, 0.5°C in temperature, 10% in relative humidity, and 5mm rainfall per day.
3. There is no tilt in the vertical between 850hPa and 300hPa.

4. In phase with the rainfall perturbation is a deep warm anomaly with a cold surface pool (presumably from evaporation from the rain).
5. Maximum rainfall occurs about four days ahead of the peak intensity in 850 hPa westerly wind.

The ENSO is discussed further in Chapter 5.3 where a relationship between the SOI and cyclone activity in the Australian region is investigated.

The next most significant would be TC's. This is because of the intensity of the systems and the capacity for them to do damage to shipping and land based installations. The early development of these systems is the focus of this study and is discussed in more detail later.

Within the Equatorial trough large lows can develop which do not reach the intensity of a TC. They are still capable of doing significant damage. Should a low move over land, the heavy rainfall often associated with them will cause significant flooding. These are known as Monsoon lows. Monsoon lows have been studied by Ramage (1971), Davidson and Holland (1987), Manton and McBride (1992) and many others.

Smaller features such as Meso-scale convective systems (MCC's) are reasonably common systems. However some of these continue to develop into TC's and so are usually monitored carefully. These have been quite well studied by Ruprecht and Gray (1976 a, b), Johnson and Houze (1987), Williams and Houze (1987) along with many others.

An MCC is described as a persistent area of cumulonimbus convection often with an associated altostratus deck of cloud. The diameter of the area of convection may only be a few hundred kilometres although the associated rotational circulation may extend to 1000 - 1500 kilometres. McBride and Gray (1980) found that MCC's have an upper warm core. They also found that upwards motion was as much as 100 hPa per day.

While often associated with the monsoon trough, McBride and Keenan (1982) found that 16% in the Australian region were not. Zehr (1992) found that 35% were not associated with the equatorial trough in the western North Pacific.

3.3 Conclusions

The atmospheric state in the tropics shows long periods of stable or steady state flow interrupted by periods of increased or more active weather. The scale of this activity varies from years to minutes but the results can still be extreme.

4.0 HISTORY OF RESEARCH IN TROPICAL CYCLOGENESIS

Research into cyclogenesis has taken place over many years and based at many research schools and Meteorological organisations. In this chapter we look at the history of the study of TC's primarily in Australia

- Research in the Australian region
- Research based on the North West of Western Australia

Unfortunately much research that relating to the North West has been incidental to other studies. This means that inferences must be taken and applied to the area of interest.

4.1 General

World wide, research has taken place in many areas over a long period of time. The earliest document this author was able to actually sight (as distinct from being seen quoted in other texts) was Algué (1904) which was actually a revision of an earlier document (originally printed in 1899). Algué gives a broad description of the then understanding of TC's. The understanding of the structure was quite well understood although the theory of development was very primitive.

Since then progress in the study of TC's has been almost continuous with many schools taking an interest in the problem at different times.

4.2 Australian Region

Much Australian research into cyclogenesis has been by taking the Australian region as a whole (105E - 165E) without particularly separating the two basins. Comment on the western basin has tended to be incidental to the overall project.

In 1955 a conference was held in Brisbane at which such aspects of cyclones as structure, movement and forecasting TC's were discussed. Seas, surf, swell associated

with TC's as well as theories of formation, intensification and "filling" were also discussed (Bureau of Meteorology 1955).

In 1956 the "Tropical Cyclone Symposium", an international conference was held in Brisbane at which such 'immortal' names as Palmen, R.H. Simpson, H. Reihl and C.S. Ramage were in attendance. This conference looked at Analysis, climatology, forecasting, structure, formation and movement of TC's (Bureau of Meteorology 1956).

In 1973 the "Regional Cyclone Seminar" was held in Brisbane (Bureau of Meteorology 1973).

The "Symposium on the impact of tropical cyclones on oil and mineral development in north-west Australia" was held in Perth in 1976. (Bureau of Meteorology 1976).

1979 saw the "international conference on tropical cyclones" in Perth, Western Australia. Topics included modification, structure, observations, formation, energetics, climatology, movement, rainfall and modelling of TC's (Bureau of Meteorology 1979).

4.3 In the north of Western Australia

A conference in Perth in 1973 discussed the effects of TC's on the north west of Western Australia with particular emphasis on the effects on the oil and mineral industries. While many of the topics were engineering in nature, there was some discussion on the meteorology of the problem. Topics such as genesis, characteristics, detection and forecasting of TC's were included. There was also an assessment of the extreme effects of TC's.

Milton (1978) continued a previous thread of enquiry by looking at the link between the movement of anticyclones over Western Australia and cyclogenesis. He suggested that anticyclones influence cyclogenesis through the mechanism of low level cyclonic shear, in conjunction with the monsoon trough. Milton (1978) also suggested that the

advection of dry continental air into near coastal depressions could also influence development.

In the 1980's a consortium from Murdoch University, Curtin University and the University of Western Australia created a study group to look at the problem of TC's with particular emphasis on Western Australia.

Foster and Lyons (1984) looked at two depressions that originally formed over land and then moved off the coast. Subsequently one of the lows developed into a tropical cyclone. They did further work (Foster 1987, Foster and Lyons 1988) by taking a detailed look at two cyclone seasons, 1979/1980 and 1980/1981. They compared developing and non developing systems.

In a further work, Foster (1987, 1988) demonstrated that mean differences in pre-storm flow as found by McBride and Keenan (1982) and Davidson and Holland (1987) were not necessarily apparent for individual situations.

The use of multi channel satellite observations of TC's was explored by Prata et al (1986) where they looked at several sensors to establish the state of systems of the coast of Western Australia.

Nichols (1979, 1984, 1985, 1992, 1998) has for many years looked at the association between the SOI and TC formation in the Australian region. In his most recent paper he gives a formula for predicting cyclone activity in a coming season. This explained further in Chapter 5.3 of this thesis. While his studies included both sides of the Australian continent, there is some interesting material relating to this study area.

The most recent work was presented by Broadbridge and Hanstrum (1998) where they looked specifically at the relation between the Southern Oscillation Index (SOI) and the frequency of tropical cyclones in the Western Australian region. While not trying to quantify the relationship (as did Nichols 1992), they did find a significant statistical

relationship between the SOI and cyclone activity. They reported that there was an increase in the number of cyclones, number of coastal impacts and number of early season cyclones. When there was a negative SOI there tended to be fewer cyclones and they were typically later in the season. One interesting result of their research was that the more negative the SOI the further east along the coast the impacts tended to be. They also found that there was very little relationship between SOI and mid season cyclone activity.

Research in recent years has been mainly to do with mature systems, looking at changes in direction and also intensity changes. One recent study in the same area as this thesis was Van Burgel (1999) where he used the MSU sounder on the NOAA series of satellites to estimate the intensity of a TC by looking at the upper level warm temperature anomaly.

4.4 Conclusions

Research in to cyclones in general and cyclogenesis in particular has taken place over many years. Organised research into the Australian region has been undertaken in a structured manner since at least the 1950s. Cyclones in the north of Western Australia are often studied as part of a larger study on the problem. There have been sporadic attempts to investigate cyclone activity in the north of Western Australia and this thesis is one small contribution to the effort. While much of the emphasis on TC research has been on mature systems,, there has been some on genesis.

5.0 DESCRIPTION OF TROPICAL CYCLOGENESIS

In this chapter we discuss the processes understood to be involved in the development of TC's. We look at the

- General definitions used in this paper
- Describe the synoptic patterns associated with cyclogenesis
- Describe seasonal factors associated with cyclogenesis
- Describe the dynamics of cyclogenesis

By doing this we develop a theoretical framework on which to develop the case studies. The theory used in this chapter is part of the basis for testing hypotheses in the case studies.

5.1 Definitions of cyclogenesis

5.1.1 General

One of the first problems encountered in discussions on cyclones is that of terminology. History and geography have led to different terms being used in different cyclone basins for what is essentially the same event or process. The appendices (Chapter 11) give some of these definitions and comparison of terms used among basins. In this study the terminology as used by the Australian Bureau of Meteorology for the Australian basins will be used consistently.

On average, each year 83.7 tropical cyclones occur throughout the world and about two thirds of these reach severe tropical cyclone stage (Neumann, 1993). Twice as many tropical cyclones form in the northern hemisphere (ie two thirds of all cyclones) as the southern hemisphere and twice as many form in the eastern hemisphere as the western hemisphere.

5.1.2 Genesis and Intensification

It is useful to consider two separate stages in the development of tropical cyclones. Zehr (1992) makes the convenient split into the genesis stage and the intensification stage. The genesis stage includes development from the “fair weather state” atmosphere through the tropical disturbance stage to tropical depression stage. Once the system reaches tropical cyclone stage, genesis processes are thought to have finished. Any further development is considered to be intensification. An example of a system which has gone beyond genesis and into intensification would be any named tropical cyclone in the Australian region. Intensification is well studied elsewhere and will not be further considered in this document.

Gray (1988) considers that for cyclogenesis to occur an external process must act on an area or system. This compares with intensification stages when internal processes dominate.

Dvorak(1972, 1975, 1984) has developed a system for monitoring cloud systems in the tropics using satellite imagery. He has also developed a model for tropical cyclone development based on cloud patterns and changes in the patterns as shown in figure 5.1. He has quantified this into a T-number system (where T stands for tropical) in which the number increases during development and decreases as the system dissipates. Dvorak also described a number he calls the Current Intensity (CI) which for a developing system is the same value as the T-number (shown in table 5.1). The minimum pressure to mean maximum wind speed relationship was derived empirically. The minimum pressure for the NW Pacific were recommended by Shewchuck and Wier (1980, quoted in Dvorak 1984).

In his model for development, Dvorak stated that development takes place in a series of surges but in such a way that the T-number increases by about a value of 1 each day.

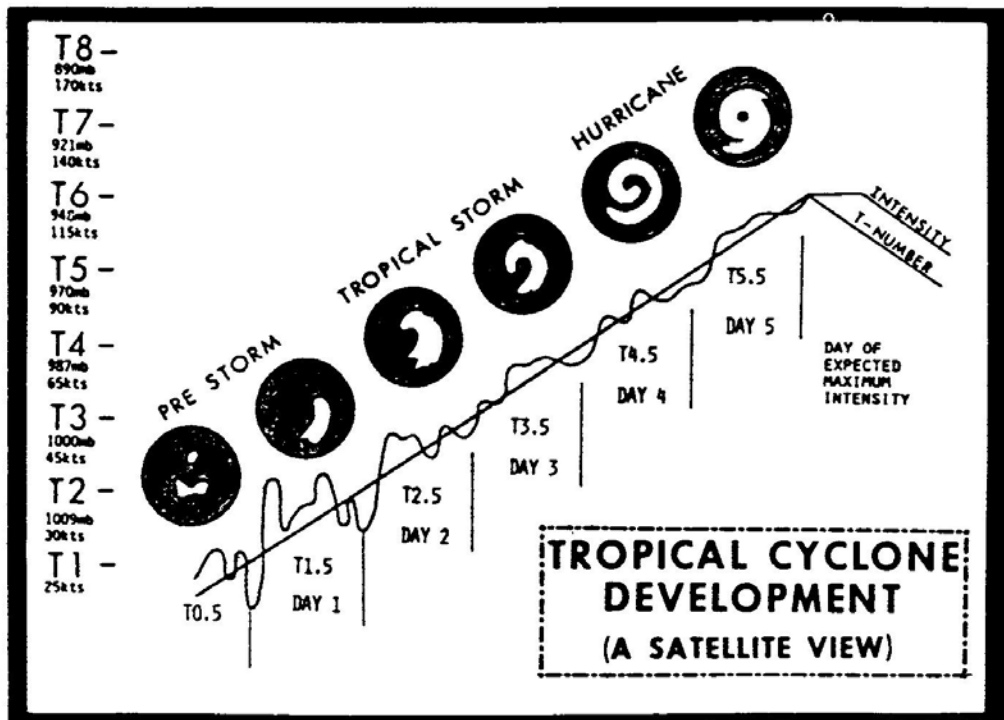


Figure 5.1 Model of tropical cyclone development used in intensity analysis (curved band pattern type). Taken from Dvorak (1984).

The T-number is defined as;

$$\text{T-number} = (\text{CF} + \text{BF} + \text{Vert Depth}) + \text{Rules}$$

Where

CF is the central feature

BF is the Banding feature number and

Vert Depth is the vertical depth of the system either estimated from VIS imagery or calculated from digital IR imagery

Rules are a series of rules developed in the appendix to Dvorak (1984)

By following the stepwise process in the appendix, one is able to obtain a T-number and hence a CI from which the intensity of the system can be established.

CI Number	Mean wind speed (knots)	MSLP (Atlantic)	MSLP (NW Pacific)
1	25		
1.5	25		
2	30	1009	1000
2.5	35	1005	997
3	45	1000	991
3.5	55	994	984
4	65	987	976
4.5	77	979	966
5	90	970	954
5.5	102	960	941
6	115	948	927
6.5	127	935	914
7	140	921	898
7.5	155	906	879
8	170	890	858

Table 5.1 A comparison of tropical cyclone intensity, the mean maximum wind speed and the minimum sea level pressure (MSLP) in tropical cyclones.

Dvorak's intensity scheme is in widespread use but it requires experienced analysts to use the scheme effectively as there remains a considerable amount of subjectivity in its application, particularly in the developmental stages of the system (Van Burgel, 1999).

Gentry et al (1980) proposed a technique using regression equations to determine current and forecast intensity of TC's

Dvorak's system has been further developed by Veldon, Olander and Zehr (1998) where they used equivalent blackbody temperatures from geostationary satellites to remove the subjectivity of the Dvorak intensity analysis scheme. Using events where aircraft reconnaissance was available, they were able to get better results with their Objective Dvorak Technique (ODT) than the average of three tropical analysis centres.

The Bureau of Meteorology in Australia currently uses the Dvorak method of estimating cyclone intensity. Within the Bureau of Meteorology Regional Office in Perth, the technique is applied to all systems being monitored.

5.1.3 Development and non-development

Systems are further subdivided into whether or not they continue from the genesis stage to the intensification stage. Developing systems (Tropical Cyclone Study Group 1982; Lunney 1988) are those which continue from the genesis stage to the intensification stage. Non-developing systems are those which start but do not continue developing to the 'named' system stage.

Of particular interest to residents in the tropics and to forecasters is the differentiation between developing and non-developing systems. Zehr (1976) made a considerable study of the difference between developing and non-developing systems. Mc Bride (1981) made a study of cyclogenesis in the Australian region using compositing techniques that included developing and non-developing systems. He then went on to compare these systems (McBride and Zehr, 1981).

Zehr (1992) stated that the two stages of genesis of a system that eventually became a TC were characterised by different primary activities. In stage one of development the most significant feature was an increase in relative vorticity in the lower layers of the atmosphere. He suggests that mean relative vorticity increases from less than $5 * 10^{-5} \text{ s}^{-1}$ to nearly $30 * 10^{-5} \text{ s}^{-1}$. During stage 2 the dominant feature was a decrease in pressure. He suggests here that pressure will drop from the environmental value (typically about

1010hPa) to about 997 hPa. By this stage the maximum wind speed has increased to 17.5ms^{-1} .

In the case of a non-developing system, Zehr (1992) suggests that the primary difference is that mean relative vorticity never gets above about $10 * 10^{-5} \text{ s}^{-1}$ and also minimum pressure does not drop below about 1005 hPa and maximum wind speeds do not get above 12.5 ms^{-1} .

5.2 Synoptic

5.2.1 General

Tropical cyclones are seasonal in nature with a distinct maxima in occurrence in the late summer to early autumn period.. Neumann (1993) updated a climatology on cyclones and classified them into seven basins. The basin of interest in this study being the one designated Australia/southeast Indian Ocean.

McBride (1995, Ch3 in Elsberry 1995) makes the distinction between core formation and large scale vortex formation. A small change in momentum in the large scale vortex can lead to a large change in momentum in the core due to the import of momentum. As has been said earlier, genesis is considered to finish when the system reaches average wind speeds of 17.5 m/s (34 knots).

Gray (1968) gives two primary environmental conditions for tropical cyclone formation and these are

- (a) sea surface temperature (SST) and,
- (b) location of the Inter Tropical Convergence Zone (ITCZ).

These are optimised for cyclone development in the Australian region in January to March.

In a further expansion on the pre-requisite conditions, Gray (1968, 1975, 1979), in his climatological studies showed that there were six environmental parameters that contributed to cyclone formation, these being;

- (a) large values of low level vorticity
- (b) located at least a few degrees from the Equator (significant planetary vorticity)
- (c) weak vertical shear in the horizontal winds
- (d) sea surface temperature at least 26C and a deep thermocline.
- (e) conditional Instability through a deep layer of the atmosphere
- (f) high humidity levels in the lower and middle atmosphere.

The first three points , (namely a, b, c) are functions of the horizontal dynamics of the atmosphere and could change quite rapidly depending on the current synoptic situation. The last three points, (namely d, e, f) are functions of the thermodynamic structure of the atmosphere and ocean and would tend to vary only slowly with time

Frank (1987) pointed out that Gray's factors were not mutually exclusive. He modified Grays list by combining (a) and (b), and by deleting (e). Frank added one item to the list, namely mean upward vertical motion.

Within the Australian basins, three sub-basins have been identified. These are the Coral Sea, Gulf of Carpentaria and the Timor Sea. It is this last area on which the present research is concentrated. McBride and Keenan (1982) found that about 50% of all tropical cyclones formation points (ie classified as a tropical cyclone and therefore named) occurred within 300 km of the of Australian coast. They also found that severe tropical cyclones were more likely in the Timor Sea than in the other sub-basins. McBride and Keenan (1982) and Holland (1984) showed that the vast majority of TCs formed within the monsoonal trough. This gives an interesting feature in giving a mid season relative minimum in TC frequency as the monsoon trough is located over the Australian continent. They also showed that early and late season TCs formed nearer to the equator than mid season systems.

Another interesting feature of their studies was the observation that approximately half of the TCs that form off the north west coast of Australia actually developed from pre-existing disturbances that developed over the continent and then moved off the coast. As this type of development has been investigated elsewhere (Foster 1984), it will not be discussed further in this research.

Observational studies have shown that there are seven large scale conditions that have found to be necessary for TC formation. These have been listed in McBride (1995) and elsewhere and are;

- (a) TC's form from pre-existing disturbances containing abundant deep convection;
- (b) the pre-existing disturbance must develop a warm core throughout the troposphere;
- (c) formation is preceded by an increase of lower tropospheric relative vorticity over a scale of 1000 to 2000 km;
- (d) large scale environment with little vertical shear of the horizontal wind;
- (e) an early indicator of TC formation is the appearance of curved banding features of the deep convection in the incipient disturbance;
- (f) The inner core may originate as a mid level meso-vortex that has formed in association with a pre-existing mesoscale area of Altostratus (ie a Mesoscale Convective system (MCS));
- (g) formation often occurs in conjunction with an interaction between the incipient disturbance and an upper-tropospheric trough.

5.2.2 Pre-existing Disturbance

Riehl (1954) stated *“We observe universally that tropical storms form only within pre-existing disturbances ... An initial disturbance therefore forms part of the starting mechanism. A weak circulation, low pressure, and a deep moist layer are present at the beginning. The forecaster need not look into areas which contain no circulations.”*

No studies to date have shown this statement to be false.

While most pre-existing disturbances are associated with the monsoonal trough, about 16% of pre-cyclone disturbances in the Australian region are not (McBride and Keenan 1982). This compares with 35% in the western North Pacific (Zehr 1992).

Persistence is a major factor in the determination of whether or not a TC is likely to form. Zehr (1992) found that in the northwest Pacific only 22 non-developing clusters lasted more than two days whereas in the same study period some 50 TCs formed. In this region there is about a 70% chance that a persisting cluster will form a TC. In the Australian region the time from first detection to naming is typically one to two days in the eastern sub-basin and two to four days in the western sub-basin within the occasional cluster taking up to ten days to mature (McBride and Keenan 1992).

Madden and Julian (1971, 1972) showed that there was an eastward progressing oscillation in the tropical troposphere manifesting in surface pressure, upper winds and cloudiness. This oscillation has become known as the Madden Julian Oscillation (MJO).

There is some evidence that cyclogenesis is associated with the MJO, often known as the 30-60 day oscillation. Gray (1979, 1985) first indicated that there was often a burst of cyclonic activity of 2 - 3 weeks followed by 2 - 3 weeks of relative inactivity. Lau et al (1991) and Manton and Mc Bride (1992) showed that there appeared to be super clusters of the order of 2000 - 3000 km across embedded within the 30-60 day oscillation which has a wavelength of the order of 5000-10000 km. Frank (1987) suggested that the pattern of cyclogenesis was consistent with these oscillations. Liebmann et al (1994) further showed that this relationship was consistent in both the southern and northern Indian Oceans. They further showed that there were twice as many TC's formed in the wet or low pressure phase as in the dry phase. This was due to the larger number of low pressure systems in the wet phase of the MJO. However once the low developed, there was the same probability of it becoming either a TC or a severe TC in the wet and dry phase.

5.2.3 Lower tropospheric warm core

Cloud clusters are typically warm cored in the upper troposphere and cold cored in the lower troposphere (below about 700 hPa), that is, within the area of maximum cyclonic vorticity. During development the area of maximum vorticity descends to near the top of the boundary layer indicating that the system is translating from a cold cored to a warm cored system. This stage of development is reasonably well documented (Davidson et al 1990). Presently, the reason for the downward development of the warm core is still not understood.

5.2.4 Large Scale spin up

Mc Bride and Zehr (1981) showed that the pre-existing disturbance was in an area of maximum low level vorticity indicating that the atmosphere was warmer than the surrounding area. The two AMEX TCs (Irma and Jason) showed an increase in low level vorticity from $20 \times 10^{-6} \text{ s}^{-1}$ to $40 \times 10^{-6} \text{ s}^{-1}$ about two days before formation. This spin-up may occur as a result of an increase in the flow on one or both sides of the monsoonal trough. One example is a surge from the winter hemisphere causing higher pressures along the equator hence increasing the flow into the monsoonal trough in the equator-side westerly flow (Love 1985 a, b). Similar examples have been shown by He and Yang (1981) where cold surges in the southern hemisphere have influenced the monsoon trough in the northern summer.

Spin-up can also occur as a result of an increase in the subtropical ridge in the summer hemisphere. It appears that the ridge needs to be more pole-ward of its normal position allowing stronger, deeper trade winds to develop.

A suggestion has been made that local development may occur within the monsoon trough where two areas of high potential vorticity (PV) interact and eventually merge to form a large area of enhanced PV. Guinn and Schubert (1993) proposed that an elongated PV may form separate vortices as a result of barotropic instability of the mean flow. In a similar fashion, Ritchie et al (1993) suggested that mesoscale vorticities

within mid-levels of cloud clusters may combine to form a large area of enhanced PV in certain circumstances.

The presence of a mature TC in the vicinity also has an effect on the tropical atmosphere. Frank (1982) showed that a TC affects the area within 1000-2000 km of the system centre. The result being an enhancement of cyclogenesis in the wake of the system and a suppression ahead of it.

5.2.5 Small vertical wind shear

On a seasonal basis, Gray (1984) and Shapiro (1987) have shown that there was an inverse relationship between seasonal mean vertical wind shear and the number of TCs in the Atlantic Ocean.

For individual depressions it is almost universally considered that low vertical shear is a necessary (Palmen 1956, Bureau of Meteorology 1978, Riehl 1979, Anthes 1982, Frank 1987.) The explanation being that in areas of low shear, moisture and heat can accumulate in the volume above a disturbance allowing continuing development. In contrast, in a high shear environment ventilation (removal) of the heat and moisture do not allow the low to continue developing.

There is some evidence showing that this conventional wisdom may not be entirely accurate. Zehr (1992) did a comparison of vertical shear (200 -850 hPa) for developing and non developing clusters. He found that there was very little difference in vertical shear between the two types of system. For developing systems he found that the mean shear was 10.1 ms^{-1} with a standard deviation of 5.3 ms^{-1} . In the case of non-developing systems he found that the mean shear was 10.2 ms^{-1} with a standard deviation of 5.1 ms^{-1} .

Earlier research by McBride and Zehr (1981) using radiosonde composite data found that there was typically low shear near the centre of the system but quite high shear on the equator-ward and pole-ward sides. In the case of TCs Amy and Blanche, they found

the westerly shear to be greater than 20 ms^{-1} on the pole-ward side of the pre-cursor depressions. On the equator-ward side there was similar easterly shear. This is in contrast with Dvorak (1975, 1984) where in his technique any shear is said to greatly inhibit development.

In light of above it would seem reasonable that strong *uni-directional* shear would inhibit development.

5.2.6 Curved cloud features

Pre-existing cloud clusters vary between 200 km and 1500 km in diameter although are typically about 500 km. They may consist of several Meso-scale Convective Systems (MCS's) which evolve on a time scale of 6 - 18 hours. (McBride 1995). According to Dvorak (1975, 1984) the convective elements start to form bands about 36 hours before it is named. He states that this indicates that the low centre has been in or near the deep layer convective cloud system for at least 12 hours. He further states *It is the close association of moderately curved cloud lines or bands and a sizable amount of deep-layer convection that signals cyclogenesis.*

Zehr (1992) found that in the early stages of development there was a significant convective and altostratus maxima at about 0600 local time. While he found that the peak in convection was associated with the maximum intensity increase during the intensification stage, there was another peak during the early formation phase. He found that in 80% of pre-cyclone developing lows there was a maximum in convection about three days before the systems was classified as a TC with a range of 15 hours to 8 days. This convective maxima occurs in stage one of the conceptual model developed by Zehr (1992). Steranka et al (1986) and Davidson et al (1990) both noted that this convective maximum occurs about the time the diurnal signal starts to weaken.

5.2.7 Mid -level mesoscale vortex

The concept of a Mesoscale Convective Complexes was first developed for extra-tropical cloud clusters. They were defined as long lived convective weather systems. Later similar features were observed in tropical regions and are usually called Mesoscale convective systems (MCS) (MCBride 1995). These are defined as being large areas of cloud with temperatures colder than -70°C . A pre-cyclone cloud cluster may consist of one or several MCS's. In certain circumstances an inertially stable warm cored vortex develops in the trailing stratiform region. It is referred to as a mesoscale convective vortex (MCV) (Chen and Frank 1993). As the system develops, the MCV becomes more obvious, particularly in visible satellite imagery. Valasco and Fritsch (1987) and Chen and Frank (1993) have suggested that if a MCC moves into an area suitable for cyclogenesis then the MCV may play a pivotal role in initiating cyclogenesis. Aircraft based studies by Emanuel (1993) and Lopez (1993) have shown that MCV's do in fact form in tropical MCC's. When these MCV's form they are typically about 100-200km in diameter and usually peak vorticity between 700 and 300 hPa and no appreciable vorticity near the surface. Ritchie (1993) showed that there may be several MCV's associated with areas of altostratus and strong convection within a pre-cyclone cloud cluster.

From these observations it seems reasonable that the MCV starts at mid levels and develops downwards to the surface while increasing in size as the pre-cyclone develops.

In Zehr's (1992,1993) conceptual model there are two stages in development. Initially there is a cloud cluster with some convection. The formation of a persistent MCV represents a transition stage to stage two where central pressure starts to fall and wind speeds increase to result in a TC.

5.3 Seasonal Factors

Neumann (1993) gives a table (1.1) in which he shows a 22 year sample (1968 -1989) of world wide cyclone activity by basin. In the case of the Timor Sea basin there were

152 TCs of which 75 were classified as severe. He gives an average of 6.9 per season with a standard deviation of 2.4. in the case of Severe TC's the average is 3.4 with a standard deviation of 2.1 this represents 8.2% of the global total of TC's for this period and 7.6% for severe TC's. This shows considerable variability in the Timor region with the standard deviation being about 35% of the mean. In the case of severe TCs the figure is 62%.

Nicholls (1979, 1984, 1985) has shown that there is a correlation between the Southern Oscillation Index (SOI) during the southern hemisphere winter (July to September) and the number of TC's in the Australian region in the following summer (October to April). He used the mean sea-level pressure for the preceding winter and the number of cyclone days in the following summer as the two series. In Nicholls (1985) he shows that the correlation coefficient for the two series over his 25 year sample was -0.68 (that is accounts for about 50% of the variance). In another study, Nicholls (1992) found a sudden decrease in the time series 1986 to 1991 which would have resulted in an over forecasting of the number of cyclones. While it may be real, it may also be caused by changes in satellite imagery interpretation. McBride (1995) suggests that the number of cyclones and the SOI might not be mutually exclusive. This is based on the point the Darwin is used as one of the points in the SOI calculation. A large number of cyclones in the area would reduce the mean pressure and hence affect the calculation of the SOI. When comparing the SOI for the summer period (January to March) with the number of TC's McBride (1995, table 3.1) found for the 22 year series that the correlation coefficient was +0.37 for the Australia/SE Indian Ocean region. When he removed the two strongest ENSO events he found that the coefficient dropped to +0.19. In his latest paper, Nicholls (1998) showed that while there is a correlation between the number of TCs and the SOI, there is very little correlation between the SOI and the intensity of TCs.

During an El Nino/Southern Oscillation (ENSO) warm event in the eastern Pacific Ocean, pressures tend to be high in the Australian region and there is a decrease in TC activity. The relationship between the ENSO and TC activity has been discussed in Evans and Allen (1992) where they found that the relationship was weak but significant.

They did find that there was a small increase in the number of cyclones in the eastern parts of the Australian basin (east of 170E longitude, ie well away from this study area). That is, there was a tendency for formation locations to be further east in ENSO periods.

Palmen (1948) was the first to suggest that for a TC to form the underlying sea surface temperature (SST) must exceed 26°C. Since statistically significant relationships have not been found between SST and cyclone numbers it seems reasonable that this is a threshold value rather than a proportional one. Nicholls (1984) found that there was a +0.8 correlation between SST at the start of the cyclone season and the season total number of TC's. The mid season SST - TC number correlation is close to zero and the end of season SST - Season total of TC's correlation is -0.4. To date there is no correlation between decrease in large scale SST and number of cyclones. Raper (1992) did a study of seven basins in which he correlated three month average SST with total cyclone numbers and obtained very similar results to Nicholls for the Australian region. He also found that the correlation was significant only for the start of the season.

In a later work, Nicholls et al (1998) discussed a trend that showed the cyclone activity had decreased over the last few decades. He suggested that there were several causes for this. The most important being a better understanding of the nature of TC's along with improved observational techniques leading to better discrimination between TC's and monsoonal lows. Even allowing for this there has been a downward trend in cyclone activity in the Australian basin. Somewhat surprisingly there was a reversal of trend in the number of severe TC's. In the Australian region there has been a slight increase in the number of severe TC's. This is in contrast with the Atlantic basin where there has been a downward trend in both the total number and the number of severe TC's.

Nicholls et al (1998) developed two relationships between the SOI and the number of TC's that could be expected in a season. He found that for cyclones of all categories (weak and intense), the relationship was

$$TC_{all} = 10.4 + 0.196 * SOI_{August}$$

In the case of intense TC's (defined as having central pressure ≤ 990 hPa) the relationship was

$$TC_{\leq 990} = 8.5 + 0.168 * SOI_{\text{August}}$$

He concluded by saying that the ENSO appears to play a major roll in dictating the broad scale environmental conditions that help or hinder TC genesis through out a season. However once a TC formed other local factors, not strongly related to ENSO influence whether or not the TC becomes intense or remains weak.

5.4 Dynamics

No cyclones are known to have developed within 2.5 degrees latitude of the Equator. About 87% of cyclones are known to have formed between 20 degrees north and 20 degrees south latitude. This makes sense when one considers that it requires a certain amount of vorticity to enable system of any significance to develop so that the further from the equator the easier it is to spin up a system. On the other hand it also requires enormous amounts of energy to spin up a TC and this is most readily available in low latitudes.

Holland (1983) has shown some interesting relationships between the general environment and an existing system. He found that upper tropospheric interactions can directly affect intensity change. He also found that lower tropospheric interactions will directly produce a size change, which by non linear interactions, may indirectly affect intensity change, or strengthening. Holland (1983) further suggested that CISK alone might be enough to increase intensity from tropical storm to minimal hurricane (tropical cyclone) stage.

In the same article, Holland (1983) gives a description of early genesis which goes along these lines. Angular momentum is transported by an initial surge in the monsoon and SE trades and generates a large inertally stable monsoonal depression or shear zone. If this zone is in a benevolent environment (eg Gray 1968), then loosely organised fields

of moist convection can develop. The convection aids intensification by core heating, hence pressure fall, and by inward contraction of the maximum winds region. There is also vertical recycling of heat and momentum and enhanced oceanic evaporation. A more intense depression is better able to organise convection. An Equatorward outflow channel seen to form during early development. Holland (1983) also suggests that for continuing development there needs to be a jet streak to south, or upper trough to west. These would add to the vorticity within the system.

There are possible adverse effects on a potentially developing system. Should the system move over land then the energy available would immediately decrease and development be arrested. Likewise, should an upper trough get to close or the shear within the system become excessive then there would be a decrease in the intensity of the system. The reader may remember that one of Gray's parameters was low shear (Gray 1968, 1975, 1979), McBride (1995). In a later study, Zehr (1999) pointed out that shear evidenced it self in the form of asymmetric cloud patterns over a system. He also showed that this asymmetry could be quantified by using geostationary satellite imagery to locate the centroid of the cloud area. Given that the surface centre was known, then the distance and bearing of the cloud centroid from the surface centre was a measure of the shear as well as a measure of the asymmetry of the system.

5.5 MCC's

MCCs have been described in chapter 3.2 of this document. In this section discussion is on the significance of MCC's with respect to TC development.

As has already been discussed, TC's form from a pre-existing system. The MCC is one of the pre-existing systems that can eventually develop into a TC. Should the development of the mid-level warm core in an MCC progress upwards and to the surface, then the conditions are suitable for cyclogenesis.

5.6 Conclusions

Cyclone development can be considered in two stages, an initial genesis phase, followed by an intensification phase. The genesis phase is the development from a fair weather state atmosphere until the system is named, and is the focus of this study. The primary method for monitoring development of TCs is by using satellite imagery. A technique for analysing satellite imagery developed by Dvorak is the method of choice in the Australian region.

Not all systems that form continue from the genesis phase to the intensification phase hence there are two broad groups of systems, developers, and non-developers. One of the problems for forecasters is deciding whether a system will continue to the intensification phase or not.

The environmental conditions that are conducive to TC development have been expanded on by Gray (1968, 1975, 1979). They are functions of the horizontal dynamics and of the thermodynamic structure of the atmosphere. He also includes a sufficiently warm ocean. Other studies have shown that an additional requirement of a pre-existing disturbance is needed.

Seasonal factors also influence TC development. The most obvious being the presence of the equatorial trough, which is an annual feature. The active phase of the MJO also enhances the likelihood of cyclogenesis. The ENSO is an even larger scale feature that has a demonstrated effect on cyclogenesis. During an ENSO event there is a reduced incidence of TCs.

The dynamics of cyclone development are reasonably well understood. The requirement for adequate vorticity and the presence of angular momentum in a suitable environment lead to moist convection. With vertical recycling of heat and enhanced evaporation from the ocean the system is able to continue developing.

Many processes will inhibit genesis. Should the system move over land, energy is lost and the system weakens. A change in the environment such as increased vertical shear will also cause a decrease in the organisation of the system

Cyclogenesis is a complicated and extensive process. Positive interactions at all scales act together for a cyclone to develop. Given the complexity of the process it is something of a wonder of nature that TCs form at all!

6.0 CURRENT RESEARCH INTO TROPICAL CYCLOGENESIS

While research is taking place continually, not all is relevant to this study. In this chapter we take an overview of current work taking place in Australia. In particular we look at;

- Observations
- Modeling, and
- current status of research in Australia

6.1 Observations

There is little research into the actual observation of developing systems in Australia at this time.

6.1.1 In situ observations

One interesting and potentially useful tool that is being developed by the Australian Bureau of Meteorology and partners is an 'Aerosonde'. This is an autonomous aircraft (about the size of a large model plane) which can spend extended periods flying within a system while collecting and relaying data back to a central monitoring station. This shows some promise as it would be possible to examine the environment in the vicinity of any disturbance.

At Exmouth, on the tip of North West Cape there is a series of instruments on one of the towers of the VLF communications station. This suite of instruments is capable of monitoring the low level environment of a TC but requires that the system be nearby. Unfortunately in 1999 the tower took a direct hit by a cyclone and the equipment was damaged, requiring extensive repairs.

6.1.2 Radar observations

The Australian Bureau of Meteorology has an extensive array of radars located around the north Australian coast line in such a way as to overlap in coverage. This ensures that for near coastal systems radar monitoring is almost assured. In recent years there has been an interesting development where the radars are swept at different angles and so a three dimensional picture of the system can be constructed. Using a suitably powerful work station, the sweeps can be reconstructed to show the internal structure of the TC. Since the radars are set to cycle every ten minutes, quite detailed sequences of the evolution of the system can be obtained.

In some fortunate circumstances, genesis may actually take place within range of a ground based radar station such as occurred with TC Oliver (Simpson et al 1997). TC Oliver developed near Willis Island (14.8°S, 150.0°E). A complete set of radar observations as well as radiosonde recordings and satellite imagery is available for this system.

6.1.3 Satellite observations

Satellites have grown in sophistication and capability over the years. This author can remember the days when the only images available were the twice daily NOAA passes. Since then the geostationary satellites have given much more regular and timely images along with additional bands so that the structure can be fully seen (if not understood).

The advent of the DMSP satellites in 1987 which use microwave frequency imaging meant that for the first time observers were able to “see through” the cloud and look at the internal structure of the systems. Considerable use of the data from these satellites was used in the case studies in this document.

Chou et al (1995) gives a nice summary of the characteristics of the SSM/I instruments flown on the DMSP satellites which is as follows. “The SSM/I senses the earth atmosphere at four frequencies of 49.35, 22.235, 37.0 and 85.5 GHz, with both

horizontal (H) and vertical (V) polarization except for the 22-GHz water vapour channel that observes only the vertical polarization. The SSM/I has been flown since July 1987 on a series of DMSP (Defense Meteorological Satellite Program) spacecraft in a near-circular, sun synchronous, and near polar orbit, with an orbit period of 102 min.” Because of the low orbit of the satellites there are some gaps between passes in the tropics. Every day, the 1394km swaths of the SSM/I provide data covering 87.6°S-87.6°N, except for 14 westward-propagating diamond-shaped gaps with a maximum width of about one swath in the tropics and subtropics of each hemisphere. It takes 2.5 days for a single satellite to obtain a complete coverage for the tropics and subtropics (Bates, 1991)

In even more recent times the advent of “active” satellites such as Radarsat and those similar have been a huge boost to the meteorological community. Now not only can we see through the cloud, we can now look at surface activity under the cloud. For instance, in certain circumstances, we can now measure surface wind and sea and swell under a cloud feature.

As long as it is not raining, considerable data can be obtained from satellite imagery. Unfortunately at this stage the most interesting parts of a system are often where the rain is occurring and so contaminated data is collected in that area.

6.2 Computer Modeling

Modelling has come along in enormous steps since Richardson sat in that trench in World War One making the first attempt at calculating the weather. The advent of ever more powerful computers over the years has enabled larger and more realistic models to be developed and run. In fact the desktop computer on which this thesis is being typed is quite possibly more powerful than the twin IBM 360 mainframes which took up a whole floor in the head office of the organisation this writer joined some 30 years ago.

The current generation of super computers enables modelling on a scale that could only be dreamed of even ten years ago.

In Australia, development of a tropical meteorological computer model began in the early 1980's. Davidson and McAvaney (1982) described a tropical analysis scheme which was eventually implemented in 1984. Further development occurred in 1992 with the implementation of a tropical prediction scheme (Puri et al 1992). This model was regularly upgraded both with the physics and the resolution (Puri et al 1998). Within these models further resolution can be obtained from nested models, the MESO-LAPS which has higher resolution, but a smaller area. For the tropics, TC-LAPS has been developed which is also a nested model of high resolution and which can be “moved” within the grid as the TC moves (Davidson and Weber, 2000).

6.3 Status and Problems

Holland (1983) pointed out that there was little study being undertaken on size change mechanisms. This is still the case.

The relationship between steering winds and system movement is still not well understood, particularly after the system has gone beyond the genesis phase. Future directional movement of systems remains a serious concern to forecasters.

Davidson and Puri (2001) list six factors which inhibit the effectiveness of numerical models in the tropics. These are; the sensitivity diabatic heating in 4-dimensional systems, convective heat sources are not well defined hence leading to poor initialisation, lack of dynamic framework for coupling mass and wind fields, current observational networks fail to adequately define important structures such as TC's and monsoon lows, inability to adequately define convective and stratiform cloud, and finally, significant weather often occurs at scales less than meso-scale and so are not well represented in models.

6.4 Conclusions

In situ observations of TCs continue to be difficult, in fact they can be quite dangerous for the observer when actually inside the system. In situ observations are rare and usually accidental.

Observational techniques took a major step forward with the advent of satellites. The ability to monitor systems in data sparse areas has greatly enhanced operational, and indeed research meteorology. The more recent addition of active satellites has further improved observations of systems. Radar is a useful tool when a system is close enough to a radar site.

Computer modelling is helping to understand the processes occurring within a system. With the advent of satellite derived data being used to initialise the model, better forecasts are being made for the systems.

7.0 CASE STUDIES, OBSERVATIONS AND ANALYSIS

Now this text changes direction slightly as it turns from theory to practice. In this chapter we look at the raw data that was collected with a view to making the case studies possible. In particular we look at;

- Satellite Observations
- Numerical models
- in situ observations, and
- Classification of the case studies

7.1 Satellite Observations

7.1.1 DMSP Observations

The DMSP series of satellites have been operational since 1987 although access to the data was restricted for many years. In recent times the data has become almost real time and can be accessed via the internet. One site that makes the data readily available is Remote Sensing Systems at <http://www.ssmi.com>. It was from this site that the DMSP data in the case studies was obtained. A description of the DMSP satellite and the SSM/I sensors is given in chapter 6.1.3.

Because of the low orbit of the satellites there are some gaps between passes in the tropics. Every day, the 1394km swaths of the SSM/I provide data covering 87.6°S-87.6°N, except for 14 westward-propagating diamond-shaped gaps with a maximum width of about one swath in the tropics and subtropics of each hemisphere. It takes 2.5 days for a single satellite to obtain a complete coverage for the tropics and subtropics (Bates, 1991) In fact this was a persistent problem in analysing data for TC “Tim” where for several passes the system was between or on the edge of the pass. The same happened for TC “Isobel” where on the day of the naming, the system was right in the middle of a gap.

The data as collected from the web site <http://www.ssmi.com> can be downloaded as a single 1.8M .gz file for each day. The file is then unzipped into a 10.1M file containing a 1440*720*10 array of data. Using a program written in C (shown in Appendix 11.3), this author was able to extract the relevant parts of the arrays. In the case of this study the corners of the data were (275,381) and (338,521). The corners were built into the program, although there is an inbuilt capacity to change the corners as necessary by simply running the program from a script or batch job. When the program runs, it extracts the data and then write ten separate files, each containing just the data for one parameter over the Timor Sea. It was this data that was analysed and used in Chapter 8 of this document.

Further processing of the separate files was undertaken by importing each file into an open source GIS called Geomatica Freeview. This program can be downloaded from <http://PCIGeomatics.com>. Originally data was extracted from a histogram taken from Freeview. Later the separate files were parsed through a program called Matlab to confirm the results from Freeview. Only minor changes were necessary. While the files were being displayed in Freeview, a screen capture was taken of the image and imported into a program called Paint Shop Pro and then saved as a .jpg file, making it available to any word processor for importing as a figure. These are the figures shown in the case studies.

A summary below is taken from a web site description of the data. A full description is available at http://www.ssmi.com/ssmi/ssmi_description.html

The data is 8 bit data and so in the range 0 to 255 count values where the count value is;

255 = landmass

254 = no SSM/I observations

253 = SSM/I observations exist, but are bad

252 = sea ice (locations where >0% ice)

251 = regions of rain on wind speed map or heavy rain on water vapor map

0 to 250 = valid geophysical data

In order to convert the 8 bit data into the relevant field it is necessary to multiply the raw value as follows:

Time of day:	multiply by 6.0 to get time ranging from 0 to 1500 minutes
Wind speed:	multiply by 0.15 to get 10 meter wind speed ranging from 0 to 37.5 m/s
Water vapour:	multiply by 0.3 to get water vapor ranging from 0 to 75 mm
Liquid water:	multiply by 0.01 to get liquid cloud water ranging from 0 to 2.5 mm
Rainfall:	multiply by 0.1 to get precipitation rate ranging from 0 to 25 mm/hr

The algorithm used and description of the data for wind speed is given in Wentz et al (1997). The water vapour imagery is described in Wentz et al (1997b). Rainfall algorithms and description is given in Wentz (1997a)

The data extracted are shown in Tables 8.1, 8.5 and 8.9. In each case the morning pass was used so that the data would be as near as possible to the same time as the computer model data.

7.1.2 GMS observations

A Japanese satellite is located in Geostationary orbit above longitude 135E. This satellite has provided hourly images for many years. In fact it is probably one of the most useful tools in operational meteorology for routine weather monitoring (personal experience as a forecaster). GMS4 was able to provide IR and VIS images on an hourly basis. The latest satellite, GMS5, is able to provide IR, VIS and water vapour imagery.

7.1.3 NOAA Series of Satellites

The NOAA series of satellites have been in use since the 1960's and prior to the geostationary satellites were the only source of imagery. Due to the nature of the orbit these satellites they become a bit of a mixed blessing. The lower orbit enables higher resolution of the imagery. The sun synchronous nature of the orbit means images from an individual satellite are 12 hours apart.

The more useful aspects of the polar orbiting satellites these days are with instruments such as TOVS which provide data very useful for initialising computer models.

7.2 Numerical models

7.2.1 Global Models

Global Models have been the basis on which much forecasting and development work has been based over the years. In the forecasting office that this author works there is routine access to the ECMWF model (colloquially known as the "EC"), the UK model, the US model and the GASP model. Unfortunately each model provider supplies different amounts of data. Currently the only supplier of a complete suite of data is the GASP which is an 'in house' product of the Bureau of Meteorology (Seaman et al 1995, Burke et al 1995).

It is the Gasp that is used for the evaluation of model data. The data was obtained from the archives of the Australian Bureau of meteorology. It was then passed through a variant of the program used to extract the SSM/I data, shown at appendix 11.4. The individual files resulting were then loaded into a Microsoft Excel spread sheet (one work book for each days worth of data). This was convenient as there were many functions and macros which could be used to do the calculations such as vorticity, shear and Zehr's parameter. It is the data from these workbooks that is used in the tables given in chapter 8 of this thesis.

7.2.2 Regional Models

When this study first started the regional model that the forecasting Centre had access to was a Bureau of Meteorology product known as the RASP. It was a product that was initialised from and nested in the GASP. More recently the RASP has been superseded by a product known as the LAPS. A version of the LAPS known as TLAPS was designed to better handle tropical meteorology. More recently still a product known as TCLAPS has become available on an operational basis (Wang 1999).

Unfortunately the models were considered to be not very good during the period. Given that they were nested in the GASP, it was decided to use the GASP analysis fields for data analysis.

The TCLAPS is much improved and currently is used in operational meteorology. It would have been very useful to have it available for the case studies.

7.3 In-situ Observations

Almost no observations are available for the area of interest in this study. The Indonesian archipelago is on the northern border and some synoptic observations are available. Within the study area only the Australian Islands, Christmas Island and Cocos Island are available. Christmas Island provides synoptic observations. Cocos Island provides both synoptic observations and upper atmospheric observations. On the south eastern border of the study area there are several sites along the Australian north west coast which provide synoptic and upper atmospheric observations.

Sadly very few reports are received from ships in the area. There is considerable shipping along the north west coast and to the north. Presumably there would be very heavy shipping traffic along the Indonesian Archipelago. Very few reports reach the forecasting office.

On rare occasion floating buoys are deployed through the area but unfortunately none were available within reasonable proximity of the case studies.

On one occasion this author lamented to a ships captain about the lack of consideration by ships in the vicinity of a TC. The thought was that it would be very useful for ships to continue through the TC to give a good data set, rather than change course away from the system as they currently do. The response was not repeatable in any company let alone a learned document like a thesis!

7.4 Classification of case studies

One of the major difficulties in forecasting is picking systems that form in data sparse areas. Actually deciding if and where system will develop is the initial problem. Secondly deciding where or not the system will continue to develop is also difficult.

This study is an attempt to look at efficient methods of monitoring tropical systems in a remote area and then to look at signals which might indicate further development. An attempt is made to see how early these signals might be seen.

Tropical cyclones that form in remote areas and then later impinge on the Australian continent are a significant problem. As was indicated in the introduction to this paper, the north west of Western Australia is an socially and economically important part of Australia. Disruption to activities in this area has considerable consequences for the State of Western Australia and also the Commonwealth of Australia.

7.5 Conclusions

A variety of data were used in the case studies in this thesis. The prime source of information was the American DMSP series of satellites. Also used is imagery from the Japanese GMS satellites. Data from several computer models were inspected before deciding to stay with the Australian GASP model.

The methodology used in the case studies has also been described.

8.0 REVIEW OF CASE STUDIES

In this chapter three case studies will be discussed, these being

- TC “Tim”
- TC “Elaine”, and
- TC “Isobel”

In each case we will look at firstly the observations available and secondly some model data from over the Timor Sea to ascertain the processes taking place in the environment of the systems. In each case we will look at

- GMS Satellite imagery
- Sea Surface temperatures
- DMSP imagery
- Model data available (taken from GASP)
- The environment using Gray’s parameters (Gray 1979)
- Discussion of the data analysed

Tropical cyclones are named in the Australian region only after exceeding an intensity of T2.5 using the Dvorak scheme (Dvorak 1982). These case studies look at the antecedent conditions and attempt to see how early signals can be recognised showing changes within the system. For the sake of clarity comparison with the “normal” state of the atmosphere is looked at. The Normal state is assumed to be ten (10) days before the system was named. Developments over the next ten days (until naming) are monitored with a view to recognising signals which may indicate further development.

Three cyclones were used in these case studies. The map below showing the positions at which they were named.

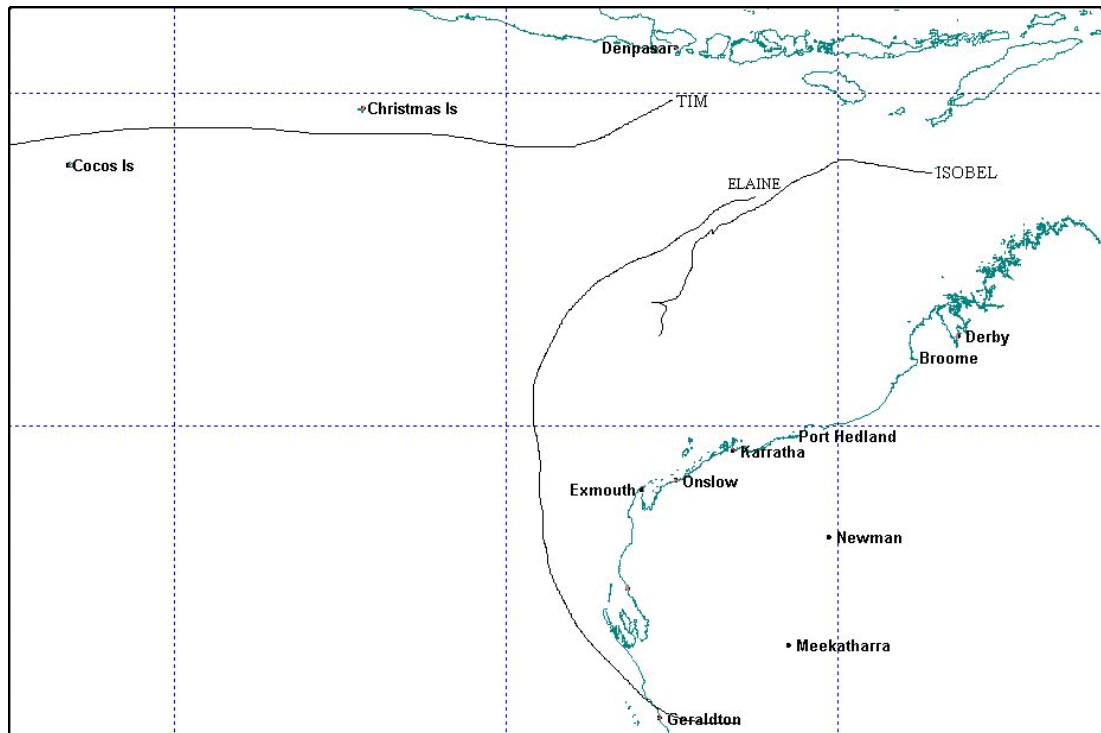


Figure 8.1: Map showing the point at which each of the tropical cyclones used in this study were named and the subsequent track.

Two of the TC's, Tim and Isobel subsequently dissipated over the ocean with no ill effects on the State of Western Australia. TC Elaine crossed the coast near Geraldton and caused extensive flooding in the northern agricultural parts of the South West Land Division (the area to the south east of Geraldton). The town of Moora was evacuated at one point due to flood waters encroaching into the town.

The diagrams presented in sections 8.1 (case study one: TC Tim), 8.2 (case study two: TC Elaine), and 8.3 (case study three: TC Isobel) are shown at the end of each section. The sequence in each case is that of SST, GMS satellite imagery, and finally the DMSP data.

In the case of the SST diagrams, which show the three weekly charts leading up to the naming of the cyclone, the charts are self evident. The lines represent SST isotherms at one degree intervals. There are heavier lines at five degree intervals so in the case of these diagrams the 25°C and 30°C lines are so marked. These diagrams were cropped from Weekly Sea surface temperatures from the Darwin Regional Meteorological Centre.

The GMS imagery is IR and is therefore a representation of the temperature at the top of what ever the satellite is looking at. Black represents warmer temperatures while white represents colder temperatures. By implication a whiter colour would be higher in the atmosphere. Further analysis is required to ascertain whether the cloud is just higher or indeed thicker, that is whether one is looking at a cirrus shield or at a thunderstorm. The images presented are extracted from global images. The section shown are from 5°S to 22°S and from 105°E to 130°E.

The DMSP imagery are in each case sampled over the same sub-set. Since the data was received in digital form it is possible to precisely define the corners, or in this case the centre point of the corner pixel. Each pixel represents a 0.25 degree by 0.25 degree sample of the Earth with the centre point defined by the data source centre. For this study the edge pixels were defined as 5.625°S to 21.5°S and 95.125°E to 130.125°E. A description of how the digital data was reconstructed into “visible” images was given in chapter 7. There are four pieces of useful information that is available in each pass, these being water vapour, liquid water content, rainfall and surface wind speed.. For the sake of consistency, the morning pass was used to match as closely as possible the computer model data. The diagrams presented are in the following order, water vapour, liquid water content, rainfall, and surface wind speed. As was explained in chapter 7, the raw data contains additional information. Data values of 0 to 250 represent valid geophysical data. Data values of 251 to 255 represent other information pertinent to the pass. Because of the number and detail of the diagrams given in the case studies, examples are given below in figures 8.2, 8.3, 8.4, and 8.5 with keys to explain the content of them.

For each type of image (that is, water vapour, liquid water content, rainfall and surface wind speed), the digital value was translated into a grey scale for presentation in this document. The scale was set so that a digital value of 0 (zero) was black scaling through grey to a value of 255 being white. The highest value with valid data is 250. This presents on the page (and indeed on the screen when the diagrams were being generated) as white. Unfortunately most printers used these days are not capable of displaying the entire range 0 to 250 so there is some degradation of the quality of the image as

presented on the printed page. There is however sufficient sensitivity to get a good appreciation of the variation in signal across an image.

The GASP model data was taken from the archives of the Bureau of Meteorology in Melbourne. After parsing the data through a cropping program (shown in appendix 11.4), the individual files were imported into Microsoft Excel spreadsheets for manipulation. The results of these processes are summarised in the tables 8.2, 8.6, and 8.10.

The model data is timed at 23Z on a given date, which is 7am local time the next morning local time. That is, 23Z on 18th January is 7am Western Standard Time (WST) on the 19th. The dates in tables have been set to WST dates for easier comparison with the satellite imagery. In other words, the model data (at date/23Z) is set at only an hour before the 00Z image dated the next day. This should make for easier comparison of the computer model data with the satellite imagery.

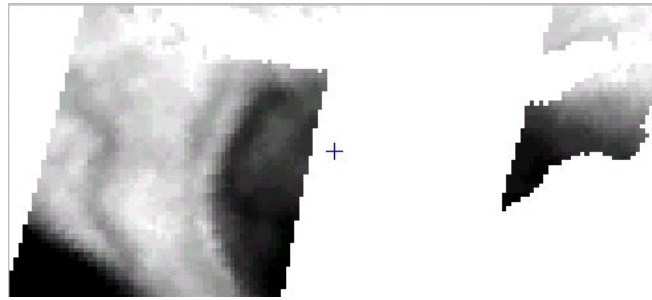


Figure 8.2a: Example DMSP image of the study area. In this case showing water vapour (mm) over the Timor Sea on the morning of 20 March 1994 with a scale giving the grey scale shading.

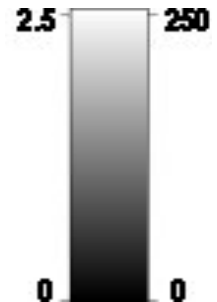
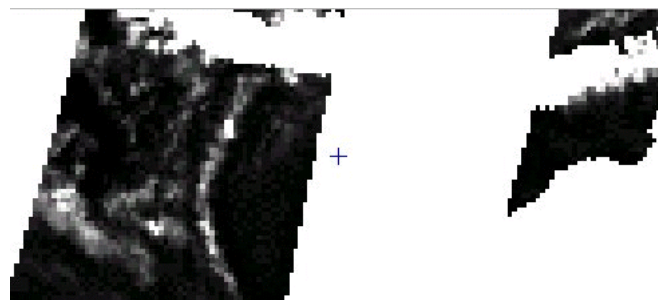


Figure 8.2b: Example DMSP image of the study area. In this case showing liquid water content (mm) over the Timor Sea on the morning of 20 March 1994 with a scale giving the grey scale shading.

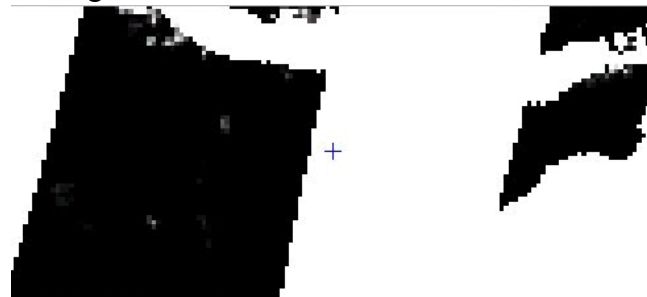


Figure 8.2c: Example DMSP image of the study area. In this case showing rainfall (mm/hr) over the Timor Sea on the morning of 20 March 1994 with a scale giving the grey scale shading.



Figure 8.2d: Example DMSP image of the study area. In this case showing surface wind speed (m/s) over the Timor Sea on the morning of 20 March 1994 with a scale giving the grey scale shading.

In order to assist with the navigation of the images used in the case studies, the following two diagrams (Figures 8.3a and 8.3b) show the latitude and longitude of the GMS images and DMSP images respectively used in case studies 1, 2, and 3.



Figure 8.3a: GMS IR image of the Timor Sea showing the latitude and longitude markings. In this case the image was at 00Z on March 20, 1994.

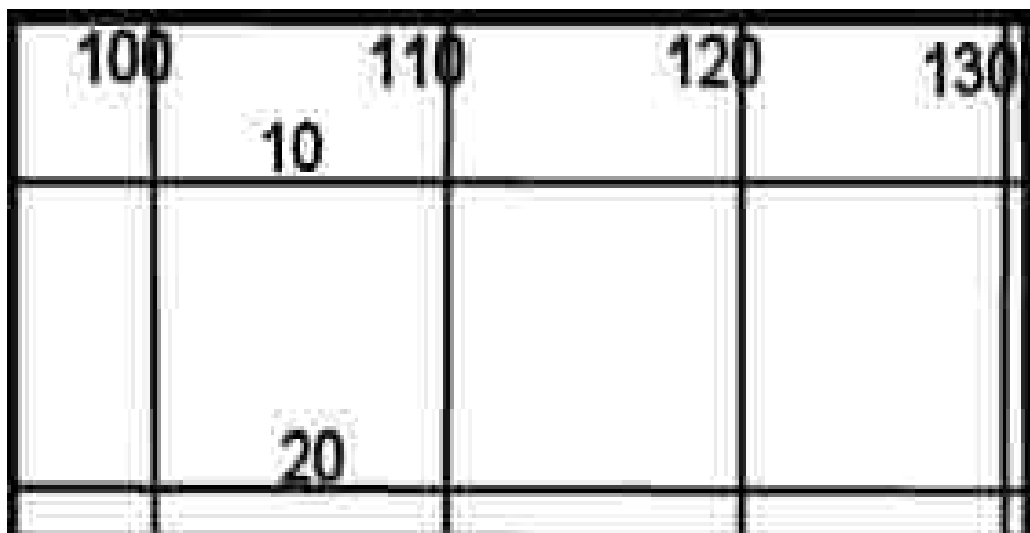


Figure 8.3b: Navigation for the DMSP images of the Timor Sea showing the latitude and longitude markings. For this study the corner pixels were defined as 5.625°S, 95.125°E and 21.5°S, 130.125°E.

8.1

Case 1. - TC “Tim”

Tropical cyclone “Tim” was named on 30 March 1994. Atmospheric conditions from the 20th March 1994 until naming are examined in the following discussion. Figure 8.4 shows the particular area of interest within the Timor Sea.

The system was first logged in the Perth Tropical Cyclone Warning Centre (TCWC) on the 28th March, 1994 at 10.0°S, 115.0°E and subsequently named on the 30th March, 1994 at 11.6°S, 112.0°E.

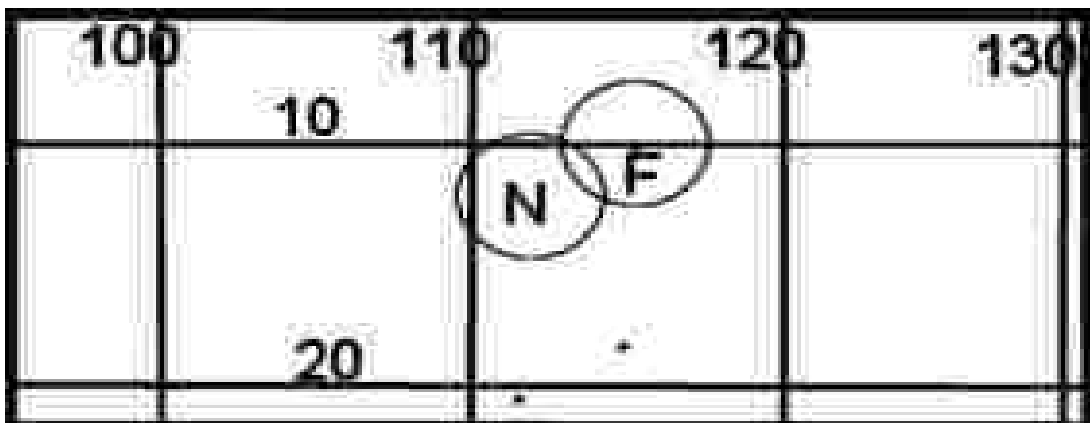


Figure 8.4: Map showing the location of the area where the system that became TC Tim was first identified (marked F) and where it was eventually named (marked N).

Description of the imagery used in this case study is given in section 8.0. A brief description of the GMS IR satellite imagery is that the whiter the colour in the image, the colder the temperature at the top of the cloud, that is, the higher the cloud is in the atmosphere. Figure 8.3a gives the navigation for the GMS imagery. In the case of the USA DMSP imagery, the blacker the colour in the image the lower the value of the parameter being displayed. Calibration for the DMSP images are shown in figures 8.2 to 8.5 where scales for water vapour, liquid water, rainfall, and surface wind speed respectively are given along with sample images. Figures 8.3b and 8.18 give the

navigation for each of the DMSP images. A full description of the DMSP imagery is given in section 7.1.1.

8.1.1 Antecedent Conditions

For the sake of this study, it was assumed that the atmosphere was in a “normal” or undisturbed state ten days before the system was named.

In this case the pre existing conditions are set as 20th March 1994.

8.1.1.1 GMS Satellite imagery

GMS IR Satellite imagery, obtained from the Bureau of Meteorology (Perth Office Archive), relevant to this event are shown in figures 8.6a to 8.6r. The images are for 00Z and for 12Z GMS for the study area.

On 20th March, 1994 the satellite imagery shows no cloud over the Timor Sea and only scattered thunderstorms over the Indonesian Archipelago. Interestingly, on the 21st, cloud activity is even more suppressed suggesting that a surge of SE trade winds from the mid latitude high had extended right through the Timor Sea, bringing drier air to the region. The 22nd and 23rd shows increasing cloud over the Indonesian Archipelago but no increase in cloud over the formation area. There is, however, an increase in cloud to the west associated with an active phase of the Madden-Julian Oscillation that was moving into the area. The 24th and 25th continue to show an increase in cloudiness over the Indonesian Archipelago with very little cloud over the study area.

March 26th shows the first visible indications that cloud is developing near the point that the depression was later seen to develop (10°S, 115°E). By March 27th a well developed cloud cluster is evident in the area. This development continues through March 28th as both the size and the development of the system increase. By March 29th the system is well developed and showing signs of increasing organisation. As has been

mentioned, TC “Tim” was named on the 30th indicating that all the parameters had been met as well as persisting long enough for the system to develop.

8.1.1.2 Sea Surface temperatures

One of the preceding conditions for tropical cyclone development is a sufficiently warm sea. Generally it is considered that SSTs greater than 26°C are necessary but not sufficient condition for cyclogenesis (Gray 1979). SSTs relevant to this case study are shown in figures 8.5a to 8.5c.

In the case of TC “Tim” the pre-existing SST was well in excess of this with temperatures in the vicinity of 28.5°C to 29.0°C in the area. There was a slight cooling just before the study period commenced for reasons that at this stage are unexplained. Given the cloud free conditions there was probably some oceanographic process occurring. From the 20th to the 27th the 29°C isotherm essentially remains in the same area indicating a stable oceanographic regime in the area. Hence a more than adequate SST is evident for formation of a tropical cyclone.

8.1.1.3 DMSP Satellite imagery

A brief description of the DMSP and SSM/I are given in chapter 7.1.1. In that same section was described the source of the data used in this study. In the introduction to this chapter, a description is given as to how to interpret the images presented at the end of each case study. Table 8.1 below shows a summary of data collected by the USA DMSP satellite passes. In this case the particular satellite was DMSP 11. Viewing the passes as imaged in the figures below (figures 8.7 to 8.10) shows only too clearly the problem with polar orbiting satellites. In several cases the passes were such that the data gap between satellite passes was right over the area of interest. In this case data was taken from the edge of the available passes.

From March 20th to the 23rd there was very little activity over the area. From the 24th an increase in humidity can be seen as the water vapour values start to increase. This

would indicate the start of the collection of heat and moisture in the area. This increase continued on March 25th with some evidence of isolated showers in the target area. A few pixels showed a marked increase in liquid water content and rainfall. There was a decrease on March 26th and 27th which, in fact, may be real as comparison with the GMS imagery shows something of a decrease in organisation on the afternoon GMS image for March 27th (figure 8.6p). This is in contrast with the general trend of increasing cloud and organisation on the GMS imagery.

In this particular case, the passes on March 26th and 27th were such that the system was in the data gap between the edges of successive passes. These dates are significant in that the data now leads to two different possible interpretations. The apparent decrease over these days could be for one of two reasons. Firstly, the system was so far into the gap that valuable signal was not present, that is, that the passes were too far away from the system to give representative information. The second possible cause for the apparent decrease in organisation was that there was an actual decrease in intensity of the system and that it almost “died” during that stage.

The consequence of this is that it is not possible to definitively decide whether the Dvorak model of intensification (linear increase) or the Zehr model which implies development in a series of stages, is the appropriate model to use to explain the development of TC Tim.

From March 28th to the 30th there was a steady increase in all parameters being measured.

Systems are named when the mean wind speed around the core reach Gale Force, which is 34 knots or 17.5 m/sec. Given that the system was named on the 30th and that this was the day that wind speed exceeded 17.5 m/sec is a compliment to the skill of the meteorologists monitoring the system. In 1994, DMSP data were only available about 24 hours after the passes. The only way to decide on the intensity of the system in near real time was to use the Dvorak system. The Dvorak system is well verified in the Pacific and Atlantic Oceans, but with the data sparse regions around Australia, it is not

as well proven as it could be. This author was not able to find a reference showing conclusively a relationship for Dvorak T number and central pressure for the Australian region.

As was mentioned in chapter 7, global data was downloaded from a site in the USA. This data file was then parsed through a program (Imcrop.c, shown in the appendix 11.3) which extracted the individual parameters before saving only the portion over the Timor Sea (figure 8.3b). The much smaller and more manageable individual parameter files were then processed with particular attention in the vicinity of the area of eventual development (the area marked “F” in figure 8.4) until the system was recognised and then followed until it was eventually named (shown at the position marked “N” in figure 8.4). The table below, Table 8.1 is a summary of data extracted from the “single parameter” files.

Date (March 1994)	Surface Wind Speed (m/sec)	Water Vapour (mm)	Liquid water (mm)	Rainfall (mm/hr)
20	7.5	48	0.1	0
21	7.5	30	0.01	0
22	11.5	33.9	0.03	0
23	9.3	33.3	0.06	0
24	6.6	53.1	0.03	0
25	4.2	59.4	0.03	0
26	3	54	0.03	0
27	11.3	52.8	0.32	0
28	9.45	57	0.61	7.7
29	13.2	49.5	0.72	25
30	19.8	60.3	0.85	25

Table 8.1: A comparison of maximum values of surface wind speed, columnar water vapour, cloud liquid water, and precipitation rate (rainfall) taken from DMSP 11 orbits over the study area between the 20th and 30th 1994.

8.1.1.4 Model data

The primary meteorological computer model data available for the area at the time was an Australian model known as the GASP. In 1994, this model was executed on a 1.5 degree grid. This gives a 28 by 13 grid for the study area. For each day the 23Z model data were used which, in fact, is for 7am local time the next morning. Therefore 23Z on the 19th is 7am local time on the 20th. The model data was supplied from the Bureau of Meteorology electronic archive in Melbourne, Australia.

Data taken from the grid point nearest the point of interest are presented in table 8.2. Where necessary, another grid point was selected as the system moved so as to keep the reference point as close as possible to the centre of the system. The following discussion is summarised by table 8.2.

Unfortunately, for this event, the humidity data could not be extracted from the computer model data stored in the Head Office, Bureau of Meteorology, Melbourne.

There is surprisingly little variation in temperatures from the GASP model during the ten days of the study for this cyclone. If one calculates the mean temperature for each level (850, 700, 500, and 200 hPa) for the ten days of interest, then the daily variation from the mean is very rarely more than 0.5°C. There is a very slight rise in temperature at all levels from the 21st to the 23rd March followed by a 0.6°C drop at 700, 500, and 200 hPa on the 24th March. Temperatures then rise again until the 26th March, followed by another decrease until the 29th. Finally, there is a very slight rise on the 30th March.

Analysis of the computer model data shows that there is almost no reaction in the model as the system develops. The two heights at which one would have expected to see the initial warming, 700 and 500 hPa are in fact the levels at which there is the least reaction to the developing system. This could be due firstly to the coarse grid of the model and secondly as a result of the known insensitivity of the model to the tropics.

Apart from the 28th March, winds at 850 hPa remain Easterly for the whole period. From the 21st March until the 25th, winds were southeasterly or easterly. From the 26th March, winds became more north easterly. However, on the 30th March, the day of naming, the winds turned south easterly again. Winds were below 10 m/sec apart from the 23rd March when they achieved a speed of 10.1 m/sec. There is a slow increase in speed from 4.4 m/sec on the 27th March until the 30th March when the speed achieved by the model was 7.4 m/sec. This is still well below what would be expected in the vicinity of a developing storm. That the winds stayed easterly for almost the whole period and south easterly for most of the first half of the study period is an indication that the system developed south of the equatorial trough.

The 200 hPa fields show that winds were below 10 m/sec throughout the study period. In fact the maximum wind generated by the model was 8.9 m/sec on the 29th March. The direction of the wind is quite variable and given the light speeds, one would have to come to the conclusion that for much of the time a col l was near or over the low level features. This would help in maintaining a low shear environment

The relatively light winds and the uniform temperatures throughout the study period would lead to the conclusion that the GASP model never really recognised the presence of a developing system over the Timor Sea.

Date	850 Temp (K)	700 Temp (K)	500 Temp (K)	200 Temp (K)	850 RH (%)	700RH (%)	850 Wind (U, ms ⁻¹)	850 Wind (V, ms ⁻¹)	200 Wind (U, ms ⁻¹)	200 Wind (V ms ⁻¹)	Zehr's GP
21	290.3	283.0	267.3	220.5			-1.7	3.1	-1.6	3.0	0.0
22	290.1	282.4	268.9	219.8			-8.3	1.0	2.4	5.4	0.0
23	290.6	282.6	269.3	221.9			-10.1	1.1	0.2	8.6	0.0
24	290.5	282.1	268.6	220.3			-5.6	-0.3	-4.4	7.4	0.0
25	290.1	283.5	267.5	220.5			-4.8	1.4	-2.7	1.3	0.0
26	290.5	284.0	268.7	221.7			-7.5	-1.0	0.2	-7.8	0.0
27	289.8	283.7	268.6	220.2			-2.3	-3.8	2.0	-0.3	0.0
28	289.8	282.9	267.6	218.7			0.7	-4.6	2.9	1.1	0.0
29	289.6	282.3	267.4	219.9			-2.4	-5.6	5.5	7.0	0.0
30	289.9	282.4	267.4	220.6			-6.0	4.4	1.5	2.1	0.3

Table 8.2: Table showing information taken from the daily computer model (GASP) runs and giving some of the key data which should show any changes in the environment. Unfortunately relative humidity data were not able to be retrieved for this event. The convention with winds is that Westerly and Southerly winds are positive.

8.1.1.5 Gray's Parameters

In chapter five, an article by Gray (1979) was discussed in which he listed six parameters necessary for development of TC's. These are listed below for information.

- large values of low level vorticity,
- located at least a few degrees from the Equator (significant planetary vorticity),
- weak vertical shear in the horizontal winds,
- sea surface temperature at least 26C and a deep thermocline,
- conditional instability through a deep layer of the atmosphere, and
- high humidity levels in the lower and middle atmosphere.

Low level vorticity can be inferred from the increase in cloud activity in a region in that any increase in cloud is a result of vertical motion; the most probable cause in the tropics being a low level circulation. Isentropic flow at such low latitudes would be negligible in most circumstances and can be ruled out as a major contributor to uplift. Cloud cover and its increase has already been discussed in section 8.1.1.1 GMS Satellite Imagery. Computer models provide data in an efficient form for the calculation of vorticity and the GASP model data are used to provide the table below.

As can be seen in table 8.3, vorticity in the area of development varies significantly until March 27th when there is a local minimum. This is quite interesting in that a large cloud cluster, visible on the 00Z image collapses during the day (see figure 8.6m and 8.6n). By the time of the 12Z image in the evening, only stratiform cloud is present in the area. After that time the vorticity increases and it is during this period that the system develops.

Date	21st	22nd	23rd	24th	25th	26th	27th	28th	29th	30th
value	-0.9	-0.7	-1.7	-0.4	-0.6	-0.9	-0.4	-1.5	-1.8	-3.5

Table 8.3: Table showing 850hPa vorticity value at the computer grid point nearest to the development of the tropical system during March 1994. The value shown is in units of s^{-1} .

The next point in Gray's list is "located at least a few degrees from the Equator (significant planetary vorticity)". The system was first logged by the Perth TCWC at 10°S 115°E on the 28th March 1994. It then moved towards 11.6 °S 112.0 °E by March 30th. Given that it is considered that systems needed to be at least 5 degrees from the Equator to develop, TC "Tim" was well within the pre-condition as specified by Gray.

The next point in Gray's list is "weak vertical shear in the horizontal winds". The table below (Table 8.4) shows how vertical shear over the area of interest changes during the study period.

Date	21st	22nd	23rd	24th	25th	26th	27th	28th	29th	30th
value	0.1	11.6	12.7	7.8	2.1	10.3	5.5	1.5	11.1	7.8

Table 8.4: Table showing vertical shear between 850hPa and 200hPa at the grid point nearest to the development of the tropical system. The values shown are in knots. The data were extracted from the GASP model runs by the Bureau of Meteorology and are for the dates in March 1994 as indicated.

As can be seen from the above table, vertical shear varied quite dramatically during the period. It is interesting that on March 27th there was a local maximum in the shear which occurs concurrently with the decrease in vorticity (and the decrease in convective activity). The rapid decrease in vertical shear over the last two days is consistent with Grays requirement of a low shear environment.

Continuing with Gray's list, we come to "sea surface temperature at least 26C and a deep thermocline". Figures 8.5a to 8.5c show the sea surface temperature over the Timor Sea in the period up to the 27th March 1994. Given that SST changes only slowly then it can be quite reasonably assumed that these were the temperatures experienced as the system moved over the water. While there are no measurements of the thermocline easily available for this time, the fact that the TC developed suggests that the thermocline was certainly sufficiently deep. The figures indicate that the SST was about 28.5 C in the area of development.

The second last in Gray's list is "conditional Instability through a deep layer of the atmosphere". Unfortunately, moisture was not archived in the model data stored in 1994. Direct calculation of the stability is very flawed without moisture parameters. There is an indication that the atmosphere was in a sufficiently unstable state due to the formation of convective cloud in the area. It would have been interesting to calculate the conditional instability particularly around March 27th.

Finally, Gray's last point is "high humidity levels in the lower and middle atmosphere". Again due to the lack of moisture data in the GASP model this cannot be validated numerically. The DMSP data however is an excellent indicator of the moisture processes occurring in the area. The table, table 8.1 shows Water Vapour, Liquid Water content and Rainfall near the system. As can be seen from the table, all these items increase with time with a noticeable increase from March 28th onwards. Accepting the SSM/I data leads to the conclusion that there was sufficient humidity in the lower and middle levels of the atmosphere to allow cyclogenesis to take place.

In conclusion, the parameters defined in the first four of Grays points are able to be directly measured or calculated for this system. Each of the parameters complies with the requirements as laid down by Gray. The final two points were not able to be directly measured in this case, however, evidence from the GMS IR imagery and the SSM/I sensors show that instability and moisture were sufficient for the system to form. The final piece of evidence that there was sufficient instability and moisture is that the

system actually continued developing into a cyclone, showing that all parameters were in place to facilitate development.

8.1.2 Discussion

Satellite imagery of the target area showed a relatively quiet region for the first few days of the study period. Cloud activity was generally confined to the Indonesian Archipelago. Only after March 25th did cloud become evident in the area. This cloud steadily increased in organisation and size until March 30th when the system was named.

Microwave imagery of the Timor Sea (table 8.1) for the same period also shows a relatively quiet scene for most of the study period. Water vapour, liquid water and rainfall data extracted from the DMSP satellite all indicate little activity over the Timor Sea until March 27th. The pass on March 28th shows a jump in activity consistent with the system becoming established. Examining the DMSP data (table 8.1), one would have to conclude that the forecasters did a good job in naming the system at the time they did.

Surface wind speed increases on March 22nd and 25th are not reflected in the model outputs for those days. There is actually a slight increase in 850 hPa wind speed a day later in each case, but it is only short lived, lasting for only a day. If a surge in the south east trades or in the monsoonal north westerlies was taking pace, it would be expected to last for several days.

Temperatures at 850 hPa remain remarkably steady throughout the period and the coldest temperature recorded was on the 29th when it was 289.6K. On the 30th March, the temperature at 850hPa increased by 0.3K while at 700hPa the temperature increased by 0.1K and at 500 hPa the temperature remained steady. This indicates a very slight decrease instability of the atmosphere on the day of naming. It would be consistent with the system developing.

GASP model output winds show that the Timor Sea was not very windy throughout the study period. Winds were typically less than 10 m/sec. On March 27th and 28th there was a further decrease in the low level winds to 4 m/sec. On the same days the 200 hPa

winds decreased from 9 m/sec to 4 m/sec. This is clearly a marked decrease in the vertical shear on these days. The slight increase in wind speed at 850 hPa combined with the continuing light winds at 200 hPa indicates that there was very little venting of the system in the two days before naming, thus allowing a build up of heat and moisture which added to the energy available to the system.

The question arises as to how the system actually developed. For the first eight days there was very little activity and so no obvious signal as to what was about to happen. The presence of a col in the vicinity of eventual development helps bring about decreased venting in the area. As has been shown above, all of Grays parameters have been met, hence the environment was suitable for development of a system. The steady development of the system into TC Tim was such that once it started, the increase in intensity was almost continuous. When compared to the Dvorak model and the Zehr model, one would have to conclude that in this instance Dvorak more reasonably represented the processes occurring. Zehrs model suggests that there are two stages and can be a gap between them. If there were two stages in the development of TC Tim, then the gap was very short, perhaps of the order of a few hours and certainly missed by the various monitoring systems.

After a period of stable conditions, a col moved into the vicinity of the area of genesis enhancing the pre existing latent conditions suitable for cyclogenesis. A cloud cluster that developed in the vicinity was then in an area conducive to further development, which is what happened.



Figure 8.5a: Sea Surface Temperature for the week ending 13 Mar 1994. Taken from a product issued by the Darwin RSMS (Australian Bureau of Meteorology).



Figure 8.5b: Sea Surface Temperature for the week ending 20 Mar 1994. Taken from a product issued by the Darwin RSMC (Australian Bureau of Meteorology)



Figure 8.5c: Sea Surface Temperature for the week ending 27 Mar 1994. Taken from a product issued by the Darwin RSMC (Australian Bureau of Meteorology)

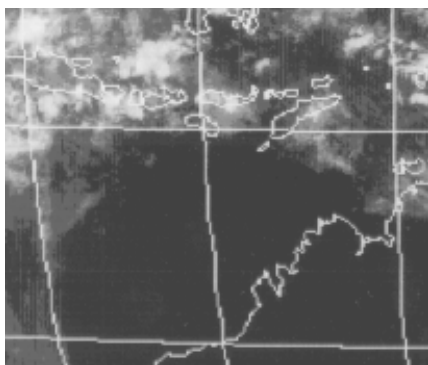


Figure 8.6a: GMS4 image of the Timor Sea 00Z 20 Mar 1994.

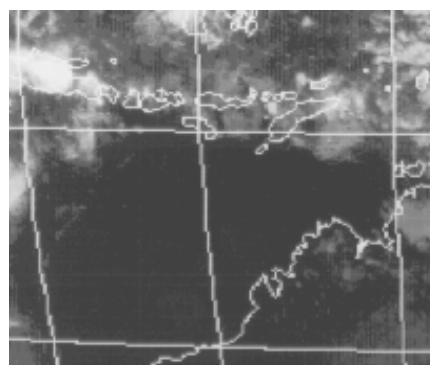


Figure 8.6b: GMS image of the Timor Sea 12Z 20 Mar 1994

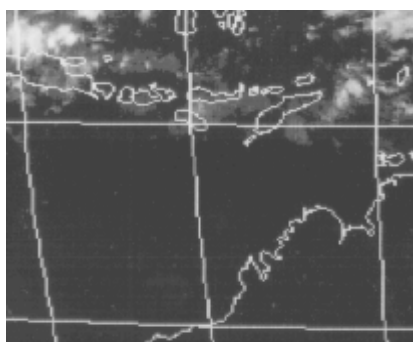


Figure 8.6c GMS4 image of the Timor Sea 00Z 21 Mar 1994

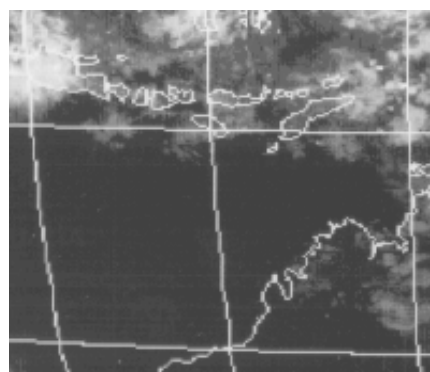


Figure 8.6d GMS4 image of the Timor Sea 12Z 21 mar 1994

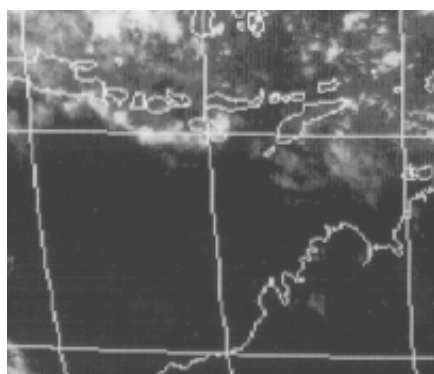


Figure 8.6e GMS4 image of the Timor Sea 00Z 22 Mar 1994

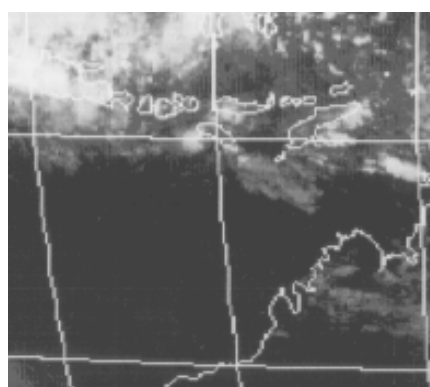


Figure 8.6f GMS4 image of the Timor Sea 12Z 22 Mar 1994

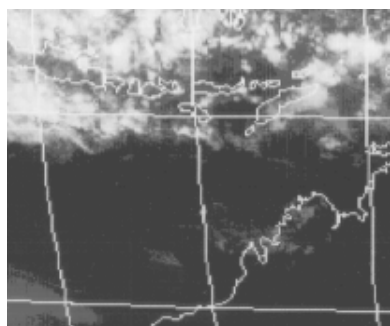


Figure 8.6g GMS4 image of the Timor Sea 00Z 23 Mar 1994

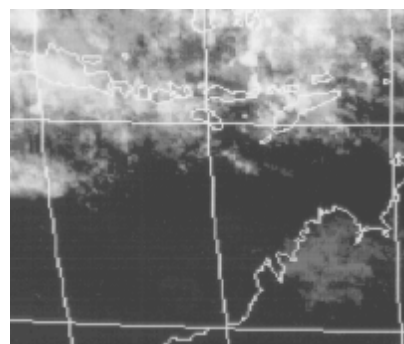


Figure 8.62h GMS4 Image of the Timor Sea 12Z 23 Mar 1994

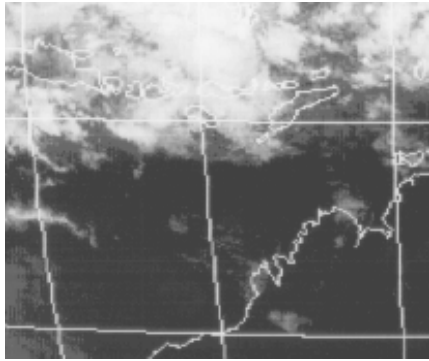


Figure 8.6i GMS4 image of the Timor Sea 00Z 24 Mar 1994

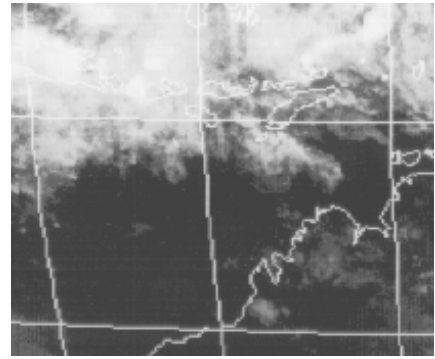


Figure 8.6j GMS4 image of the Timor Sea 12Z 24 Mar 1994

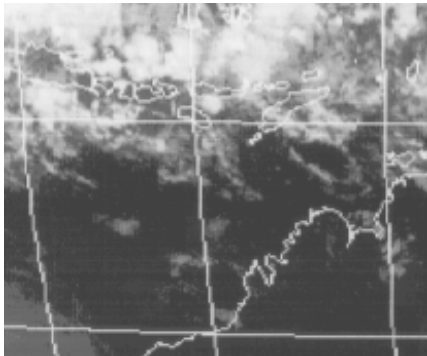


Figure 8.6k GMS4 image of the Timor Sea 00Z 25 Mar 1994

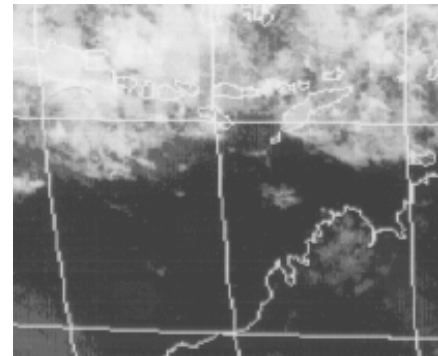


Figure 8.6l GMS4 image of the Timor Sea 12Z 25 Mar 1994

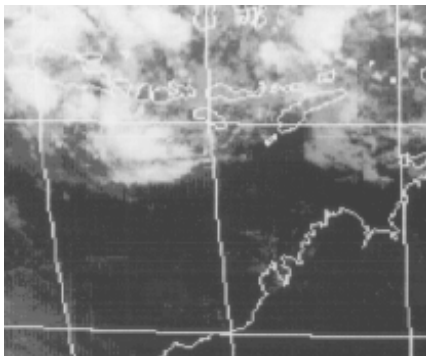


Figure 8.6m GMS4 image of the Timor Sea 00Z 26 Mar 1994

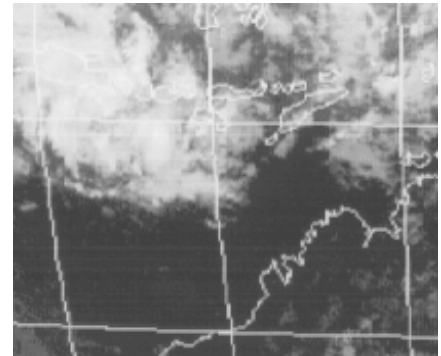


Figure 8.6n GMS4 image of the Timor Sea 12Z 26 Mar 1994

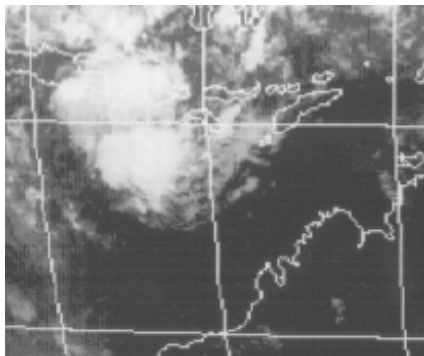


Figure 8.6o GMS4 image of the Timor Sea 00Z 27 Mar 1994

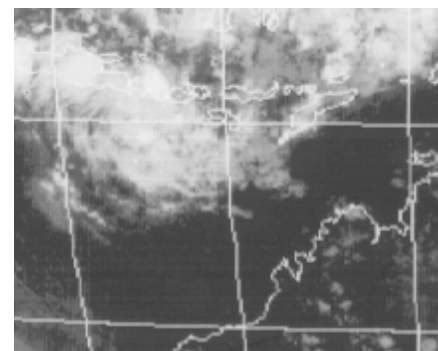


Figure 8.6p GMS4 image of the Timor Sea 12Z 27 Mar 1994

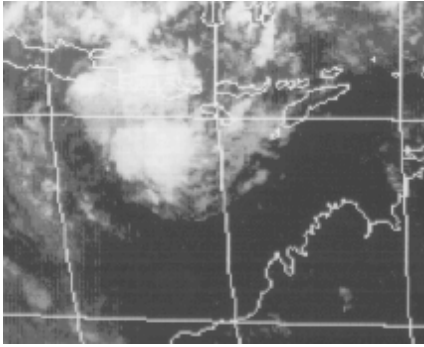


Figure 8.6q GMS4 image of the Timor Sea 00Z 28 Mar 1994

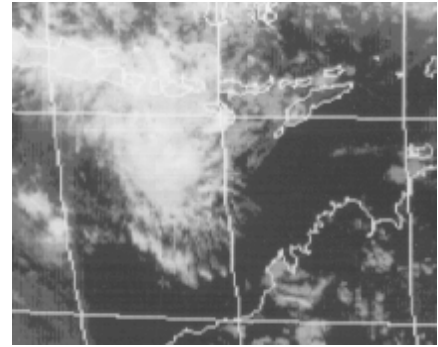


Figure 8.6r GMS4 image of the Timor Sea 12Z 28 Mar 1994

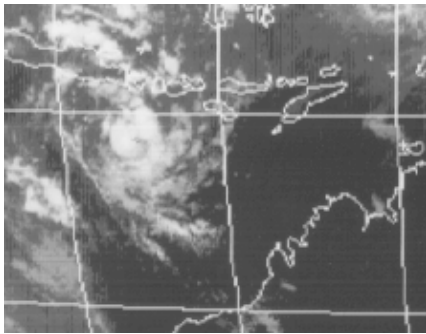


Figure 8.6s: GMS4 image of the Timor Sea 00Z 29 Mar 1994

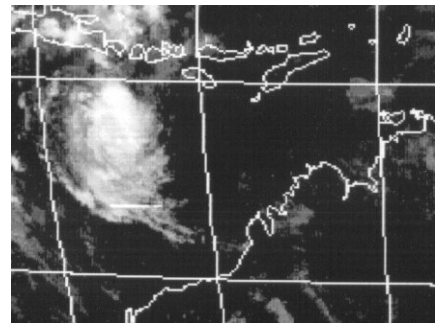


Figure 8.6t: GMS 4 image of the Timore Sea 12Z 29 Mar 1994

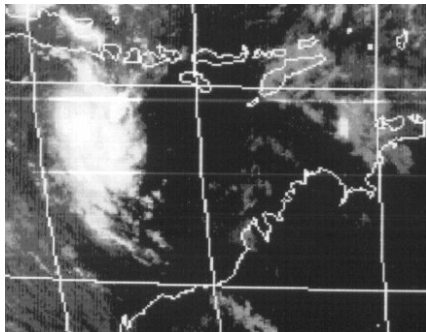


Figure 8.6u: GMS4 image of the Timor Sea 00Z 30 Mar 1994

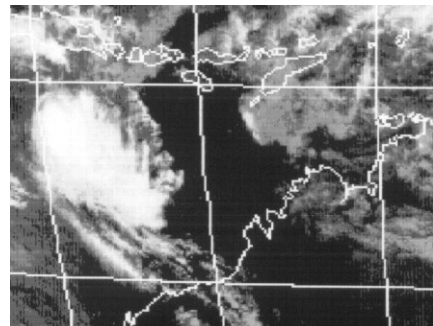


Figure 8.6v: GMS 4 image of the Timor Sea 12Z 30 Mar 1994



Figure 8.7a: Water vapour image of the Timor Sea am 20 Mar 1994.

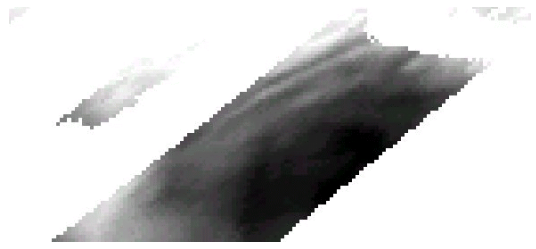


Figure 8.7b Water vapour image of the Timor Sea am 21 Mar 1994



Figure 8.7c Water vapour image of the Timor Sea am 22 Mar 1994

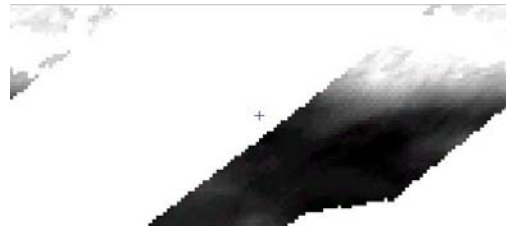


Figure 8.7d: Water vapour image of the Timor Sea 23 Mar 1994



Figure 8.7e: Water vapour image of the Timor Sea 24 Mar 1994



Figure 8.7f: Water vapour image of the Timor Sea 25 Mar 1994



Figure 8.7g: Water vapour image of the Timor Sea 26 Mar 1994



Figure 8.7h: Water vapour image of the Timor Sea 27 Mar 1994



Figure 8.7i: Water vapour image of the Timor Sea 28 Mar 1994



Figure 8.7j: Water vapour image of the Timor Sea 29 Mar 1994

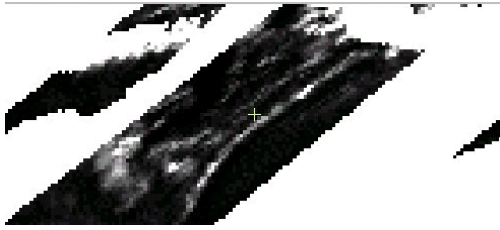


Figure 8.8a: Liquid water content over the Timor Sea am 20 Mar 1994.

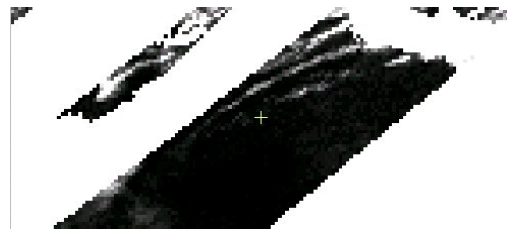


Figure 8.8b: Liquid water content over the Timor Sea am 21 Mar 1994

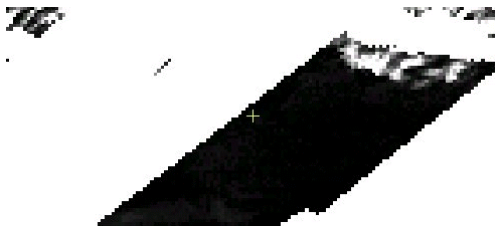


Figure 8.8c: Liquid water content over the Timor Sea am 22 Mar 1994



Figure 8.8d: Liquid water content over the Timor Sea am 23 Mar 1994

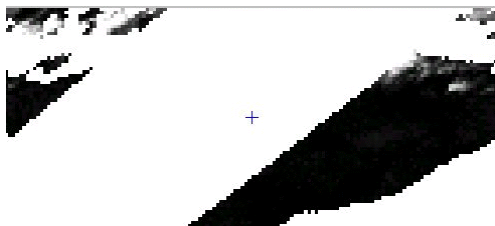


Figure 8.8e: Liquid water content over the Timor Sea am 24 Mar 1994



Figure 8.8f: Liquid water content over the Timor Sea am 25 Mar 1994

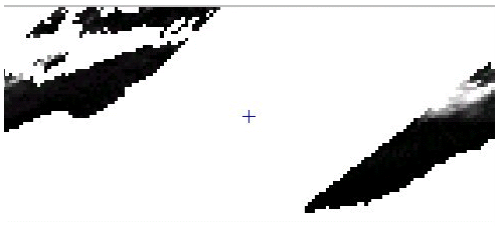


Figure 8.8g: Liquid water content over the Timore Sea am 26 mar 1994

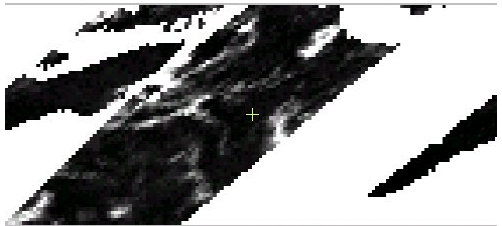


Figure 8.8h: Liquid water content over the Timore Sea am 27 Mar 1994

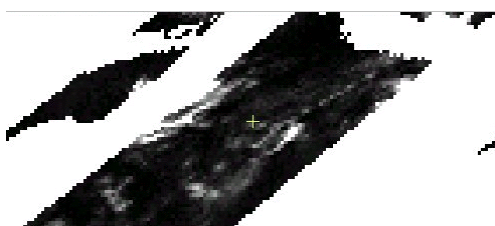


Figure 8.8i: Liquid water content over the Timor Sea am 28 Mar 1994

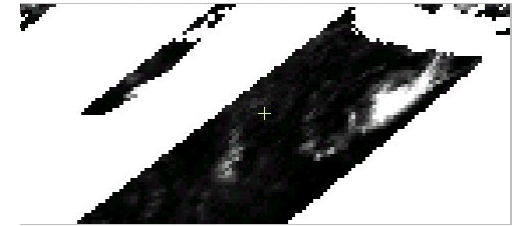


Figure 8.8j: Liquid water content over the Timor Sea am 29 mar 1994



Figure 8.9a: Rainfall over the Timor Sea am 20 Mar 1994.



Figure 8.9b: rainfall over the Timor Sea am 21 Mar 1994



Figure 8.9c: Rainfall over the Timor Sea am 22 mar 1994

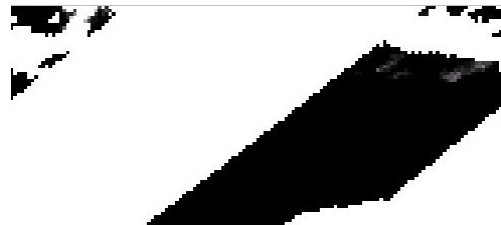


Figure 8.9d: Rainfall over the Timor Sea am 23 Mar 1994



Figure 8.9e: rainfall over the Timor Sea am 24 Mar 1994



Figure 8.9f: Rainfall over the Timor Sea am 25 Mar 1994

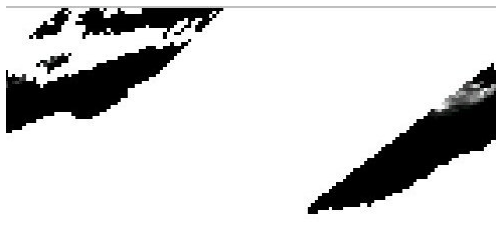


Figure 8.9g: Rainfall over the Timor Sea am 26 Mar 1994



Figure 8.9h: Rainfall over the Timor Sea am 27 Mar 1994



Figure 8.9i: Rainfall over the Timor Sea am 28 Mar 1994



Figure 8.9j: Rainfall over the Timor Sea am 29 Mar 1994



Figure 8.9k: Rainfall over the Timor
Sea am 30 Mar 1994



Figure 8.10a: Surface wind speed over the Timor Sea am 20 Mar 1994.



Figure 8.10b: Surface wind speed over the Timor Sea am 21 Mar 1994



Figure 8.10c: Surface wind speed over the Timor Sea am 22 Mar 1994

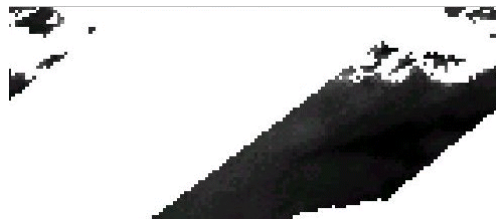


Figure 8.10d: Surface wind speed over the Timor Sea am 23 Mar 1994



Figure 8.10e: Surface wind speed over the Timor Sea am 24 Mar 1994



Figure 8.10f: Surface wind speed over the Timor Sea am 25 Mar 1994

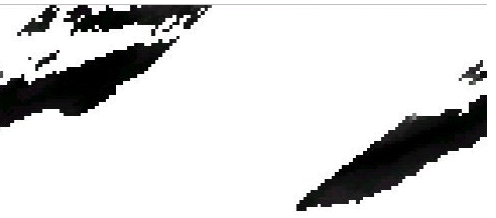


Figure 8.10g: Surface wind speed over the Timor Sea am 26 Mar 1994



Figure 8.10h: Surface wind speed over the Timor Sea am 27 Mar 1994



Figure 8.10i: Surface wind speed over the Timor Sea am 28 Mar 1994



Figure 8.10j: Surface wind speed over the Timor Sea am 29 Mar 1994

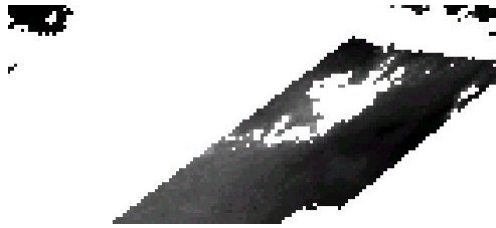


Figure 8.10k: Surface wind speed
over the Timor Sea am 30 Mar 1994

8.2 Case 2. - TC “Elaine”

Tropical cyclone “Elaine” was named on 16th March 1999. Atmospheric conditions from the 06th Mar 1999 until naming are examined. In this case March 17th was also checked due to little signal being present on the 16th. Figure 8.11 shows the Timor Sea with the genesis area marked with an “F” in a circle and the place at which TC Elaine was named marked with an “N” in a circle.

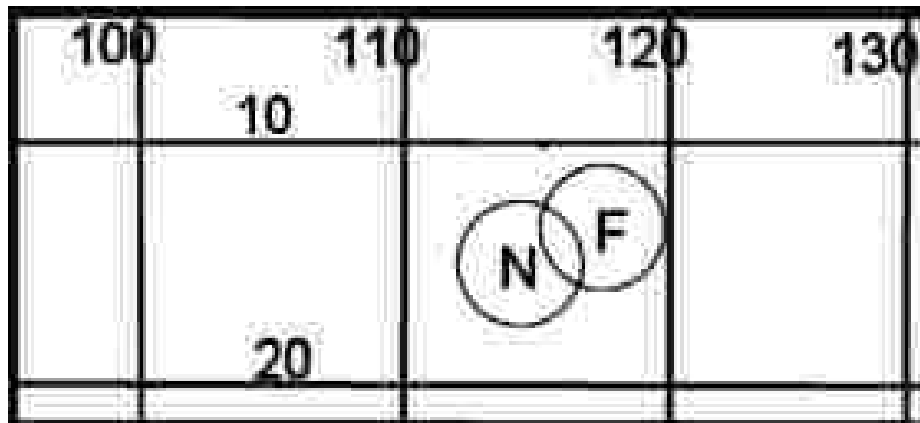


Figure 8.11: Map showing the location of the area where the system that became TC Elaine was first identified (marked F) and where it was eventually named (marked N).

Description of the imagery used in this case study is given in section 8.0. A brief description of the GMS IR satellite imagery is that the whiter the colour in the image, the colder the temperature at the top of the cloud, that is, the higher the cloud is in the atmosphere. Figure 8.3a gives the navigation for the GMS imagery. In the case of the USA DMSP imagery, the blacker the colour in the image the lower the value of the parameter being displayed. Calibration for the DMSP images are shown in figures 8.2 to 8.5 where scales for water vapour, liquid water, rainfall, and surface wind speed respectively are given along with sample images. Figures 8.3b and 8.18 give the navigation for each of the DMSP images. A full description of the DMSP imagery is given in section 7.1.1.

8.2.1 Antecedent Conditions

For the sake of this study, it was assumed that the atmosphere was in a “normal” or undisturbed state ten days before the system was named. In this case the pre existing conditions are set as 06th March 1999.

Unlike the situation for TC “Tim”, satellite imagery shows that on March 6th there is an active phase of the MJO with considerable amounts of cloud over the Timor Sea.

8.2.1.1 GMS Satellite imagery

Satellite imagery relevant to this event are shown in figures 8.13a to 8.13u. The figures presented are the 00Z and the 12Z GMS IR pictures of the study area over the Timor Sea. An explanation of the navigation and grey scale is given in chapter 8.0.

There is a considerable amount of cloud over the area on the 6th and 7th with several cloud clusters being observed in the IR imagery. The clusters continue on the 8th although low level cloud decreases generally over the area. By the 9th there is a slight decrease in general activity although some thunderstorm activity persists along about 13 degrees south latitude. During the 10th and 11th cloud activity increases but contracts northward on the 12th and 13th. During the 14th a cloud cluster develops to the north east of the position where the TC eventually develops. This cluster moves south west and becomes more organised during the 14th and 15th. The system was named at 0100Z (0800WST) on the 16th March 1999 while at a position of 14.0S 115.8E.

A sequence of satellite photos are shown at figures 8.13a to 8.13u which show the 00Z and 12Z satpix of the Timor Sea for the period 6th March 1999 until 16th March 1999

8.2.1.2 Sea Surface temperatures

SST's were in excess of 29°C for the entire month. Given that one of the basic requirements for cyclogenesis is SST's above 26.5°C, then in this case there is ample energy available within the ocean for this cyclone to develop.

These SST diagrams were cropped from weekly sea surface temperatures from the Darwin Regional Meteorological Centre and are shown at figures 8.12a to 8.12c. They show the weekly SST as derived from satellite imagery. The isotherms are at 1°C intervals with the multiples of 5°C isotherms marked in a heavier font.

8.2.1.3 DMSP Satellite imagery

Table 8.5 below shows a summary of data taken from the American satellite DMSP 14. Portions of the global images are shown in figures 8.14a to 8.17l. In each case the portion over the Timor Sea has been extracted for inclusion in the figures. In chapter 8.0 a description of the navigation and grey scales are given.

Columnar water vapour in the region (shown in figures 8.14a to 8.14l) show a similar pattern to that of the GMS satellite imagery. Between March 6th and the 9th there is an increase in moisture followed by a decrease until the 13th. Then there is little change until March 16th when there is a dramatic increase. In fact, the channel was saturated as the water vapour value increased from 49 to 75mm.

Figures 8.15a to 8.15l show liquid water content over the Timor Sea. Liquid water shows a very similar pattern to the columnar water vapour. The first few days shows reasonable amount of liquid water which is consistent with the amount of cloud in the area at the time. There is a relatively long period of very little liquid water between March 10th and 15th before a dramatic increase on March 16th and 17th. This is also consistent with the GMS IR imagery which shows a decrease in cloud through that period.

Rainfall over the Timor Sea is shown in figures 8.16a to 8.16l. There is a peak in rainfall on March 8th which is consistent with the thunderstorm activity over the area. Small amounts of rain are evident the following two days. The next five days give no rain in the vicinity of the eventual development of the system. On March 16th and 17th there is a rapid increase in the amount of rain in the vicinity of the system.

Finally, wind speed over the Timor Sea derived from DMSP is shown in figures 8.17a to 8.17l. This shows a remarkably quiet period consistently from March 7th until the 15th. Only on March 16th does the wind increase over 5 m/sec (10 knots). An increase on March 17th to 12m/sec is actually outside the rain affected area. This shows that the system developed rapidly overnight.

Date (March 1999)	Surface Wind Speed (m/sec)	Water Vapour (mm)	Liquid water (mm)	Rainfall (mm/hr)
07	2.9	59.1	0.9	0.0
08	3.0	57.3	1.2	8.8
09	3.3	63.0	1.2	0.3
10	4.5	62.4	0.3	0.3
11	3.2	54.0	0.0	0.0
12	3.5	54.9	0.3	0.0
13	2.6	48.6	0.0	0.0
14	4.1	57.0	0.0	0.0
15	3.8	48.6	0.2	0.0
16	6.1	75	0.5	9.6
17	11.7	75	1.7	15.4

Table 8.5: A comparison of maximum values of surface wind speed, columnar water vapour, cloud liquid water, and precipitation rate (rainfall) taken from DMSP 13 orbits over the study area between the 07th and 17th March 1999 for TC Elaine.

It is interesting to note that wind speeds measured during this event were only about half of the speed measured during the lead up to TC Tim. Even on the last two days when speed doubled compared with the rest of this event (TC Elaine), they were still lighter than for the TC Tim (case study 1).

Water vapour was much more consistent in value than was the situation in case study 1. This is consistent with the amount of cloudiness over the area.

Liquid water content was relatively low compared to case study 1 until the last three days when there was dramatic increase from near zero values to 0.85mm on the last day.

Rainfall in this case study follows closely the convective cloud patterns over the Timor Sea. Early in the period there was some convective cloud (as seen in the GMS IR images). There is very little convection during the middle period of the study. An increase in convection on the 13th marks the start of events that eventually led to TC Elaine.

8.2.1.4 Model data

Model information was taken from the Australian global model GASP. Table 8.6 shows data extracted which was near the location of the low development and later the cyclone.

As with TC Tim, the data shows an indication of a false start. Between March 6th and 9th there is an increase in 700 hPa temperatures as would be expected with a cloud cluster developing. However from March 10th onwards there is a cooling followed by a fairly steady temperature.

The upper atmospheric temperatures at 500 hPa and at 200 hPa show a remarkable steadiness throughout the period

Moisture as generated by the model shows an unfortunate trend at both 850hPa and at 700hPa. At both levels the humidity actually decreases in the model! One would expect the moisture in the vicinity of the system to increase as time goes on.

The one potentially useful parameter that can be calculated and which would show the atmosphere becoming more amenable to a cyclone developing is Zehr's Daily Genesis Parameter (ZDGP). The ZDGP was calculated for this event using the GASP model output data and is presented in the last column of table 8.6. It was consistent with the remainder of the information extracted in that it was inconclusive to say the least.

Date	850 Temp	700 Temp	500 Temp	200 Temp	850 RH	700RH	850 Wind	850 Wind	200 Wind	200 Wind	Zehr's
March	(K)	(K)	(K)	(K)	(%)	(%)	(U, ms ⁻¹)	(V, ms ⁻¹)	(U, ms ⁻¹)	(V ms ⁻¹)	GP
1999											
06	291.2	282.8	268.6	220.3	77	58	4.7	2.0	-13.0	4.0	0.0
07	290.5	282.4	268.7	219.7	80	64	1.8	2.9	-10.3	3.4	0.0
08	291.4	283.5	267.5	220.1	73	60	-0.9	2.1	-10.2	4.0	0.0
09	292.5	284.0	267.4	219.9	58	51	-3.2	0.8	-9.0	1.1	0.0
10	292.1	282.8	268.7	219.9	62	62	-3.0	-1.7	-9.3	3.0	0.0
11	290.9	282.5	268.2	220.3	69	67	-1.4	-2.9	-1.7	-0.8	0.0
12	292.4	282.5	268.4	219.8	64	66	-4.8	-0.6	-7.2	-0.1	0.1
13	292.7	282.2	269.0	220.0	67	75	-4.3	0.4	-3.1	-1.1	0.0
14	292.5	282.9	268.1	219.9	65	57	-4.1	-0.4	0.0	2.1	0.0
15	291.3	281.9	268.8	220.8	61	60	-6.9	-2.3	-1.7	7.0	0.0
16	293.1	283.8	268.2	220.5	61	55	-8.3	3.0	-7.1	2.1	1.3

Table 8.6: Information taken from the daily computer model (GASP) runs for TC Elaine and giving some of the key data which should show any changes in the environment.

8.2.1.5 Gray's Parameters

As with case study 1, Gray's parameters (Gray 1979) will be reviewed. These are listed below again for information.

- large values of low level vorticity
- located at least a few degrees from the Equator (significant planetary vorticity)
- weak vertical shear in the horizontal winds
- sea surface temperature at least 26C and a deep thermocline
- conditional instability through a deep layer of the atmosphere
- high humidity levels in the lower and middle atmosphere.

To ascertain the low level vorticity in the vicinity of the developing system, vorticity at 850 hPa was calculated from the GASP model data. The data shown below in table 8.7 is taken from the grid point nearest to the position where the system was located. The negative values throughout the period apart from the 10th and 11th are indicative of the model not having relevant information on the developing situation. In fact the apparent decrease in vorticity as the system eventually forms shows that no valid information was being presented by the model.

Date	06th	07th	08th	09th	10th	11th	12th	13th	14th	15th
value	-1.0	-1.2	-0.5	-1.0	0.3	0.3	-0.2	-0.3	-0.9	-0.8

Table 8.7 Table showing 850 hPa vorticity at the computer grid point nearest to the development of TC Elaine for a sequence of days in March 1999. The value shown are in units of s⁻¹.

Significant planetary vorticity is the next parameter to be studied. The system was first identified by the Australian Bureau of Meteorology at 13.1°S 117.5°E at 0100Z on 15 March 1999. TC Elaine was named at 0700Z on the 29th March 1999 located at 14.0°S 115.8°E. Since these latitudes are considerably further away from the Equator than five degrees, there is sufficient planetary vorticity for the system to develop.

Weak vertical shear is also needed for a system to develop. In the case of TC Elaine, shear was particularly weak. The shear between 850hPa and 200hPa as taken from the GASP is shown below at table 8.8. The data in this table were taken from the same grid point as was used to calculate the vorticity shown in the table above (table 8.7). The shear shows a more or less steady decline throughout the period apart from on March 14th when there was a slight increase. Given that the winds used to calculate the vorticity showed no sign of the system developing, one would have to be very cautious about using these data.

Date	06th	07th	08th	09th	10th	11th	12th	13th	14th	15th
value	17.8	12.1	9.5	5.8	7.9	2.1	2.6	1.9	4.8	-0.8

Table 8.8 Table showing vertical shear between 850hPa and 200hPa at the computer grid point nearest to the development of TC Elaine for a sequence of days in March 1999. The values shown are in knots

The second last parameter in Gray's list is conditional instability. Given that the computer model was not adequately handling other aspects of the environment through the study period, any calculation of the instability would also be suspect. There are two indicators that suggest that there was a deep layer of conditionally unstable air. First, and most obviously was that the system developed into a cyclone. Secondly, the deep convection which had been seen in the vicinity and upstream of where the low eventually developed shows that the atmosphere was at least conditionally unstable.

Finally, a necessary condition is the need for a deep layer of moist air. A study of table 8.5 shows that throughout the study period there was a significant amount of moisture in the atmosphere with the water vapour having values in excess of 50mm. Even on the driest days, March 13th and 15th, there was 49mm of water vapour in the atmosphere. There is also the satellite imagery (GMS IR, figures 8.13a-u) showing widespread cloud through the region. This cloud shows that there is a quantifiable amount of uplift occurring across the Timor Sea. Since isentropic flow is negligible at these latitudes, it

would be reasonable to assume that convection was a primary cause of the cloud formation and heat redistribution in the area.

8.2.2 Discussion

The satellite imagery and the microwave imagery were quite consistent in that there was early activity over the entire region of interest. This activity decreased by about March 9th when it remained quiet for a day or so. By March 12th cloud activity had increased again throughout the area. A cloud cluster becomes evident on March decrease 14th in the area that the low eventually develops and persists while moving Southwestwards. There is a decrease in activity around the cluster on the 14th and this becomes particularly noticeable on the 15th and 16th.

Unfortunately the passes of the satellite were not ideally located to support this research and the system was in satellite data gaps at significant stages in the development.

The system remained as a cloud cluster for about two days before increasing quite quickly to cyclone stage. This is consistent with the Zehr model of cyclone development which gives a two stage growth pattern.

The table 8.5 shows a good summary of the development of the system. After an initial period of activity, there was a period of quiet and then suddenly, at the end of the period, a sudden development into the cyclone occurs.

Table 8.6 shows a summary of the model output which is inconclusive given the lack of diagnostic information provided for activity over the Timor Sea. Given this information, a forecaster would be tempted to not give the system the attention that it required.



Figure 8.12a: Sea Surface Temperature 28 Feb 1999.

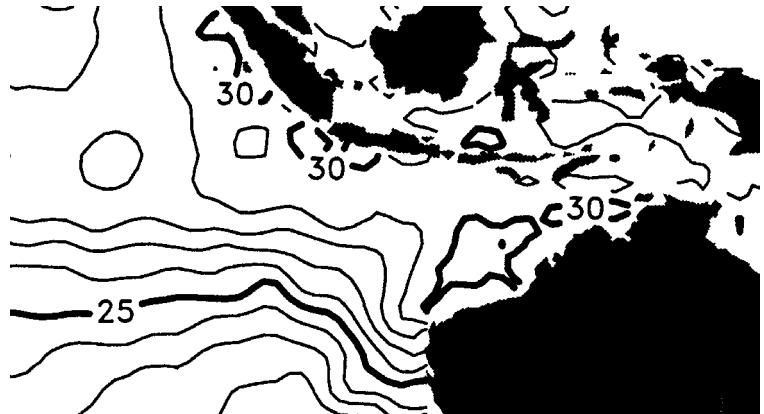


Figure 8.12b. Sea Surface Temperature 07 Mar 1999



Figure 8.12c. Sea Surface Temperature 14 Mar 1999

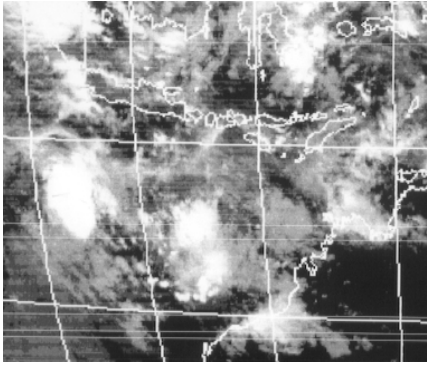


Figure 8.13a: GMS image of the Timor Sea 00Z 06 Mar 1999.

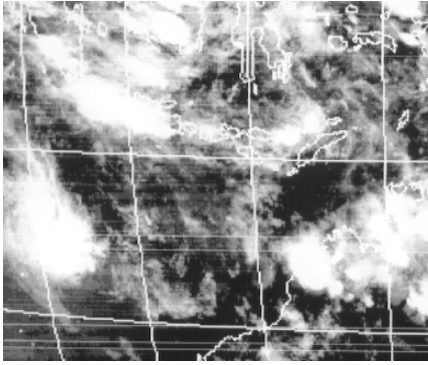


Figure 8.13b. GMS image of the Timor Sea 12Z 06 Mar 1999

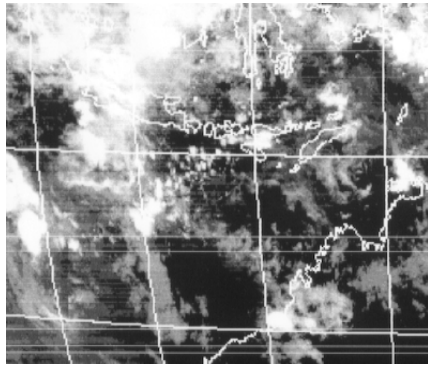


Figure 8.13c. GMS image of the Timor Sea 00Z 07 Mar 1999

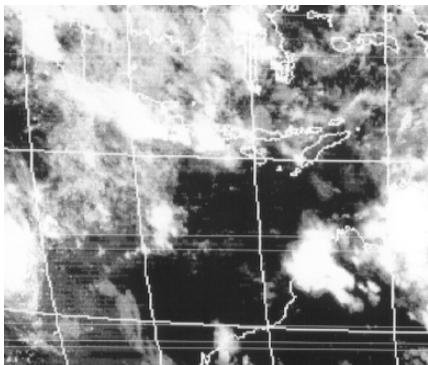


Figure 8.13d. GMS image of the Timor Sea 12Z 07 Mar 1999

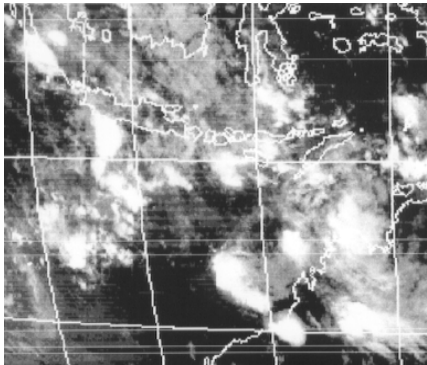


Figure 8.13e. GMS image of the Timor Sea 00Z 08 Mar 1999

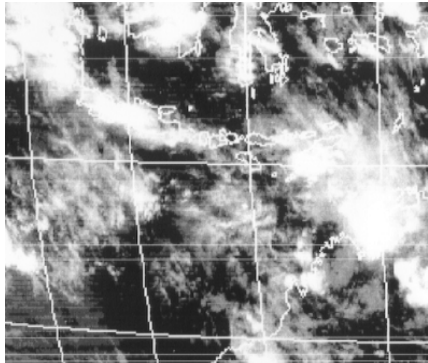


Figure 8.13f. GMS image of the Timor Sea 12Z 08 Mar 1999

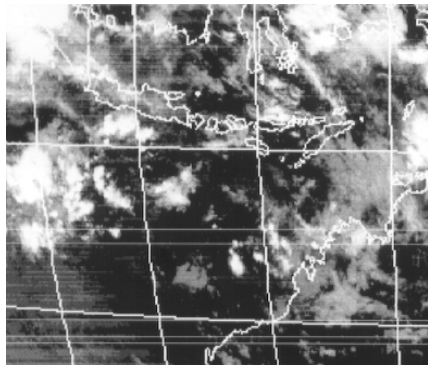


Figure 8.13g. GMS image of the Timor Sea 00Z 09 Mar 1999

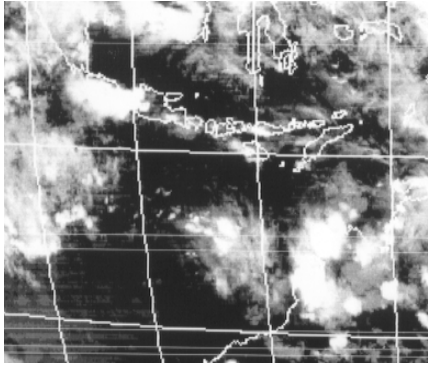


Figure 8.13h. GMS image of the Timor Sea 12Z 09 Mar 1999

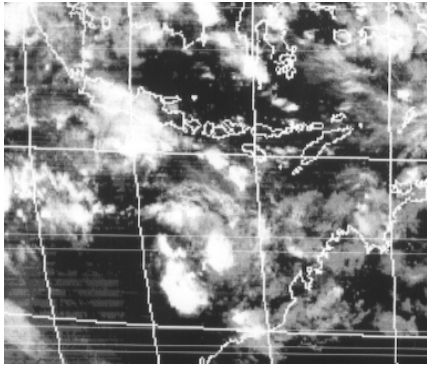


Figure 8.13i. GMS image of the Timor Sea 00Z 10 Mar 1999

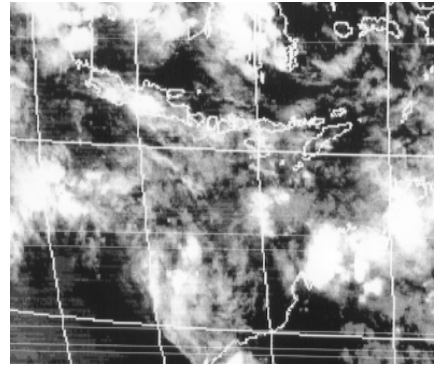


Figure 8.13j. GMS image of the Timor Sea 12Z 10 Mar 1999

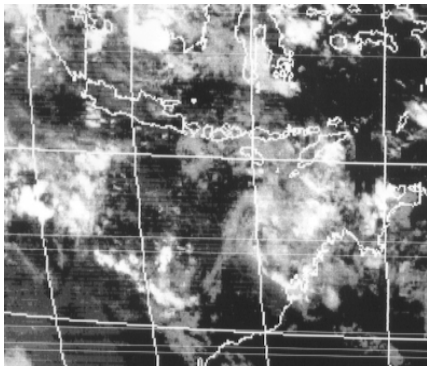


Figure 8.13k. GMS image of the Timor Sea 00Z 11 Mar 1999

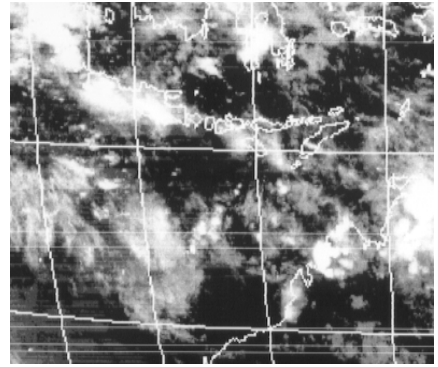


Figure 8.13l. GMS image of the Timor Sea 12Z 11 Mar 1999

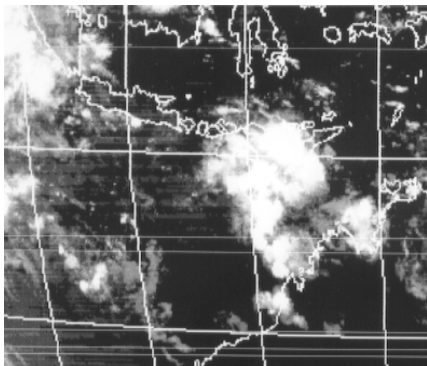


Figure 8.13m. GMS image of the Timor Sea 00Z 12 Mar 1999

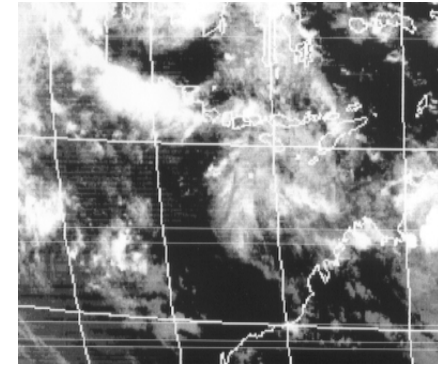


Figure 8.13n. GMS image of the Timor Sea 12Z 12 Mar 1999

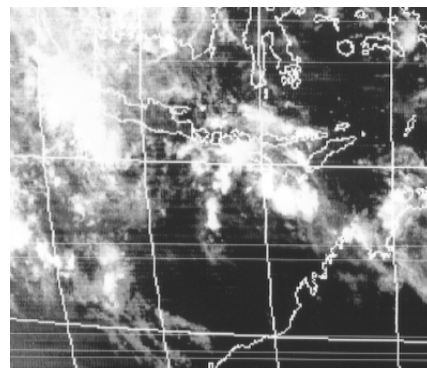


Figure 8.13o. GMS image of the Timor Sea 00Z 13 Mar 1999

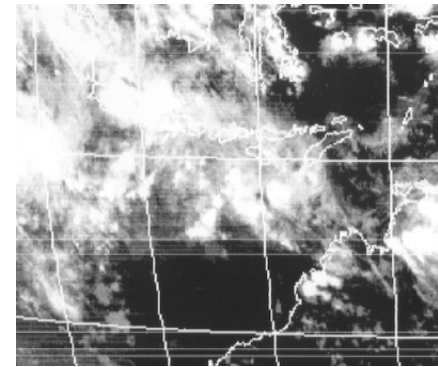


Figure 8.13p. GMS image of the Timor Sea 12Z 13 Mar 1999

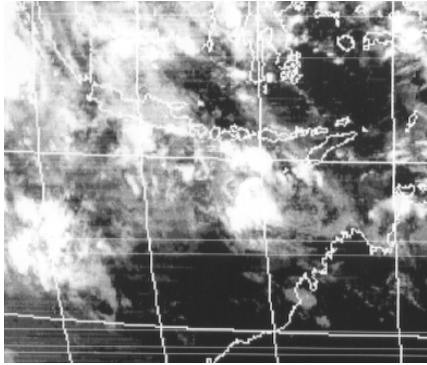


Figure 8.13q: GMS image of the Timor Sea 00Z 14 Mar 1999

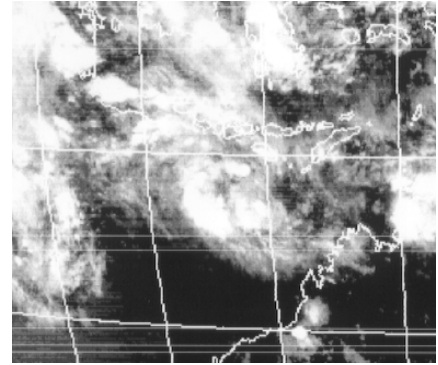


Figure 8.13r: GMS image of the Timor Sea 12Z 14 Mar 1999

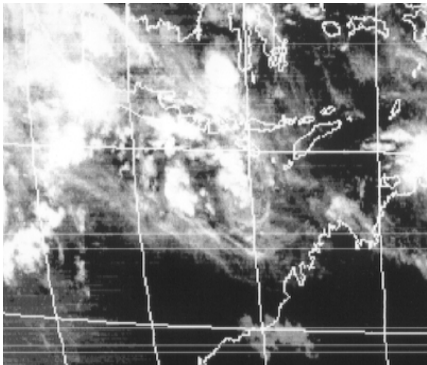


Figure 8.13s: GMS image of the Timor Sea 00Z 15 Mar 1999

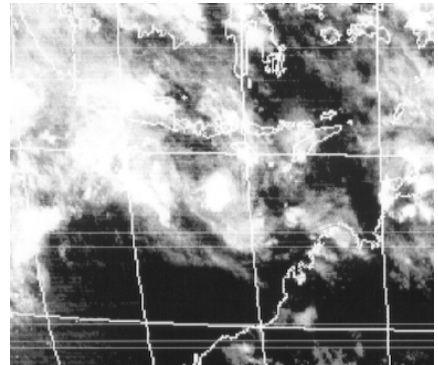


Figure 8.13t: GMS image of the Timor Sea 12Z 15 Mar 1999

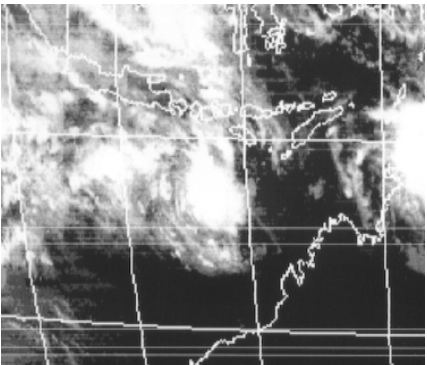


Figure 8.13u: GMS image of the Timor Sea 00Z 16 Mar 1999

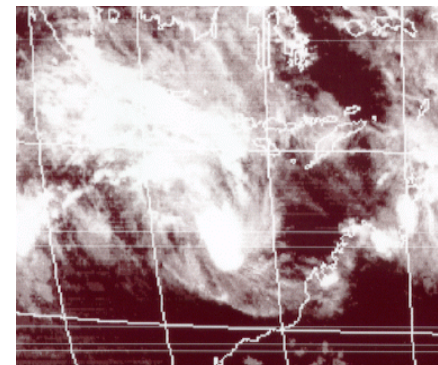


Figure 8.13v: GMS image of the Timor Sea 12Z 16 Mar 1999

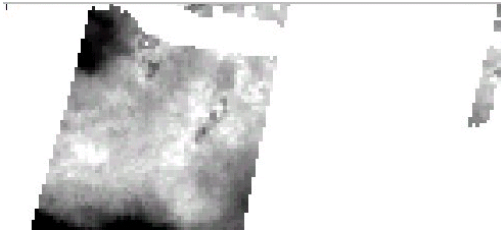


Figure 8.14a: Water vapour image of the Timor Sea 00Z 06 Mar 1999.

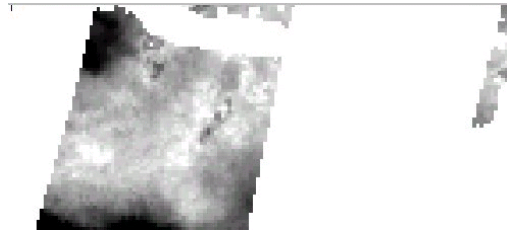


Figure 8.14b. water vapour image of the Timor Sea am 07 Mar 1999

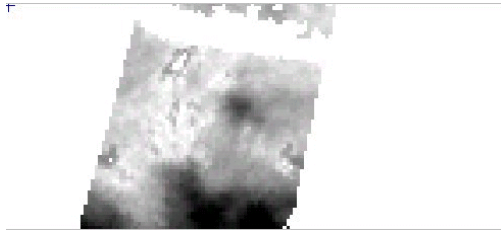


Figure 8.14c. water vapour image of the Timor Sea am 08 Mar 1999

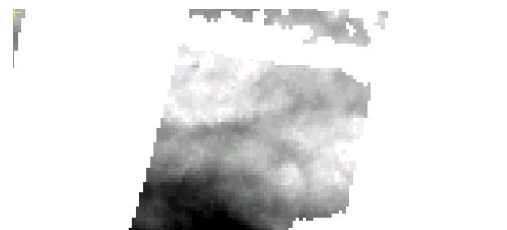


Figure 8.14d. water vapour image of the Timor Sea am 09 Mar 1999

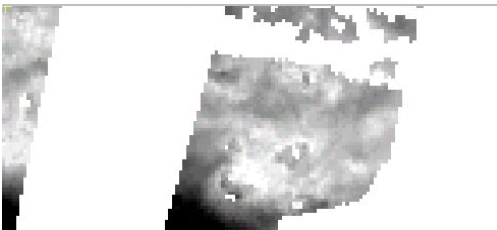


Figure 8.14e. water vapour image of the Timor Sea am 10 Mar 1999



Figure 8.14f. water vapour image of the Timor Sea am 11 Mar 1999

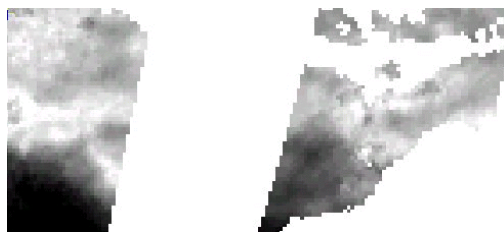


Figure 8.14g. water vapour image of the Timor Sea am 12 Mar 1999

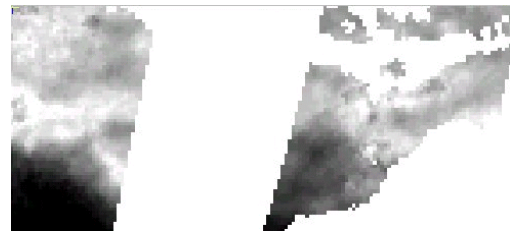


Figure 8.14h. water vapour image of the Timor Sea am 13 Mar 1999

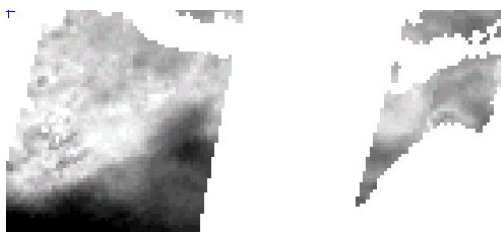


Figure 8.14i. water vapour image of the Timor Sea am 14 Mar 1999

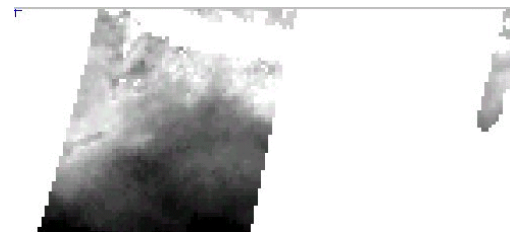


Figure 8.14j. water vapour image of the Timor Sea am 15 Mar 1999

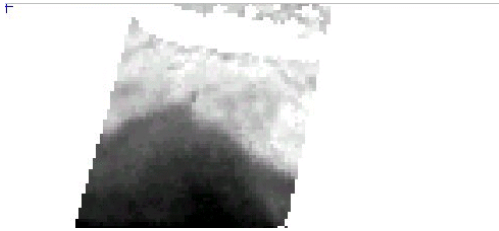


Figure 8.14k. water vapour image of the Timor Sea am 16 Mar 1999

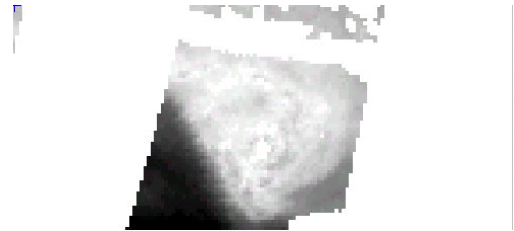


Figure 8.14l: water vapour image of the Timor Sea am 17 Mar 1999

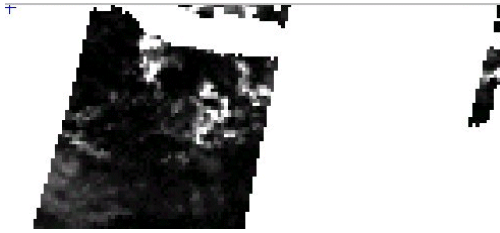


Figure 8.15a: liquid water image of the Timor Sea am 06 Mar 1999.

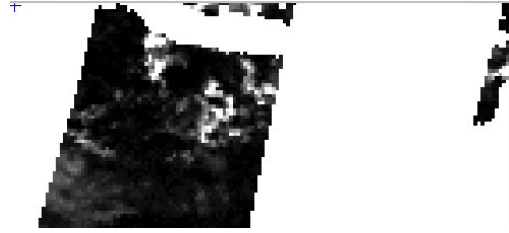


Figure 8.15b: liquid water image of the Timor Sea am 07 Mar 1999



Figure 8.15c: liquid water image of the Timor Sea am 08 Mar 1999

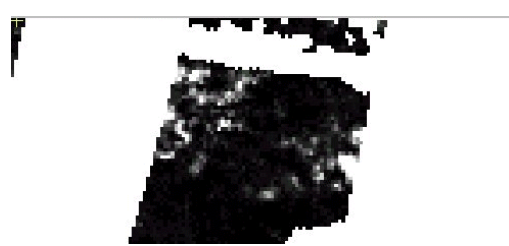


Figure 8.15d: liquid water image of the Timor Sea am 09 Mar 1999

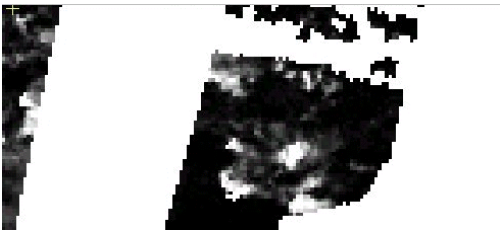


Figure 8.15e: liquid water image of the Timor Sea am 10 Mar 1999

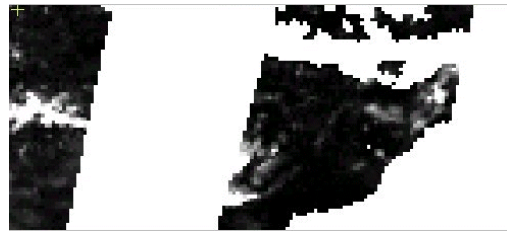


Figure 8.15f: liquid water image of the Timor Sea am 11 Mar 1999

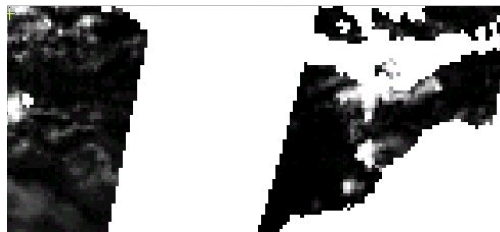


Figure 8.15g: liquid water image of the Timor Sea am 12 Mar 1999.

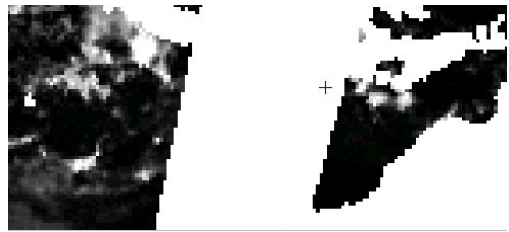


Figure 8.15h: liquid water image of the Timor Sea am 13 Mar 1999.



Figure 8.15i: liquid water image of the Timor Sea am 14 Mar 1999

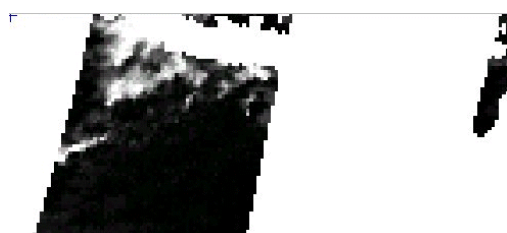


Figure 8.15j: liquid water image of the Timor Sea am 15 Mar 1999

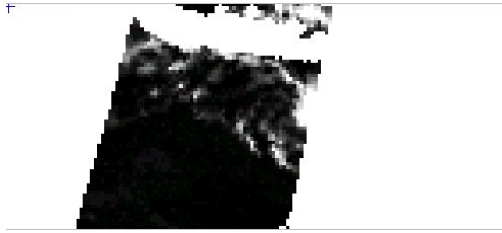


Figure 8.15k. liquid water image of the Timor Sea am 16 Mar 1999



Figure 8.15l: liquid water image of the timor Sea am 17 Mar 1999

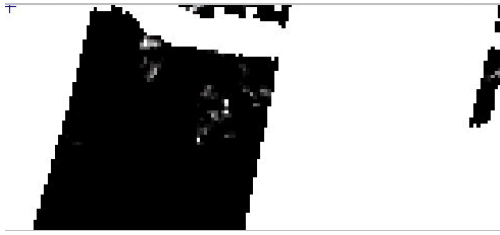


Figure 8.16a: Rainfall over the Timor Sea am 06 Mar 1999.

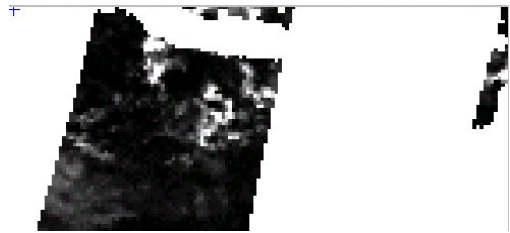


Figure 8.16b. Rainfall over the Timor Sea am 07 Mar 1999

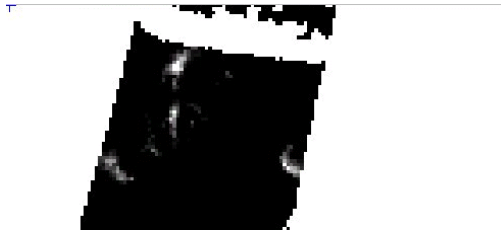


Figure 8.16c. Rainfall over the Timor Sea am 08 Mar 1999



Figure 8.16d. Rainfall over the Timor Sea am 09 Mar 1999



Figure 8.16e. Rainfall over the Timor Sea am 10 Mar 1999



Figure 8.16f. Rainfall over the Timor Sea am 11 Mar 1999



Figure 8.16g. Rainfall over the Timor Sea am 12 Mar 1999



Figure 8.16h. Rainfall over the Timor Sea am 13 Mar 1999



Figure 8.16i. Rainfall over the Timor Sea am 14 Mar 1999



Figure 8.16j. Rainfall over the Timor Sea am 15 Mar 1999



Figure 8.16k. Rainfall over the Timor Sea am 16 Mar 1999



Figure 8.16l: Rainfall over the Timor Sea am 17 Mar 1999

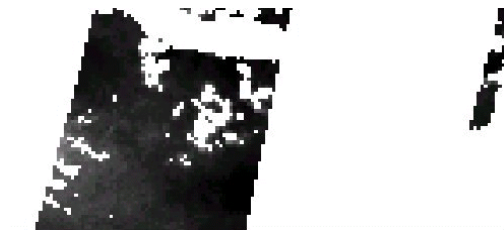


Figure 8.17a: Surface wind speed over the Timor Sea am 06 Mar 1999.



Figure 8.17b: Surface wind speed over the Timor Sea am 07 Mar 1999

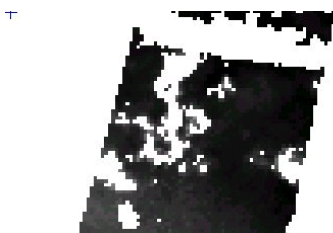


Figure 8.17c: Surface wind speed over the Timor Sea am 08 Mar 1999



Figure 8.17d: Surface wind speed over the Timor Sea am 09 Mar 1999



Figure 8.17e: Surface wind speed over the Timor Sea am 10 Mar 1999

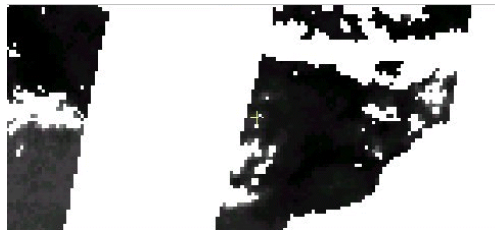


Figure 8.17f: Surface wind speed over the Timor Sea am 11 Mar 1999



Figure 8.17g: Surface wind speed over the Timor Sea am 12 Mar 1999



Figure 8.17h: Surface wind speed over the Timor Sea am 13 Mar 1999



Figure 8.17i: Surface wind speed over the Timor Sea am 14 Mar 1999

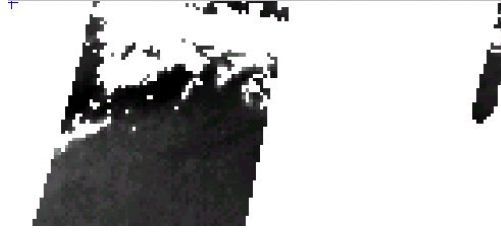


Figure 8.17j: Surface wind speed over the Timor Sea am 15 Mar 1999



Figure 8.17k. Surface wind speed over the Timor Sea am 16 Mar 1999



Figure 8.17l: Surface wind speed over the Timor Sea am 17 Mar 1999

8.3 Case 3. - TC “Isobel”

Tropical cyclone “Isobel” was named on 29th January 1996. Atmospheric conditions from the 19th January 1996 until naming are examined. This was actually the third time that the name was used. TC’s in 1974 and again in 1985 had the same name. Figure 8.18 shows the particular area of interest within the Timor Sea. The system was first identified on January 27th 1996 near 12.4°S 122.8°E (position marked “F” in figure 8.18) and was subsequently named when at 14.0°S 116.4°E on January 29th 1996 (position marked “N” in figure 8.18).

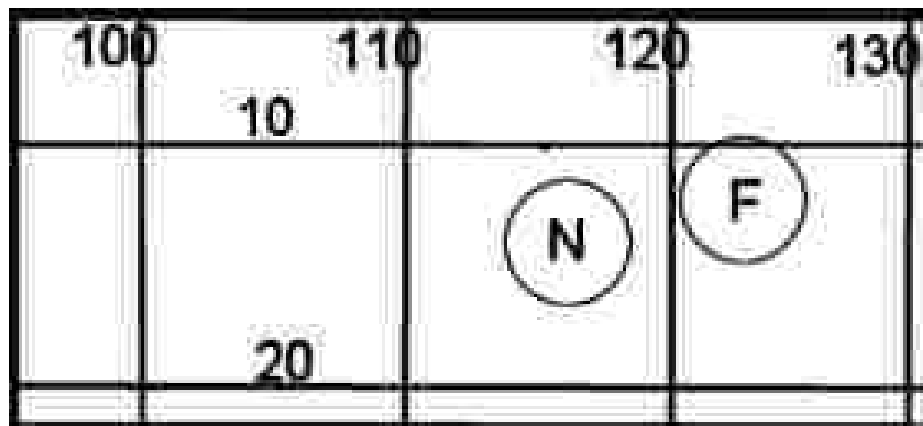


Figure 8.18: Map showing the location of the area where the system that became TC Isobel was first identified (marked F) and where it was eventually named (marked N).

Description of the imagery used in this case study is given in section 8.0. A brief description of the GMS IR satellite imagery is that the whiter the colour in the image, the colder the temperature at the top of the cloud, that is, the higher the cloud is in the atmosphere. Figure 8.3a gives the navigation for the GMS imagery. In the case of the USA DMSP imagery, the blacker the colour in the image the lower the value of the parameter being displayed. Calibration for the DMSP images are shown in figures 8.2 to 8.5 where scales for water vapour, liquid water, rainfall, and surface wind speed respectively are given along with sample images. Figures 8.3b and 8.18 give the navigation for each of the DMSP images. A full description of the DMSP imagery is given in section 7.1.1.

8.3.1 Antecedent Conditions

For the sake of this study, it was assumed that the atmosphere was in a “normal” or undisturbed state ten days before the system was named. In this case the pre existing conditions are set as 19th January 1996.

8.3.1.1 GMS Satellite imagery.

Satellite imagery relevant to this event are shown in figures 8.20a to 8.20u. Presented are the 00Z and the 12Z GMS IR images of the study area over the Timor Sea.

Satellite imagery on January 19th shows active thunderstorms over the Indonesian Archipelago. Over the Australian continent, diurnal thunderstorms are evident. During January 20th an area of thunderstorms drifts south from Indonesia to about 10°S latitude and even further south in the east of the study area. This activity persists for the next two days although with marked diurnal variation. By January 23rd two more concentrated areas of thunderstorm activity distill out of the general area of storms. One near 15°S, 100°E and the other near 10°S, 115°E longitude. These features both move west on January 24th and 25th. Diurnal thunderstorm activity persists over the Kimberley region of Western Australia. Of general interest is the solitary bore seen on the image 8.3.2n which is travelling out from thunderstorms which collapsed the previous night.

On January 26th a cloud cluster develops near 12°S 122°E which persists through the 27th and 28th while drifting slowly westwards. It is this system which was named TC “Isobel” at 0700Z on January 29th. It is interesting to note that there was marked suppression of convective activity over the Timor Sea on January 28th and 29th as the system developed.

8.3.1.2 Sea Surface temperatures

Sea surface temperatures are shown in figures 8.19a to 8.19c. As can be seen from the figures, SST's were in excess of 29°C for the entire period of interest. For the week leading up to January 21st the temperature reached 30°C in the genesis area. From January 21st to the 28th there appears to be a very slight cooling of 0.5°C or less. Given that SST are still well in excess of the limiting temperature of 26°C, this is of little consequence.

Hence SST is more than adequate for the formation of a tropical cyclone.

8.3.1.3 DMSP Satellite imagery

Table 8.9, below, shows a summary of the meteorological products collected by the USA DMSP satellite. In this case the particular satellite was DMSP 13. Viewing the passes as imaged in the figures below shows only too clearly the problem with polar orbiting satellites. In several cases the passes were such that the gap between coverage was right over the area of interest. In this case, data were taken from the edge of the From January 28th to the 30th there was a steady increase in all parameters being measured.

Water vapour values are shown in column three of table 8.9. Water vapour imagery for this event are shown at figures 8.21 a-j. Water vapour over the area of interest reflects the processes seen in the GMS IR imagery. Relatively low values of column water vapour at 43.8mm at the start of the period increase to 61.8mm on January 22nd as a thunderstorm cluster moves through the area. These values decrease as the system dissipates on January 24th. Water vapour values remain steady on January 24th, 25th and 26th before increasing on January 27th and further increasing until January 29th corresponding to the date when the system was named. Of general interest in the imagery is the decrease in moisture from the north to the south. This is consistent throughout the period. Also the dry air streaming off the Australian continent can be seen, particularly in figures 8.21d to 8.21j (the very dark area to the west of the

Australian continent). This causes a significant moisture gradient to the south of the developing system. If the drier air was ingested into the system it would have been a strong inhibitor to further growth of the cluster. Studying the wind fields, there is no evidence that drier air was advected into the system. This is confirmed by the relatively rapid increase in intensity once development started.

Integrated liquid water content in the area of interest is shown in table 8.9 at column four. Liquid water shows the same trend as does water vapour in that there is an increase from the start of the study period to January 22nd when values of 1.74 mm are reached. There is then a drop to 0.47 mm on January 25th which is consistent with the cloud activity becoming isolated over the area of interest. Varying values between January 23rd and the 27th are consistent with isolated thunderstorm activity over the study area. Liquid water imagery for this event is shown at figures 8.22 a-j. Liquid water content is a good analogy for cloud within an area. Early in the period there is a cloud band extending from about the centre of the left edge of the image (figure 8.22a) which dissipates over the next three days. For the remainder of the study period the southern parts of the area remain clear. In the north, significant amounts of liquid water content are evident near the Indonesian Archipelago throughout the period. Liquid water content increases in the area to the north of the Australian continent by the 25th and continued to increase until the end of the period, when the system was named. Over the last three days (January 27th to 29th), liquid water content increased in the western parts of the study area indicating a general increase in activity in the Timor Sea.

Rainfall is shown in table 8.9 at column five. This again shows the pattern of the thunderstorms moving through the area of interest. Rainfall peaks at 12.0 mm on January 21st and 22nd before decreasing to zero until January 26th. On January 27th and 28th there is a rapid increase in rainfall as the system becomes developed. Rainfall imagery for this event is shown at figures 8.23 a-j.

Surface wind speed is shown in table 8.9 at column two. This parameter shows the same features as the remainder of the data with an increase in wind speed to 10.8 m/sec on January 22nd and 13.7 m/sec on 23rd, before easing back to about 7 m/sec for a few days.

A marked increase takes place on January 27th and 28th. The wind recorded on the 28th is actually on the edge of a rain affected area and so is almost certainly higher nearer the system. Wind speed imagery is shown at figures 8.24 a-j.

Date (January 1996)	Surface Wind Speed (m/sec)	Water Vapour (mm)	Liquid water (mm)	Rainfall (mm/hr)
19	7.8	43.8	0.5	0.0
20	8.5	59.7	0.81	9.6
21	9.3	61.2	0.89	12.0
22	10.8	61.8	1.74	12.0
23	13.7	61.5	0.93	0.0
24	5.4	55.8	0.81	0.0
25	7.7	55.5	0.47	0.0
26	6.6	55.8	0.96	0.0
27	14.1	59.4	0.71	17.7
28	17.7	62.4	1.74	25.0
29	-	-	-	-
30				

Table 8.9: A comparison of maximum values of surface wind speed, columnar water vapour, cloud liquid water, and precipitation rate (rainfall) taken from DMSP 14 orbits over the study area between the 19th and 29th January 1996.

8.3.1.4 Model data

Model output data taken from the GASP runs relevant to this system development are shown at table 8.10. This table is in the same format as for case studies one (table 8.2) and two (table 8.6). As with the previous case studies, the data were taken from the model grid point nearest to the point of interest. Data were taken from the point nearest the “F” (12.4°S 122.8°E) in figure 8.18 until the system moved to the southeast and then the point was moved as necessary. The final data were taken from the grid point nearest the position marked “N” (14.0°S 116.4°E) in figure 8.18. The dates shown in table 8.10

have been adjusted to local time so as to make comparison with the satellite data easier. The model data are timed at 23Z on a date, which is 7 am local time the next morning. That is, 23Z on 18th January is 7 am Western Standard Time (WST) on the 19th January.

The temperatures at 850 hPa, 700 hPa and at 500 hPa are remarkably consistent. At the lower two levels, temperatures change by less than one degree (1°C) throughout the study period. At 500 hPa there is a rise of 1.8°C on January 23rd. Apart from that, there is no real changes in signal within the data supplied by the model. The 200 hPa temperature shows a slight but steady increase in temperature from January 18th when it was 218.9K to 221.4K on January 26th. There was marked cooling of 1.5K on January 27th and this persisted on January 28th.

The patterns in the 850 hPa humidity column of the table 8.10 show that humidity was generally within 5% of 70% RH from January 19th until January 23rd. There was a dramatic drop in humidity to 51%. This is somewhat surprising as there was a decrease in cloud cover over the Timor Sea the day before. By the 25th cloud had again increased in the area. Humidity did increase from January 25th to the 27th. There is an unexpected decrease in humidity on January 29th when the value dropped to 57%. Given that the TC was nearby and that there was a considerable amount of cloud in the vicinity, this is rather surprising. The humidity at 700 hPa shows a similar pattern except that the sudden drying out occurred on January 23rd.

Surface wind speed, as obtained from the DMSP satellite, remained below 10 m/sec apart from on January 22nd and 23rd until the 27th when the winds started to increase as the system developed. By the January 28th, winds were in excess of 17.5 m/sec. This, combined with the heavy rainfall implies that the cyclone may have been named a day late. Winds from the GASP model are somewhat ambivalent about the event. The 1000 hPa winds actually peak on January 27th at 14.8 m/sec in the vicinity of the system and decrease on January 28th to 6 m/sec in the vicinity of the system. 850 hPa winds from the GASP model show a slight increase in wind speed over the last four days of the study period, peaking at 16.6 m/sec on January 29th. Winds at 200 hPa from the GASP model show a slight but steady decrease over the last three days, which is not what

would be expected. As with the 1000 hPa winds, the 200 hPa winds actually peaked on January 27th. This would imply that the model started to get hold of the system, but unfortunately, somehow, lost it again at the vital time when it actually “took off”.

Vorticity can be calculated from the GASP wind fields, and was done for this event. As with the 1000, 850, and 200 hPa winds, there was a peak in vorticity at 850 hPa on the 27th at -5 s^{-1} . The vorticity then decreased until on the 29th when it was -0.3 s^{-1} .

Zehr’s parameter was also calculated for this event. This was inconclusive as there was no signal at all. The value remained at zero for the entire event.

Drawing together the points so far we can come to the following conclusions. The GMS satellite imagery showed a convectively active Timor Sea throughout the period. From this we can conclude that there was conditional instability over a large portion of the Timor Sea. This also signifies that moisture was being introduced through considerable depth over a large area. The DMSP imagery reflects the information in the GMS imagery in showing widespread moisture, both as vapour and as liquid. The surface winds from the DMSP show an interesting trend which was also seen in case studies one and two. There is a distinct drop in wind speed between about five and three days before the system is named. This would enable moisture to concentrate in an area rather than being vented by the winds. With increasing moisture would come increasing cloud and increasing thermal energy in the atmosphere. The rapid increase in Liquid water content and eventually in rainfall as the system finally develops would be as a consequence of this.

The GASP model data has a similar feature to the DMSP data in that there is a marked lull in wind speed through the period January 21st to 25th when the winds start to increase again. Unfortunately, the model appears to have lost the plot on January 28th and 29th when it indicated a decrease in activity in the vicinity rather the development of a tropical cyclone. The calculated values of vorticity and Zehr’s parameter showed no trend towards increasing activity just at the time that the system actually developed.

Looking at the rainfall and wind fields from the DMSP, one would have to come to the conclusion that the system was named a day late.

Date January 1996	850 Temp (K)	700 Temp (K)	500 Temp (K)	200 Temp (K)	850 RH (%)	700RH (%)	850 Wind (U, ms ⁻¹)	850 Wind (V, ms ⁻¹)	200 Wind (U, ms ⁻¹)	200 Wind (V ms ⁻¹)	Zehr's GP
19	290.9	282.4	267.4	218.9	70	71	-9.9	1.6	-12.2	3.6	0.0
20	290.6	282.9	267.9	219.1	66	64	-15.0	-0.9	-12.4	3.4	0.0
21	290.2	282.9	267.6	219.1	67	68	-6.2	-1.2	-16.4	0.7	0.0
22	291.3	282.8	266.6	219.8	64	68	-4.2	-1.2	-17.6	7.4	0.0
23	291.0	282.5	267.0	219.7	70	67	-9.7	-4.2	-16.6	2.2	0.0
24	290.4	282.8	268.8	220.1	76	44	-15.1	-0.1	-16.2	4.3	0.0
25	291.9	281.9	268.6	220.0	51	60	-7.2	1.1	-11.8	3.8	0.0
26	290.6	281.2	268.7	220.6	60	55	-10.5	-1.3	-12.4	3.3	0.0
27	290.5	281.5	268.7	221.4	65	67	-9.3	0.3	-19.0	0.8	0.0
28	290.7	282.0	268.6	219.9	70	52	-12.5	2.8	-15.0	2.9	0.0
29	290.3	282.2	268.5	219.9	57	22	-16.5	-2.1	-14.7	6.2	0.0

Table 8.10: Table showing information taken from the daily computer model (GASP) runs for TC Isobel and giving some of the key data which should show any changes in the environment.

8.3.1.5 Gray's Parameters

As has been mentioned several times previously, Gray's parameters are as follows;

- large values of low level vorticity,
- located at least a few degrees from the Equator (significant planetary vorticity),
- weak vertical shear in the horizontal winds,
- sea surface temperature at least 26C and a deep thermocline,
- conditional instability through a deep layer of the atmosphere, and
- high humidity levels in the lower and middle atmosphere.

The vorticity as calculated from the GASP model data is shown below at table 8.11. In the most part, values are low with the last few days of the study period being near zero. This is not what would be expected as a system increased in intensity. Typically, for such a system, one would expect vorticity to evolve from a background value depending on where the system was developing. Whether it was developing in the Equatorial trough or in the trade wind regime to the south of the Equatorial trough would determine the background vorticity. Given the low values of vorticity calculated and also the fact that the system did develop, it is reasonable to assume that the GASP model was not handling the wind fields very well. As a result, the vorticity field is not well formulated.

Date	20th	21st	22nd	23rd	24th	25th	26th	27th	28th	29th
value	-1.6	-0.1	-0.9	-2.2	-0.6	0.7	-0.2	0.5	0.1	-0.3

Table 8.11 Table showing vorticity at the computer grid point nearest to the development of TC Isobel. The value shown is in s^{-1} .

The system was first recognised at 12.4°S and later named at 14.0°S. These latitudes are sufficiently far from the equator to provide significant planetary vorticity. Figure 8.18 shows the location of these positions.

The next parameter discussed is weak vertical shear in the horizontal winds. The shear as calculated from the model data is shown below at table 8.12 Apart from January 22nd, the shear is always below 10 m/sec which is considered a limiting value above which development is not likely to occur.

Date	20th	21st	22nd	23rd	24th	25th	26th	27th	28th	29th
value	5.0	8.1	15.9	9.4	4.5	5.3	5.0	9.7	2.5	8.5

Table 8.12 Table showing vertical shear between 850hPa and 200hPa at the computer grid point nearest to the development of TC Isobel. The values shown are in knots.

SST's have been discussed in section 8.3.1.2. There is a question as to the depth of the warm water which can be inferred as being sufficiently deep to provide the energy required by the fact that the system eventually developed into a TC. This means then that the SST was more than adequate to provide the energy needed for the system to develop

Conditional instability through a deep layer is difficult to calculate given the mediocre performance of the GASP model. There is, however, considerable amounts of cloud in the area. This along with the organised convection that can be seen in the GMS satellite imagery (figures 8.20j-u) suggests that there was a deep layer of instability.

The question of humidity levels in the area can easily be seen in the satellite imagery. The GMS imagery (figures 8.20a-u) shows considerable amounts of cloud in the Timor Sea throughout the period. Humidity values as shown in tables 8.9 (DMSP data) and 8.10 (GASP data) show values compatible with TC development. The DMSP data are generally lower than the GASP humidity values and do not show the dramatic decrease in humidity on the 24th and 25th of January in the GASP model data. There is a slight decrease of only about 2% in the DMSP data compared with about 25% in the GASP data. Given the cloud and moisture values, there was more than adequate humidity for the system to develop.

8.3.2 Discussion

Satellite imagery of the target area shows that convection was active over the Indonesian Archipelago during the first eight days of the study. Only on January 28th and 29th did convective activity decline over the islands. Near the genesis point (marked “F” in figure 8.18), isolated thunderstorm activity persisted throughout the study period. On January 24th, convective activity increased in the vicinity of the genesis point, which continued on January 26th although showing a marked diurnal trend, peaking in the morning and decreasing by evening. On January 27th the system continued to drift westwards but showed less diurnal variation. This persisted through January 28th. On January 29th the system showed even more organisation and was in fact named on this day.

DMSP Microwave imagery of the Timor Sea (table 8.9) shows similar values to TC Tim for surface wind speed and water vapour. Liquid water content was highest in TC Isobel compared to either TC Tim or TC Elaine. Rainfall is also higher for TC Isobel than for the other two case studies. Of interest is the rainfall on January 20th, 21st, and 22nd as a cloud cluster developed in the vicinity of the genesis point, but did not continue developing. This is in fact consistent with the GMS IR satellite imagery which shows consistent cloud and convection in the area.

Temperatures at 850 hPa remain remarkable steady in the GASP model data. Apart from January 22nd to the 25th when temperatures rose by one degree, temperatures at 850 hPa were within 0.5 °C throughout the study period. Temperatures remain even more consistent at 700 hPa where they remain within 0.5 °C right through the study period. 500 hPa temperatures show consistency with the lower layers although there is an increase of nearly two degrees on January 24th. Temperatures very slowly decrease over the remainder of the period. At 200 hPa, temperatures very slowly increase from January 19th to the 24th before slowly decreasing over the remainder of the period. Given the consistency of the temperatures at 850 and 700 hPa and also the slow decrease in temperatures at 500 and 200 hPa over the last four days of the study, one could infer a slight destabilisation in the middle and upper atmosphere.

Surface wind speeds, as seen in table 8.9, were quite consistent at 8 to 10 m/sec throughout the period apart from on January 24th, 25th, and 26th when they dropped to approximately 6, 8, and 7 m/sec respectively. Winds then increase over the last two days as the system developed. The winds actually reached gale force (17.5 m/sec) on January 28th.

Winds at 850 hPa show a somewhat different pattern in being below 10 m/sec apart from on January 20th and on the 24th. On January 28th and 29th, winds increase as the system develops. The direction of the wind at 850 hPa was from the western quadrants throughout and mostly from the North West. This implies that the system was on the Northern side of the Equatorial trough. Winds at 200 hPa show general consistency although there is a decrease below 15 m/sec on the 25th and 26th of January. Wind directions at 200 hPa were even more consistent being from the South West quadrant throughout the period of interest. The clear inference of this is that the system developed to the south of the upper ridge and on the Eastern limb of an outflow within the ridge. This is a minor surprise as this author would have been looking at the western limb of an outflow and hence further to the east than this system actually developed.

The process of development could be explained as follows. A cloud cluster developed in the area early in the study period bringing moisture to the area. Winds however, increased probably venting the area and causing the system to dissipate. Winds and moisture generally decreased from the 23rd to the 24th of January, quite possibly allowing evaporation to increase moisture in the area. The very slight decrease in upper temperature would have allowed a slight increase in deep convection which would have further increased instability as the depth of the moisture increased. It already has been shown that all of Gray's parameters have been met for the development of this system. Zehr's ZDGP, derived from model data (see table 8.10), on the other hand remained at zero for the whole study time. This is most likely as a result of the GASP model not fully grasping the situation, although one would have expected to see some signal, at least on the last few days.

Zehr's development model suggests that there is development in two stages. If this was the case then, as happened for TC TIM, the time gap was very short, perhaps only a few hours. More likely, once the system started developing, the process was almost continuous, which is consistent with the Dvorak model.

In conclusion to the conclusion we can make the following points;

- The DMSP data showed system development from about day -3
- The GMS IR satellite imagery showed a convectively active Timor Sea which enabled potential for TC development over a wide area.
- The cloud system that eventually became TC Isobel was evident from about January 25th. It could be tracked on the GMS imagery slowly drifting westwards.
- The GASP model data showed a light wind regime about day -5, followed by a peak in activity at day -3. There after the model weakened the system.
- From the DMSP imagery one would have to conclude that the cyclone was named a day late.

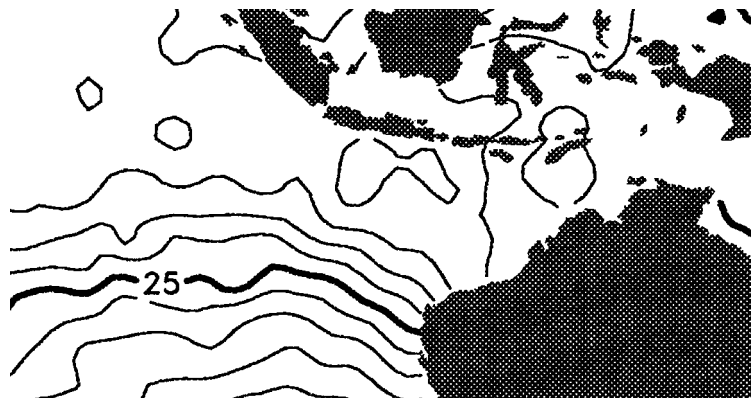


Figure 8.19a: Sea Surface Temperature for the week ending 14 Jan 1996. Taken from a product issued by the Darwin RSMC (Australian Bureau of Meteorology).



Figure 8.19b. Sea Surface Temperature for the week ending 21 Jan 1996. Taken from a product issued by the Darwin RSMC (Australian Bureau of Meteorology)

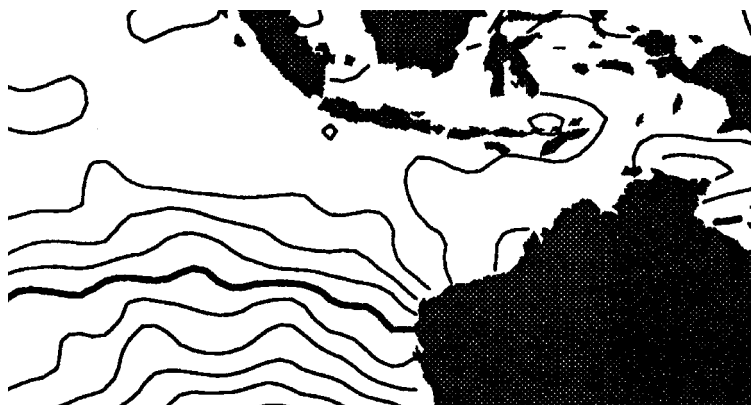


Figure 8.19c. Sea Surface Temperature for the week ending 28 Jan 1996. Taken from a product issued by the Darwin RSMC (Australian Bureau of Meteorology)

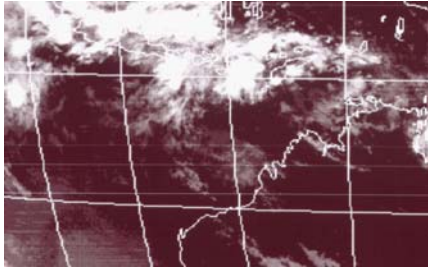


Figure 8.20a: GMS4 image of the Timor Sea 00Z 19 Jan 1996.

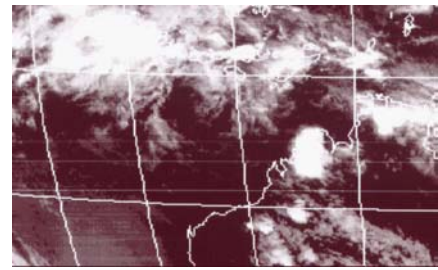


Figure 8.20b: GMS4 image of the Timor Sea 12Z 19 Jan 1996

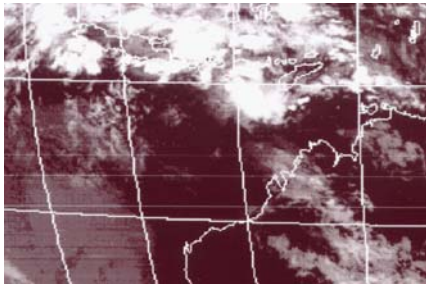


Figure 8.20c: GMS4 image of the Timor Sea 00Z 20 Jan 1996

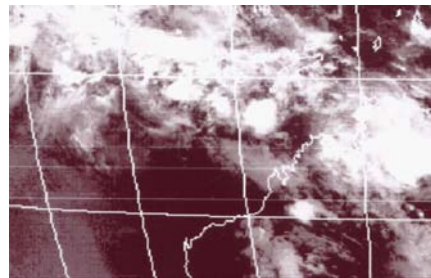


Figure 8.20d: GMS4 image of the Timor Sea 12Z 20 Jan 1996

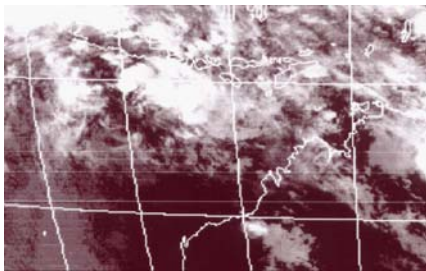


Figure 8.20e: GMS4 image of the Timor Sea 00Z 21 Jan 1996

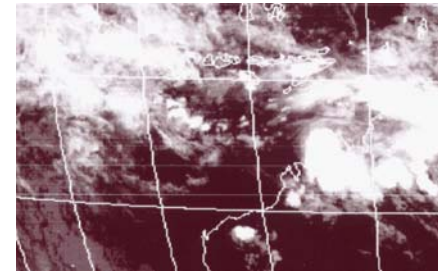


Figure 8.20f: GMS4 image of the Timor Sea 12Z 21 Jan 1996

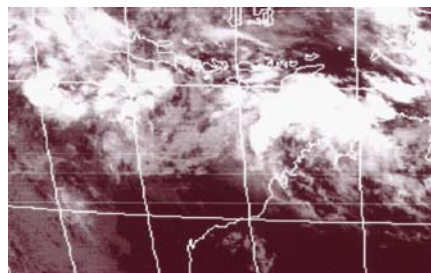


Figure 8.20g: GMS4 image of the Timor Sea 00Z 22 Jan 1996

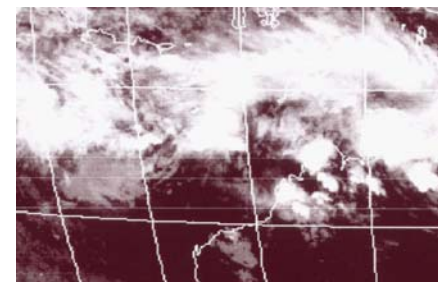


Figure 8.20h: GMS4 image of the Timor Sea 12Z 22 Jan 1996

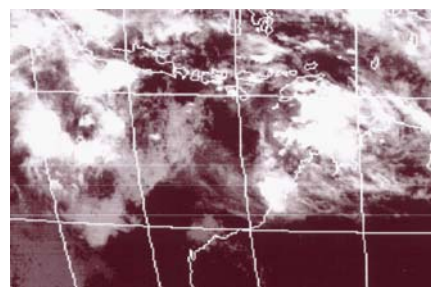


Figure 8.20i: GMS4 image of the Timor Sea 00Z 23 Jan 1996

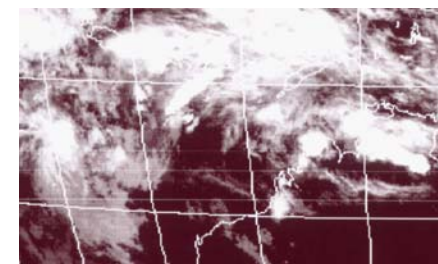


Figure 8.20j: GMS4 image of the Timor Sea 12Z 23 Jan 1996

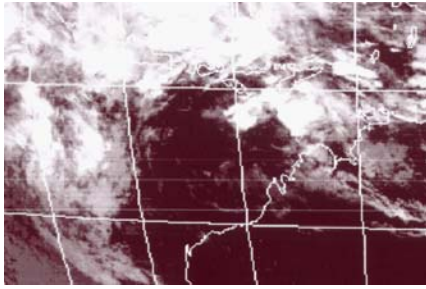


Figure 8.20k: GMS4 image of the Timor Sea 00Z 24 Jan 1996

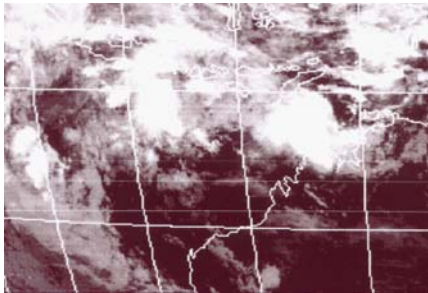


Figure 8.20m: GMS4 image of the Timor Sea 00Z 25 Jan 1996

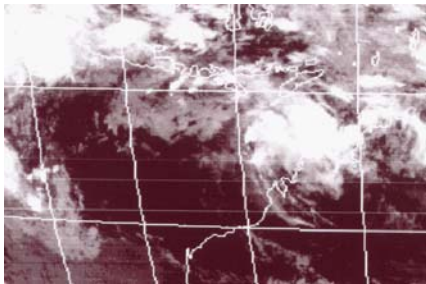


Figure 8.20o: GMS4 image of the Timor Sea 00Z 26 Jan 1996

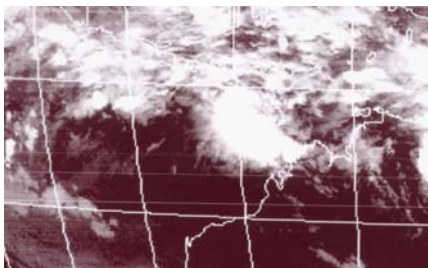


Figure 8.20q: GMS4 image of the Timor Sea 00Z 27 Jan 1996

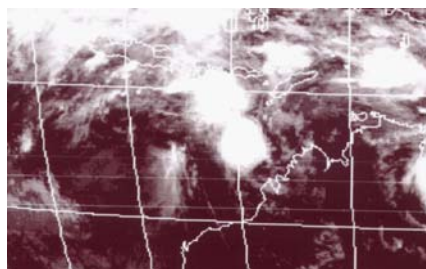


Figure 8.20s: GMS4 image of the Timor Sea 00Z 28 Jan 1996

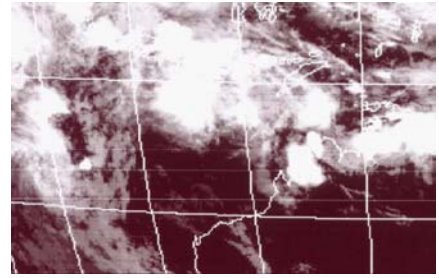


Figure 8.20l: GMS4 image of the Timor Sea 12Z 24 Jan 1996

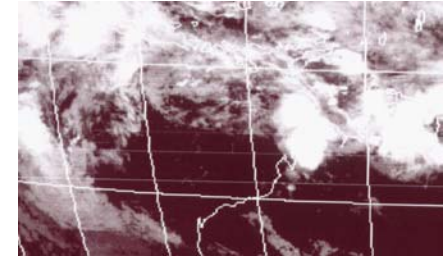


Figure 8.20n: GMS4 image of the Timor Sea 12Z 25 Jan 1996

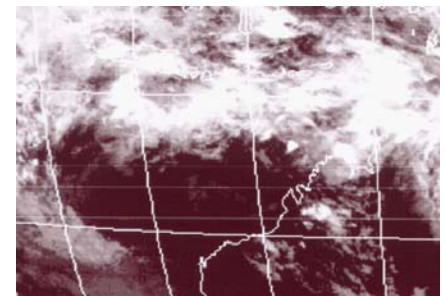


Figure 8.20p: GMS4 image of the Timor Sea 12Z 26 Jan 1996

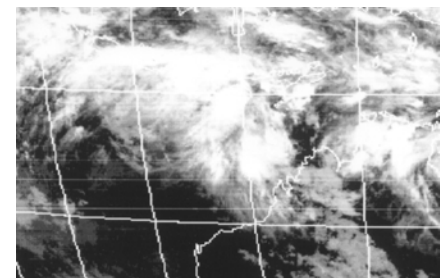


Figure 8.20r: GMS4 image of the Timor Sea 12Z 27 Jan 1996

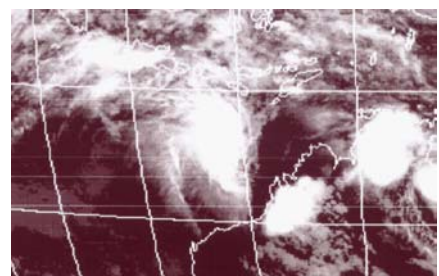


Figure 8.20t: GMS4 image of the Timor Sea 12Z 28 Jan 1996

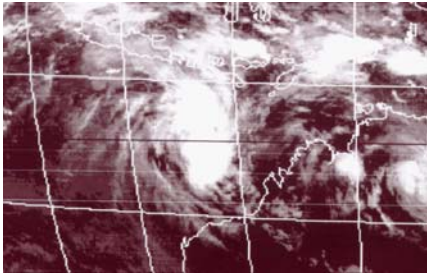


Figure 8.20u: GMS4 image of the Timor Sea 00Z 29 Jan 1996

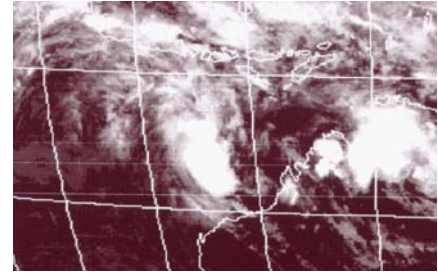


Figure 8.20v: GMS4 image of the Timor Sea 12Z 29 Jan 1996

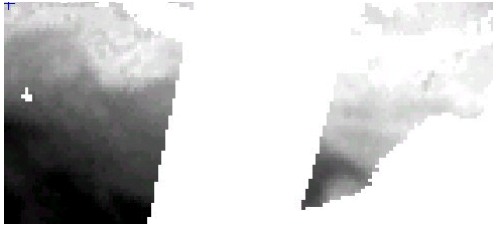


Figure 8.21a: Water Vapour image of the Timor Sea am 20 Jan 1996.

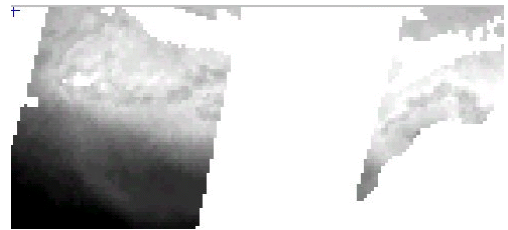


Figure 8.21b: Water Vapour image of the Timor Sea am 21 Jan 1996

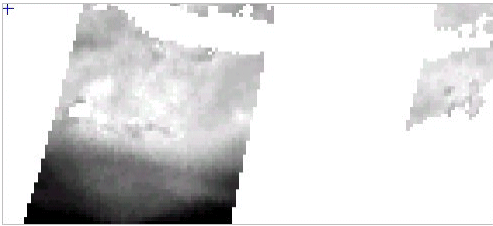


Figure 8.21c: Water Vapour image of the Timor Sea am 22 Jan 1996

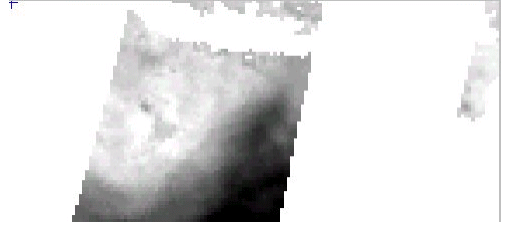


Figure 8.21d: Water Vapour image of the Timor Sea am 23 Jan 1996

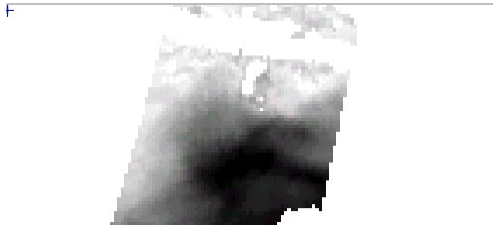


Figure 8.21e: Water Vapour image of the Timor Sea am 24 Jan 1996



Figure 8.21f: Water Vapour image of the Timor Sea am 25 Jan 1996

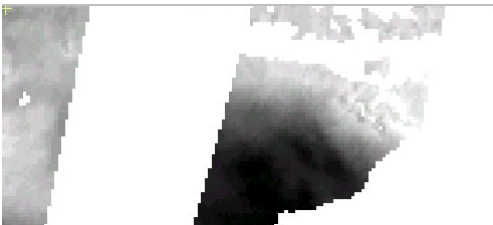


Figure 8.21g: Water Vapour image of the Timor Sea am 26 Jan 1996

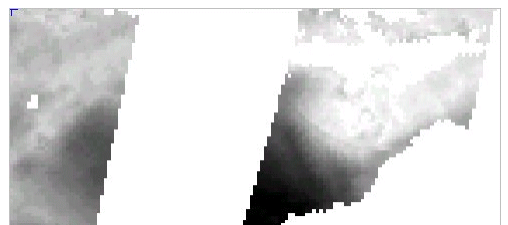


Figure 8.21h: Water Vapour image of the Timor Sea am 27 Jan 1996



Figure 8.21i: Water Vapour image of the Timor Sea am 28 Jan 1996



Figure 8.21j: Water Vapour image of the Timor Sea am 29 Jan 1996

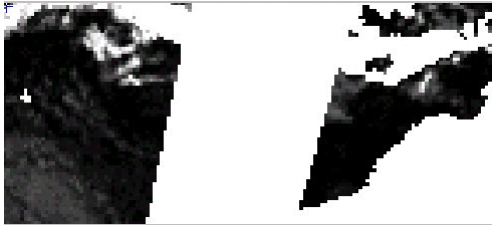


Figure 8.22a: Liquid Water content over the Timor Sea am 20 Jan 1996.

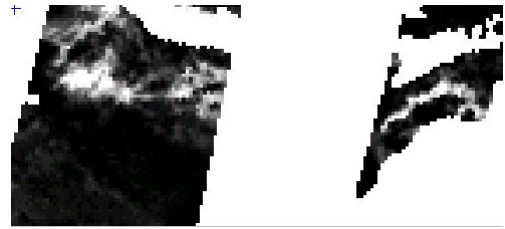


Figure 8.22b: Liquid Water content over the Timor Sea am 21 Jan 1996



Figure 8.22c: Liquid Water content over the Timor Sea am 22 Jan 1996



Figure 8.22d: Liquid Water content over the Timor Sea am 23 Jan 1996



Figure 8.22e: Liquid Water content over the Timor Sea am 24 Jan 1996



Figure 8.22f: Liquid Water content over the Timor Sea am 25 Jan 1996



Figure 8.22g: Liquid Water content over the Timor Sea am 26 Jan 1996



Figure 8.22h: Liquid Water content over the Timor Sea am 27 Jan 1996

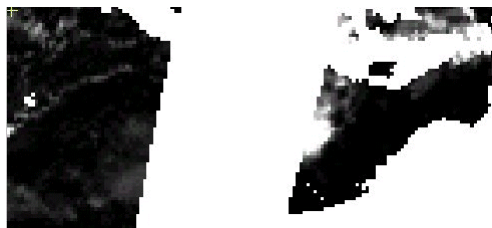


Figure 8.22i: Liquid Water content over the Timor Sea am 28 Jan 1996



Figure 8.22j: Liquid Water content over the Timor Sea am 29 Jan 1996



Figure 8.23a: Rainfall over the Timor Sea am 20 Jan 1996.



Figure 8.23b: Rainfall over the Timor Sea am 21 Jan 1996



Figure 8.23c: Rainfall over the Timor Sea am 22 Jan 1996

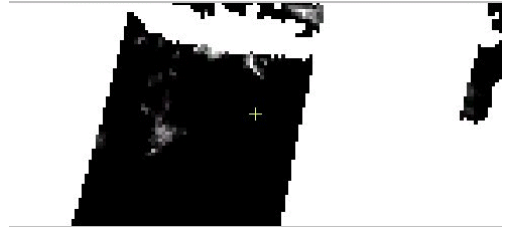


Figure 8.23d: Rainfall over the Timor Sea am 23 Jan 1996



Figure 8.23e: Rainfall over the Timor Sea am 24 Jan 1996

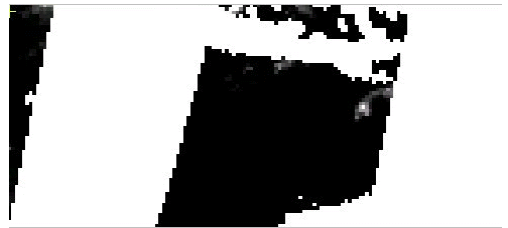


Figure 8.23f: Rainfall over the Timor Sea am 25 Jan 1996



Figure 8.23g: Rainfall over the Timor Sea am 26 Jan 1996



Figure 8.23h: Rainfall over the Timor Sea am 27 Jan 1996

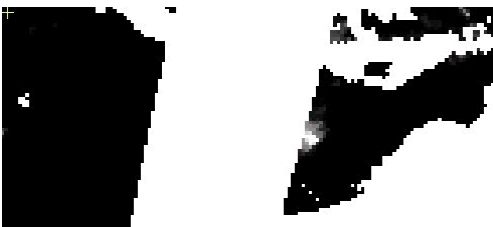


Figure 8.23i: Rainfall over the Timor Sea am 28 Jan 1996



Figure 8.23j: Rainfall over the Timor Sea am 29 Jan 1996



Figure 8.24a: Surface wind speed over the Timor Sea am 20 Jan 1996.



Figure 8.24b: Surface wind speed over the Timor Sea am 21 Jan 1996



Figure 8.24c: Surface wind speed over the Timor Sea am 22 Jan 1996



Figure 8.24d: Surface wind speed over the Timor Sea am 23 Jan 1996



Figure 8.24e: Surface wind speed over the Timor Sea am 24 Jan 1996

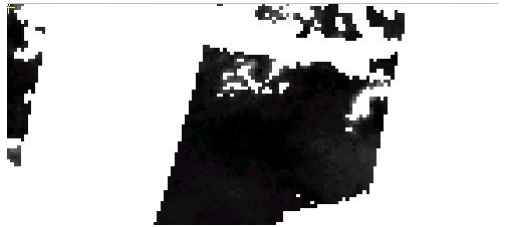


Figure 8.24f: Surface wind speed over the Timor Sea am 25 Jan 1996

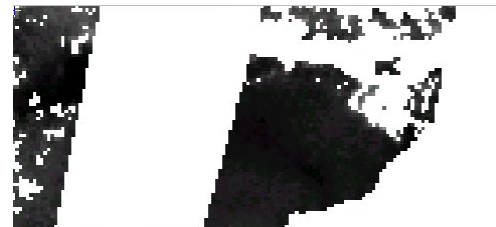


Figure 8.24g: Surface wind speed over the Timor Sea am 26 Jan 1996



Figure 8.24h: Surface wind speed over the Timor Sea am 27 Jan 1996



Figure 8.24i: Surface wind speed over the Timor Sea am 28 Jan 1996

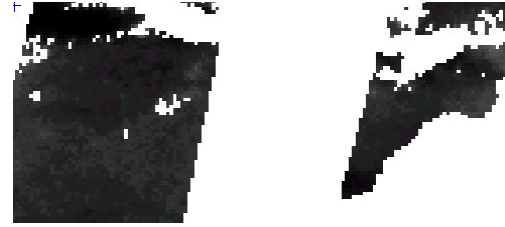


Figure 8.24j: Surface wind speed over the Timor Sea am 29 Jan 1996

8.4 Discussion of the case studies

Having studied three cyclones (TC Tim, TC Elaine, and TC Isobel), the threads will now be drawn together. In this section discussion will address the common themes, as well as a comparison between the systems. In each of the following tables, data has been reproduced from the relevant case study so that comparison or differences may be more easily seen.

An emphasis of the research to date has examined the well established, necessary but not sufficient conditions for tropical cyclogenesis. The approach adopted here is to identify either direct measures or surrogates for these criteria from measurements made by space-based sensors. In that the appropriate data sources are drawn from different satellite sensors, the task of image handling and gridding of data to a reference system has comprised a significant component of the activity.

A system is developed which could be automated in an image handling software package for monitoring the potential for development of a system

8.4.1 Comparison of the three case studies

We start by comparing each of the parameters studied separately in the case studies (see earlier). In the review which follows, case 1, 2 and 3 refer to TC systems Tim, Elaine and Isobel respectively

An interesting pattern occurs when the data are set out in the following comparative tables (tables 8.13 to 8.18 inclusive). Tables 8.13 to 8.16 relate to data from satellite observations and tables 8.17 and 8.18 are from the GASP model. At about three to four days before a system was named (day 0 in the following tables), there was a distinct decrease in many of the parameters.

The wind field in the vicinity of each of the systems are shown in table 8.13. In this table it can be seen that for the first four days (marked day -10 to day -7 in the table) of

each study period, winds were reasonably steady. Winds then decreased until about day -4 when a minimum in surface wind speed occurred. After the minimum, there was an increase in wind speed the next day followed by a slight decrease the following day for each of the case studies. Subsequently, winds increased as the system really started to develop, reaching gale force about the time of naming. The day of minimum wind speed is marked (in a light stipple shading) for each case.

Case	day -10	day -9	day -8	day -7	day -6	day -5	day -4	day -3	day -2	day -1	day 0
1	7.5	7.5	11.5	9.3	6.6	4.2	3	11.3	9.5	13.2	19.8
2	2.9	3	3.3	4.5	3.2	3.5	2.6	4.1	3.8	6.1	11.7
3	7.8	8.5	9.3	10.8	13.7	5.4	7.7	6.6	14.1	17.7	-

Table 8.13: Table comparing surface winds between the three case studies.

Looking next at the water vapour imagery, we see a similar pattern to that for the surface wind speed, shown above. Table 8.14 shows the comparison between the three case studies for water vapour. Reading table 8.14 shows that water vapour figures were somewhat variable although there appears to be maxima at about day -7 followed by a decrease approximately until day -4. From then on, water vapour increased as the systems developed into cyclones. The amount of the decrease to the minima is different for each case with TC Isobel (case 3) having the least obvious decrease. Again, the minima in water vapour are identified in table 8.14 (light stippled shading).

Case	day -10	day -9	day -8	day -7	day -6	day -5	day -4	day -3	day -2	day -1	day 0
1	48	30	33.9	33.3	53.1	59.4	54	52.8	57	49.5	60.3
2	59.1	57.3	63	62.4	54	54.9	48.6	57	48.6	75	75
3	43.8	59.7	61.2	61.8	61.5	55.8	55.5	55.8	59.4	62.4	-

Table 8.14: Table comparing water vapour content between the three case studies.

Liquid water content is presented in table 8.15. For this parameter, the changes are not so evident. In the case of TC Tim (case 1) there was very little cloud and hence little liquid water content until about three days before the system started to develop. For TCs Elaine (case 2) and Isobel (case 3) there was some cloud in the area and consequently detectable levels of liquid water. They do show a decrease to a minimum value at day-4 before an increase as the systems start to develop. The minimum values in table 8.15 are marked with shading.

Case	day -10	day -9	day -8	day -7	day -6	day -5	day -4	day -3	day -2	day -1	day 0
1	0.1	0	0	0.1	0	0	0	0.32	0.61	0.72	0.9
2	0.9	1.2	1.2	0.3	0	0.3	0	0	0.2	0.5	1.7
3	0.5	0.81	0.89	1.74	0.93	0.81	0.47	0.96	0.71	1.74	-

Table 8.15: Table comparing Liquid water content between the three case studies.

As would be expected, rainfall shows very little signature until the systems actually start to develop. A comparison of the rainfall for the three case studies is shown at table 8.16. In the case of TCs Elaine and Isobel rainfall between days -9 and day -7 were associated with separate events and not the system that developed into the cyclones. The stippled values at day -3, in this case, represent the start of the rainfall that was associated with the systems that eventually became the cyclones.

Case	day -10	day -9	day -8	day -7	day -6	day -5	day -4	day -3	day -2	day -1	day 0
1	0	0	0	0	0	0	0	0	7.7	25	25
2	0	8.8	0.3	0.3	0	0	0	0	0	9.6	15.4
3	0	9.6	12	12	0	0	0	0	17.7	25	-

Table 8.16: Table comparing rainfall between the three case studies.

The data comparisons which follow relate to information obtained from the Bureau of Meteorology's GASP model and was separately presented earlier in sections 8.1 to 8.3 inclusive.

Winds at 850 hPa for the three case studies are shown at table 8.17. The u-field and the v-fields are shown separately in this table as they were taken from the GASP model data. TCs Elaine and Isobel (case 2 and 3 respectively) show quite similar patterns with light winds throughout the period until the actual system started to develop. The winds for TC Tim (case 1) are more complicated although there is still a lull in the winds at about three days before the system was named. It is interesting to note that there is a small lull in the winds at four days before the naming (five days for TC Tim), but the most significant lull is in fact just the day before each system was named. The initial lull is at the same stage that each of the other parameters (discussed above) reach minima, but in this case, the winds had the most significant lull three days later (ie day -1). Again the minimum values in table 8.17 are marked with shading.

Case	day -10	day -9	day -8	day -7	day -6	day -5	day -4	day -3	day -2	day -1	day 0
1,u	-	-1.7	-8.3	-10.1	-5.6	-4.8	-7.5	-2.3	0.7	-2.4	-6.0
2,u	4.7	1.8	-1	-3.2	-3	-1.4	-5	-4.3	-4.1	-6.9	-8.3
3,u	-9.9	-15	-6	-4.2	-9.7	-15	-7	-11	-9.3	-13	-17
1,v	-	3.1	1.0	1.1	-0.3	1.4	-1.0	-3.8	-4.6	-5.6	4.4
2,v	2	2.9	2.1	0.8	-1.7	-2.9	-1	0.4	-0.4	-2.3	3
3,v	1.6	-0.9	-1	-1.2	-4.2	-0.1	1.1	-1.3	0.3	2.8	-2.1

Table 8.17: Table comparing 850 hPa winds from the GASP model for the three case studies. The hyphens in day -10 represent missing data. In the column marked Case, the case number and the type of field are given. For example 2,v represents the v field for case study 2 (TC Elaine).

The winds at 200 hPa show a remarkably similar pattern to those at 850 hPa. There is a small lull at day -4 (for cases 2 and 3, day -5 for case 1), but again the day with generally the light winds is in fact at day -1. A comparison of the winds at 200 hPa for the three case studies is shown at table 8.18.

Case	day -10	day -9	day -8	day -7	day -6	day -5	day -4	day -3	day -2	day -1	day 0
1,u	-	-1.6	2.4	0.2	-4.4	-2.7	0.2	2.0	2.9	5.5	1.5
2,u	-13	-10	-10	-9	-9.3	-1.7	-7.2	-3.1	0	-1.7	-7.1
3,u	-12	-12	-16	-18	-17	-16	-12	-12	-19	-15	-15
1,v	-	3.0	5.4	8.6	7.4	1.3	-7.8	-0.3	1.1	7.0	2.1
2,v	4	3.4	4	1.1	3	-0.8	-0.1	-1.1	2.1	7	2.1
3,v	3.6	3.4	0.7	7.4	2.2	4.3	3.8	3.3	0.8	2.9	6.2

Table 8.18: Table comparing 200 hPa winds from the GASP model for the three case studies. The hyphens on day -10 are missing data. In the column marked Case, the case number and the type of field are given. For example 3,u represents the u field for case study 3 (TC Isobel).

By comparing the satellite derived parameters for each of the case studies, a consistent pattern has emerged. For each parameter there was a minimum in the value at about day -4 followed by an increase toward values at which the cyclone was eventually named.

8.5 A Proposed Index for using satellite imagery to monitor cyclone development.

With the increasing amount of satellite data becoming available, it is becoming more difficult to efficiently manage those data. It is also becoming more difficult to effectively analyze the enormous amounts of information. The encouraging aspect is that computer power has increased dramatically in recent years. This increased capacity means that it is now possible to develop automated analysis systems for satellite data, even on desk top systems. It is now possible to integrate several separate sets of information into one useful screen for efficient analysis. Even with automated systems, there is a need to output the results of the analysis in a form that is readily understandable by those that are required to use the information. Software systems such as McIDAS (Suomi, 1983) are ideal for this type of data handling.

In the section of the dissertation that follows I propose a system to demonstrate the desirability for automatically combining appropriate satellite data sets into an index for monitoring the development of tropical systems.

8.5.1 Background

In recent years there has been a trend towards multi-skilling of personnel, with the sometimes unfortunate side effect of a loss of specialization. For example, an offshore oil rig may have engineers and technicians running the operations centre. They will, inevitably, make decisions based on meteorological information. Increasingly, they are expecting not only the final products, but to be able to inspect the data on which a meteorologist made his decision. Because many work places are multi disciplinary, decision making has taken on a whole new process. To be able to present meteorological information in such an environment is becoming more important. Ideally, operators who seek to use meteorological information without doubt would find it beneficial to have a decision support system associated with the actual observational data. We investigate this further below.

It is a reasonably easy process to overlay multiple data sets on a computer screen so that simultaneous views can be compared. However, it is not so easy to interpret a view that has several sets of data on a screen at the same time, particularly when the data comprises physically distinct variables. To this extent it becomes useful to combine sets of data into an index which is more easily interpreted by specialist and non-specialist alike.

Such an index would ultimately would need to be tested and refined over time. A high level of confidence would need to be established in such an index before it was promoted to users. With this in mind, the following index is proposed. For want of a name, this author will call it the “Hamilton Index” (HI). The raw data for this index are products from microwave satellite series DMSP. In future, other data sets could be included, such as the Radarsat or Quikscat scatterometer winds. Water vapour imagery from geostationary satellites or even IR imagery could be included in the set. Rainfall from the TRIM series of satellites could also be included.

At this stage, it is envisaged that the index would be calculated at all grid points within an area of interest (eg over the Timor Sea) and then overlaid on a VIS or IR satellite image so as to gain maximum benefit from the spatial structure of the physical information.

8.5.2 The Index

8.5.2.1 Implementation of the index

Using DMSP data we have fields of water vapour, liquid water content, rainfall and surface wind speed. These parameters can be combined in the following formula to provide a product which itself may be displayed on a computer screen. The proposal is that the spatial field of this index will indicate the state of development of a system. Examination of time sequential fields of this index would update the situation. As mentioned earlier, the index is called the Hamilton Index (HI). The formula is calculated by deriving a score based on the raw value of the particular parameters. Use of the

formula and associated index might suggest normalisation of the individual parameters as a means of obtaining a reasonably small but significant value for the index (van Burgel, personal communication).

A question arises as to how such disparate pieces of data, as are measured by the DMSP and other satellites, may be combined to produce a product which will give a reliable and easily interpretable product able to show the state of activity in the tropical atmosphere. In this case it was decided to use the products that were available from the DMSP satellites as the basis of an index. With the advent of newer generation satellites, similar products will become available meaning that it would be possible to generate a product more often than twice per day. How then does one include surface wind speed, water vapour, liquid water content, and rainfall into an index that would indicate the degree to which a system is developing?

The inclusion of surface wind speed in an index is somewhat problematical in that the prime measure of a system having become a cyclone is that wind speed have reached 17.5 m/sec around the core of it. Wind speed by itself is not an adequate measure of a cyclone having developed. It is possible to get gale force, or near gale force winds in the tropics without there being a TC. A surge in the trade winds can reach near gale force. Winds around a monsoonal low can be gale force. In other circumstances it is possible to have an active system with light winds near the surface. Hence there can be significant moisture with little wind.

Moisture in the atmosphere is a measure the vertical motion taking place in the atmosphere. Liquid water content is a good measure of the amount of cloud while rainfall indicates strong convection. For any given system, it would be reasonable to assume that water vapour would extend over a greater area than that of the liquid water, which in itself would have greater extent than the area of rainfall. Thus one would expect to find the area of rainfall within the area of liquid water with would be within the area of increased moisture. Any index using these parameters would exhibit a “bulls eye” type pattern in showing an active system.

Briefly, the method was to ascertain how closely related each of the parameters were related to each other. Clearly Liquid water content and rainfall are closely associated. High water vapour content can exist over large areas without there being any cloud. Wind speed can also be caused by features not necessarily associated with the system of interest. It is possible to have high wind speed but little moisture in a region. The addition of SST was considered carefully before inclusion. While not measured by DMSP, it is easily obtainable and is particularly significant in that it is the primary source of energy for a TC.

The relationship between SST and Rainfall came as a mild surprise to this author. He would have expected it to be more or less exponential, however as figure 8.25 shows, for temperatures above about 25°C, it is linear (with apologies to the author of the diagram, after this author scanned it, he could not find it again to source a reference)

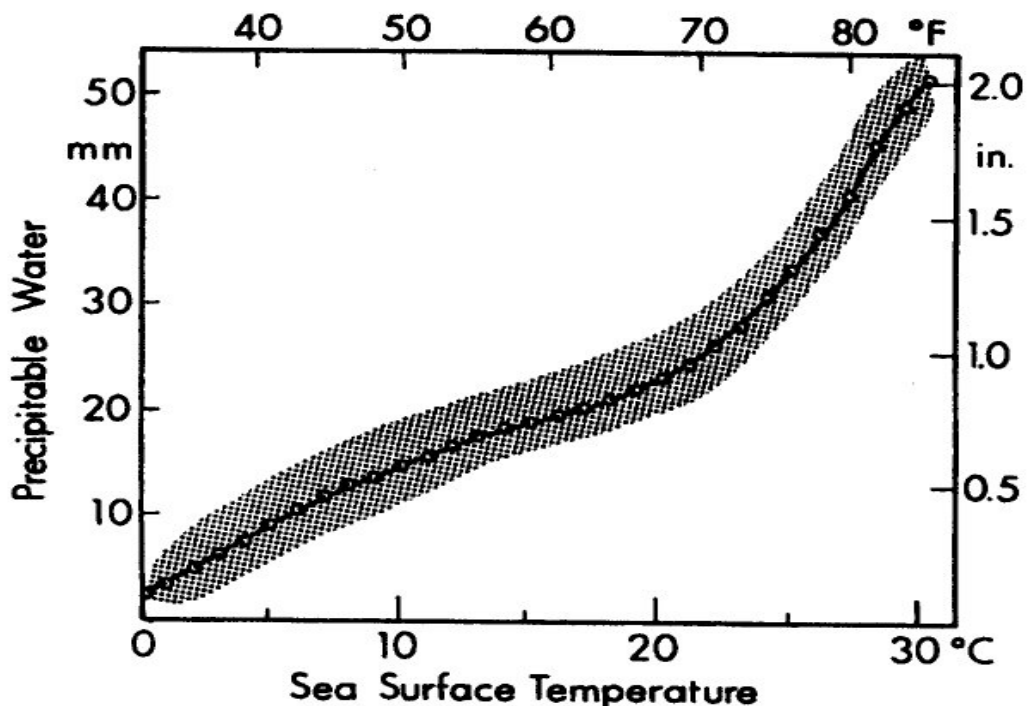


Figure 8.25: Relationship between sea surface temperature and precipitable water. Note the linear relationship above 25°C

Since precipitable water is very closely related to rainfall, and there is a linear relationship between this and SST, then rainfall and SST would have a close relationship.

In psuedocode the index is best described by,

$$\begin{aligned} \text{HI} = & \text{ ((If sst } \# \text{ 26}^\circ\text{C then HI} = 0) \\ & \text{ else HI} = (\text{wv} * (\text{lw} + \text{ra} + \text{sst}) * \text{ws}) \end{aligned} \quad (8.1)$$

where;

wv = water vapour (mm),

lw = liquid water (mm),

ra = rainfall (mm/hr),

sst = sea surface temperature ($^\circ\text{C}$), and

ws = surface wind speed (m/sec)

This psuedo code is clearly using mixed units. This is adjusted for by applying dimensional weighting factors. At this stage we will also apply a restriction on the index that SST be at least 26°C . It is now possible to develop a formula as follows,

$$\text{HI} = ((a * \text{wv}) * ((b * \text{lw}) + (c * \text{ra}) + (d * \text{sst})) * (e * \text{ws})) \quad (8.2)$$

where the units for each of the weighting factors is,

a (mm^{-1})

b (mm^{-1})

c ($\text{mm}^{-1} * \text{hr}$)

d ($^\circ\text{C}^{-1}$)

e ($\text{m}^{-1} * \text{sec}$)

until further case studies are undertaken, it is convenient to set the numerical value of each of the dimensional weighting factors at one (1).

In order to get the score value the following table is used. Eventually, when sufficient case studies have been undertaken, normalised values for each parameter could be inserted into the formula (equation 8.2) to generate the HI.

Score	wv (mm)	lw (mm)	ra (mm/hr)	ws (m/sec)	sst (°C)
0.5	# 45	0	0	# 5	# 27
1	# 55	# 1.0	# 5	# 10	# 28
2	# 65	# 2.0	# 15	# 15	# 29
3	# 74	# 3.6	# 24	# 17.4	# 30
4	75	3.7	25	\$ 17.5	\$ 31

Table 8.19: The look-up table to obtain the score values for inserting into the formula used to derive the Hamilton Index.

8.5.2.2 Rules for use with the formula

As with any formula there are circumstances as to when and where it is appropriate to use it. For this formula the following situations are appropriate for its use.

- This index is only applicable for environments where SST is at least 26°C.
- DMSP (or appropriate substitute imagery) satellite and data are available.
- The index is to be averaged over an appropriate area.
- For each parameter, find the appropriate range and then take the score from the left column (in table 8.19) to insert into the formula (equation 8.2). For example, a rainfall value of 12 mm/hr would give a score of 2.
- Calculate the index using all of the scores (in equation 8.2).

An example would be as follows,

Parameter	Value	Score
wv (mm)	68	3
lw (mm)	2.7	3
ra (mm/hr)	8	2
ws (m/sec)	5	0.5
sst (°C)	31	4
HI		13.5

Table 8.20: Example showing how to use table 8.19 to obtain a score for each parameter. These scores are then inserted into equation 8.1 to derive the Hamilton Index (HI).

Applying the values above lead to the following situation, remembering that the dimensional factors are set to one.

$$HI = (3 * (3 + 2 + 4) * 0.5) = 13.5$$

If part of the satellite scene contained a variables that were saturated then we would derive a maximum value for the index which would be as follows;

$$HI = (4 * (4 + 4 + 4) * 4) = 192$$

Similarly, the minimum value for the index would be

$$HI = (0.5 * (0.5 + 0.5 + 0.5) * 0.5) = 0.375$$

which rounds to an integer value of zero.

8.5.3 Potential usage

Such a formula has potential value in any circumstance where monitoring of the tropical environment is essential. For example, offshore oil rigs have a vital interest in the meteorology within a large radius, typically four days (or more if they could obtain it).

Even for onshore activities, information concerning the possible development of a TC in an area likely to subsequently make a landfall in the vicinity of the operation, is essential.

If the value of this product or a similar product was established then it would seem probable that there are two possible ways that this formula could be used. Organisations such as the Australian Bureau of Meteorology could easily produce a product at regular intervals which could then be directed to a web site for general consumption or, using a password, made available initially to a restricted client user base. Given the degree of value adding that is required in producing a product using this formula, another use would be to supply the product in a user pays situation where companies involved in weather sensitive operations could purchase the product as a part of a package of weather services.

The benefit of this type of product is that non-specialist operators can analyse the product with little training, allowing them to either make their own decisions, or to have greater confidence in decision making by meteorological professionals. The prime use of a product, such as would be produced using this formula, is that it is in principle potentially an excellent alerting mechanism as to meteorological activity within an area of interest. Daily monitoring of a system would show whether a severe situation is likely to continue developing or not.

8.5.4 Example using the case studies

When the data from the three case studies are used as input to the HI (equation 8.2), and then presented ideally as a time series we obtain the graph shown in figure 8.25. Of particular interest is the small dip in the graph about two days before the system was named. In fact, as a result of the data presented in figure 8.25, a re-analysis of the data in sections 8.1 to 8.4 were undertaken. The re-analysis was looking for the cause of the dip at about day -2. Somewhat surprisingly, all of the parameters decreased to some lesser or greater extent. Due to the way the formula is constructed, the more significant effects are caused by the decrease in wind speed and water vapour. It seems probable

that the change may actually be associated with increasing organisation within the structure of the system.

8.5.5 Comparison between Hamilton Index (HI) and GASP model data

The main index used with the GASP model data and which is most easily accessed is the Zehr parameter. Figure 8.27 shows the daily variation in the HI. Tables 8.2, 8.6, and 8.10 include, amongst other values, the Zehr GDI. In case 3 (TC Isobel) the index was 0.0 throughout the study. In cases 1 (TC Tim), and 2 (TC Elaine), the values remained at 0.0 and only on the last day was any significant value noted. On the last day the values increased to 0.3 for case TC Tim and 1.3 for TC Elaine. The values from the GASP model were rather disappointing although it must be remembered that the model is broadscale and probably missing most of the finer features that would be occurring within the development area of a future cyclone.

The inescapable conclusion is that the HI is more sensitive to the environment than was the GASP computer model. The HI has the added advantage that it can be calculated as soon as the satellite data is available in the office, rather than waiting for the computer model to be run at a central office and then manipulating the data to get an index.

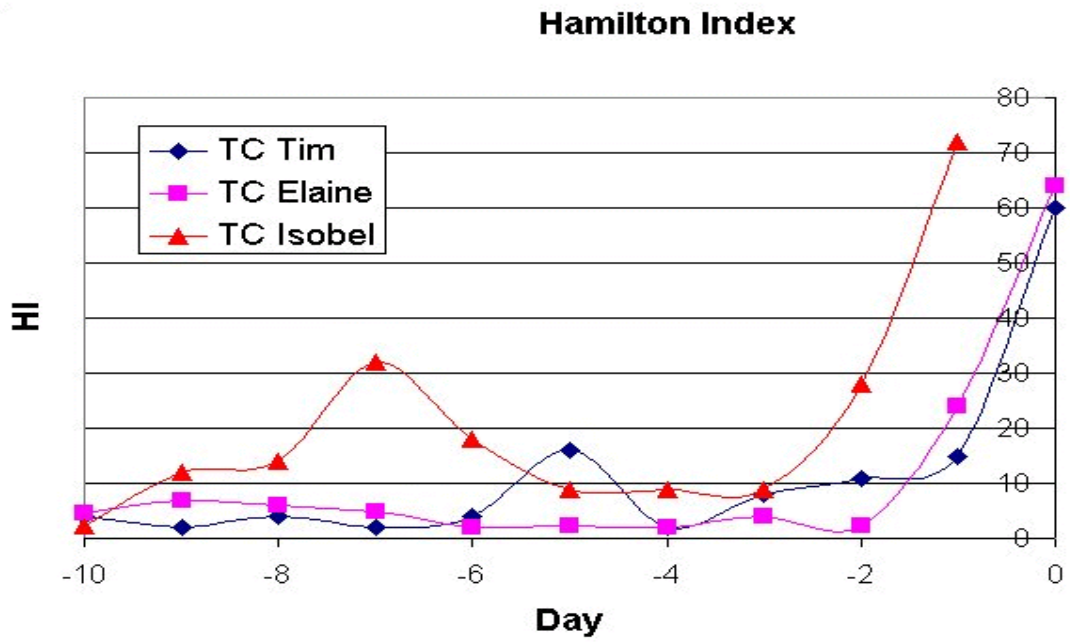


Figure 8.26: The Hamilton Index applied to the daily data from each of the case studies used in this thesis



Figure 8.27: The Zehr index applied to the daily data from each of the case studies used in this thesis

8.5.6 A review of amplitude and the temporal development of the index

A diagram of the amplitude and temporal changes of the HI are shown at figure 8.25. If the reader ignores the minor peak at day -7 in the TC Isobel graph line, which was caused by another cloud cluster moving through the target area, then the early part of each of the graph lines is reasonably horizontal and of a low value. This indicates that there was very little activity in the area. In each case, there is a small but interesting sequence about four days before the system was named. There is a slight rise followed by a slight trough, or decrease, and then the system really starts to develop. In cases 2 and 3, TC Elaine and Isobel respectively, the decrease occurs at day -2. A study of the individual parameters shows that nearly all individual parameters decreased but particularly the wind. TC Isobel was clearly named a day late but the shape of the graph is similar. Case 1, TC Tim shows a similar shape but the decrease was at day -4. After the decrease there was a slow increase for two days and then the system really developed. This would indicate that TC Tim was a slow developing system.

The graph lines in figure 8.25 represent the environment in the vicinity of the target area in the early part of each case study and then later in the vicinity of the system that was eventually named. That the individual lines on the graph are not perfectly horizontal in the early part of the study period is indicative of normal air flow in the tropics where wind speed and humidity fields vary from hour to hour, and certainly from day to day. There is a question as to how significant the minor peak and dip are between 4 and 2 days before the system is named. That it is there in all three to some extent suggests that it is real. Given that by this stage of development there is significant water vapour in the area (first term in HI) then one would expect the second and third terms to have the most influence during the later parts of the period. This appears to be the case and much of the dip at about day -2 can be attributed to a decrease in wind speed at that time.

It would take many more case studies to get a reasonable composite graph and to be able to put in values at which the cyclone is said to have formed. The three case studies here give an indication that by a value of $HI = 60$ that the minimum conditions have been met for a TC to be named.

8.5.7 Future development of the Hamilton Index (HI)

It should be remembered that the HI should not necessarily be considered the most appropriate combination of variables. The specific form that it takes has been argued previously. The thrust here was more to use it as an example of how physically derived information may be usefully combined into an index for use in a decision support system. The most obvious path for future development of the HI would be to analyse more systems. If the researcher studies non-developing as well as developing systems then a pattern should emerge which would hopefully present a clear pattern as to the intensification processes taking place. By studying non-developing systems, as well as systems that continue developing into TCs, the distinct behaviour of such an index would be revealed.

With a sufficient number of sample systems it should be possible to develop normalised values for each of the parameters. This would be advantages in that it would be much easier to program. The current system of using score values is an attempt to normalise the different parameters into a single formula.

9.0 CONCLUSIONS AND RECOMMENDATIONS

9.1 Conclusions

This thesis was undertaken as part of a Master of Science at Curtin University of Technology. As part of the professional development of the author, the topic chosen for the study was on cyclogenesis in the northwest of Western Australia. The thesis is in three, somewhat unequal, parts. These parts being, firstly a review of the theoretical understanding of cyclogenesis, secondly the undertaking of three case studies, and finally, a proposal as to an index for use with satellite data to monitor the tropical atmosphere for potential cyclogenesis.

TCs are a serious problem world-wide and the North of Australia is no exception. Disruption to commerce and trade as well as the risk to life are some of the impacts that TCs have on human habitation in the tropics. There is a significant need to improve information to support TC forecasting.

The case studies used in this thesis were taken from a study area to the north of Western Australia. The area known as the Timor Sea (figure 2.1) is a particular area of interest for meteorologists as it is an area of genesis for many of the TCs that later impinge on the North West Shelf and indeed on the State of Western Australia. This area is particularly interesting in that it is affected by the Indonesian flowthrough. The Indonesian Archipelago is to the north of the study area with the Australian continent to the south and east. Most of the area is open ocean with islands around the northern and eastern edges. Christmas Island and the Cocos Islands represent the only islands in the western part of the study area. Much of the study area has ocean depths as much as 2000m. The eastern part is significant for being the region of origin of the Leeuwin Current that flows southwards along the Western Australian coast. By way of interest, this is the only continental western coast to have a pole-ward flowing current.

The climatology of the area is such that there is a distinct monsoonal trend. A wet season from October to May is also the main cyclone season. Between 1910 and 2000 there were 250 cyclones formed in this region. This is also the main rainfall season.

Circulations in the tropics can be broken into two broad groups. Firstly, there is the “fair weather” state in which there is little activity. In the case of the study area this state is most usually observed during the dry season. During this period the dominant influence is the trade, or south easterly, winds. Wind speed varies at times depending on the location of the high pressure systems in the subtropical ridge. Occasionally, if the trade wind regime is deep enough, there may be rain showers.

The second group of circulations in the tropics are the ones that cause weather to varying degrees. These vary in scale from years down to minutes. The largest in scale is the ENSO which affects the whole globe and can last for several years. One of the dominant consequences of the ENSO is the effect on rainfall over the region. Another effect is on the amount and intensity of cyclone activity in the region. The next circulation in scale is the annual monsoon which influences weather over the entire study area. The period known in Australia as the “wet season”, which is typically from about November to about March each year, is actually the time of the north west monsoon over the continent. It is in fact the other half of the monsoon when the south east trade winds dominate the region. It is during the wet season that most cyclones develop. Even more so, the Equatorial trough which is associated with the monsoon is an area of generation of cyclones. Next in scale, and influence, is the Madden - Julian Oscillation (MJO) which operates on a 30 - 60 day timescale. This is an eastwards moving band of enhanced convective activity which typically extends over about 30 degrees of longitude. This is of particular interest during the wet season as it is during the active phase of the MJO that many TCs are formed. Monsoonal lows form regularly and are distinct from tropical cyclones in that they are cold cored, compared to the warm cored TCs. These tend to be relatively large compared to TCs. They have a significant influence in that they are often slow moving and have associated heavy rainfall. They can cause significant flooding. Winds tend to be not as strong as in TCs but can still attain gale force. The last system studied as potential sources of cyclogenesis are mesoscale convective cluster (MCC). An MCC is described as a persistent area of

cumulonimbus convection often with an associated altostratus deck of cloud. The diameter of the area of convection may only be a few hundred kilometres although the associated rotational circulation may extend to 1000 - 1500 kilometres.

A survey of the history of research into cyclogenesis shows that there has been persistent activity through out the twentieth century (and indeed into the 21st century). On a global scale, research has been more or less continuous. Research into cyclogenesis in the Australian region has been more sporadic although has increased in the latter half of the 20th century. Research into the north west in particular has been usually as an add-on to research in the Australian region in general. Since about the 1970s local research into the problem has been sporadic. Much of the research in the Australian region has been into mature systems looking particularly at movement and intensity changes, although there has been some on cyclogenesis.

The description of the process of cyclogenesis is a complex issue. Interaction at all levels of the atmosphere, particularly the middle and lower layers can lead to cyclogenesis. For the purpose of this thesis, Zehr's (1992) categorisation of genesis and intensification was used. That is, a system increases in organisation and activity until it reaches a stage when a TC can be named which is the genesis phase. From then on, any continued development is considered to be intensification. This occurs when the winds in all sectors around the centre reach at least 17.5m/sec. The purpose of this thesis was to look at systems in the genesis phase off the north west coast of Western Australia. Not all systems that start to develop actually continue to do so, hence a distinction is made between non-developing systems and developing systems. The case studies in this thesis were all on developing systems. The pre-conditions for TC genesis have been widely studied and Gray (1968, 1975, 1979) states them clearly. An interesting feature of cyclogenesis in the north west of Western Australian is that almost half of the systems developed from pre-existing lows that had formed over the Australian continent and then moved off the coast. This study restricted itself to systems whose life cycle was entirely over the ocean. Significantly, all TCs have been found to have developed from some pre-existing disturbance. Another necessity for development is that the system must become warm cored, that is be warmer in the centre of the system than at the outer edges. The development of the warm core is typically due to an

MCC being arm cored in the middle atmosphere and this warm core progressing downwards to the surface. Large scale spin-up can also assist in this process as synoptic scale processes impinge on the smaller system. Of particular importance is a vortex in the middle atmosphere. It is often from there that the warm core develops that later extends up and downwards to become the warm cored system. Seasonal factors also affect cyclogenesis. The location of the monsoon trough, the state of the SOI, and sea surface temperatures are among the factors that act together to enhance or reduce the incidence of cyclogenesis. Absolute and relative vorticity along with angular momentum transport can also enhance development. Some processes in the atmosphere can retard or even eliminate development. For example, an upper trough approaching to close to a system might increase the vertical shear to a point where excessive venting will cause the system to collapse. Cyclogenesis is a multi-faceted process in which many factors have to work together for a system to develop.

Most current research in Australia is into mature systems, that is, systems that have gone beyond the genesis phase. Observations of systems takes many forms. Satellite observations are the mainstay of monitoring in Australia. Aircraft, ship, and radar observations tend to be opportunistic (for the forecaster). Computer modelling is helping to develop an understanding of the underlying processes within a tropical system. Computer power has increased enormously in recent years enabling more detailed and more timely forecasts of these systems.

The second part of this thesis consists of three case studies and their associated description. Each TC used in these case studies developed over the open ocean. In order to adequately study them, satellite imagery was used as the primary tool. Also used was a global model (GASP), the data from which this author was able to obtain access. Two satellites were used, these being the American DMSP series of satellites and also the Japanese GMS satellites. The DMSP satellites were particularly useful in getting detailed data from within the systems. With regard to computer model data, early access to data was restricted to an Australian model, the GASP. While later access to other models became available it was decided to stay with the model data collected earlier in the project. In-situ observations for each of these systems was non existent and so had no bearing on the project.

Three case studies were undertaken. These were TCs Tim (1994), Elaine (1999), and Isobel (1996). In each case a detailed analysis was undertaken of the parameters that could be extracted from satellite data or from computer model data. The primary satellite used in these case studies was the American DMSP satellites. Data from these satellites included time of day (that the satellite crossed the equator), surface wind speed, water vapour, liquid water content, and rainfall. So as to keep the data as consistent as possible, the morning passes were used. This enabled a fair comparison with the 00Z GASP model data which was used in these case studies. One complication from using the low orbiting satellite data is that, on occasion, the swath coverage was not over the system of interest. IR satellite imagery was also used to discern the amount of, and also the organisation of cloud systems in the Timor Sea. Analysis fields from a global computer model were used as a surrogate for the observational data (which was non-existent for most of the case studies). Finally, sea surface temperatures were obtained from the Australian Bureau of Meteorology. These are generated from daily passes of the NOAA series of satellites.

The purpose of each case study was to undertake an analysis of the processes occurring in the vicinity of a system as the atmosphere increased in organisation from the fair weather state until a cyclone was named. To this end, the environment was monitored from ten days before the system was named until the day of naming. As it turned out, this was an adequate time frame. In each case environmental activity was benchmarked against Grays (1979) parameters.

Case study 1 analysed TC Tim (1994) in considerable detail. The satellite data was used either directly, or in some cases as surrogates for Grays parameters. Very little activity was observed in the vicinity of where the system eventually developed until the eighth day (day -2). Once development started, it continued quite persistently and the system was named at day 0. The evidence is that a weak trough moved into the area bringing increased instability but not increased shear, thus enabling the system to develop quickly. This is consistent with the Dvorak model of genesis.

Case study 2 analysed TC Elaine (1999). The same process was undertaken for this case study as was applied to case study 1. In this case, cloud activity was more active and

widespread over the Timor Sea. A cloud system developed three days before the day of naming but remained not very active until the last day when it rapidly developed into a cyclone. This type of development is more consistent with the Zehr model of genesis.

Case study 3 analysed TC Isobel (1996). The technique used was the same as for Case studies 1 and 2. As with case study 2, the Timor Sea was more active than was the situation for case study 1. In this case, development was more or less continuous once the system was identified. This is more consistent with the Dvorak model of genesis. The evidence would suggest that in this case the system was named a day late.

For each of the models, the satellite imagery proved to be more sensitive than the model data used. For case study one this is reasonable given the relatively primitive state of modelling in 1994. By case study 3, there was some signal in the model implying an increased sensitivity, as would be expected given the improvements that would have been implemented in the model over the years.

In the final part of the thesis, an index was developed which used satellite data to gauge the level of activity in an area of interest, in this case the Timor Sea. Data available from the DMSP satellites was brought together to build a system which could be automated in a computer system and be displayed in a manner that would be easy to interpret. Gray (1979) parameters were used throughout the case studies as a measure of meteorological activity within the area of interest. These parameters, or their surrogates can be obtained from satellite data. However, assessing some five or more indices with respect to their relative amplitudes as a function of time is difficult. This in itself makes a case for evolving and evaluating an index that can be monitoring the environment of a system, at least during the genesis period.

The index, as developed here, is admittedly only an initial attempt and would need to be validated and adjusted. Fortunately, the coefficients in the index permit a measuring and tuning based on the sensitivity of the various terms.

For want of a name, the index was called the "Hamilton Index". The formula is shown below,

$$HI = ((a * wv) * ((b * lw) + (c * ra) + (d * sst)) * (e * ws))$$

When implemented with the appropriate rules for usage, this index proves to be a sensitive indicator of the level of development within a system. Clearly, it requires further work, but when applied to the three case studies demonstrated a degree of usefulness.

9.2 Recommendations

- Remote sensing of smaller scale features within a system remain a problem. More research is needed to be able to understand the association between these features within a system
- Data storage methods are extremely varied. One of the major difficulties in this study was the comparison of data of different types and scale. A universal standard for data storage would be very useful. Data stored on a common grid would assist research enormously.
- Further research is needed on the relationship between the IOD, ENSO and TC development.
- Further testing of the index and tuning the coefficients with further case studies is required to refine the index or evolve a variant that is more appropriate.

10.0 REFERENCES

- Algué J (Rev SJ). 1904 'The cyclones of the far east'. Bureau of Public Printing
Manila (copy in Bureau of Meteorology, Perth Library)
- Anthes, R.A. 1982, 'Tropical Cyclones: Their evolution, structure and effects',
Meteor Monogr., vol. 41, Amer. Meteor. Soc., Boston MA 02108, 208pp.
- Asnani, G.C. 1993, *Tropical Meteorology*, Noble Printers, Pune 411008 (India).
Two volumes, 1202pp.
- Baines, P.G. 1989, 'The Physical oceanography of Australian waters - a review',
Aust Met. Mag vol. 37, pp.155-165.
- Bates, J.J. 1991, High-frequency variability of Special Sensor Microwave/Imager
derived wind speed and moisture during an intraseasonal oscillation.
J. Geophys. Res., vol.96 (suppl.), pp3411-3423.
- Bourke, W., Hart, T., Steinle, P., Seaman, R., Embery, G., Naughton, M., &
Rikus, L., 1995, Evolution of the Bureau of Meteorology's Global
Assimilation and Prediction system. Part 2: resolution enhancements and case
studies. *Aust. Met. Mag.*, vol. 44, pp19-40.
- Broadbridge, L.W. & Hanstrum B.N. 1998, 'The relationship between tropical
cyclones near Western Australia and the Southern Oscillation index',
Aust. Met. Mag. vol.47, pp. 183-189.
- Bureau of Meteorology, 1955, 'Report of the tropical Cyclone Conference Held at the
Divisional Office, Brisbane, Queensland 13th to 16th September 1955'.
Bureau of Meteorology, PO Box 1289K Melbourne, Vic., 3001, Australia
- Bureau of Meteorology, 1956, Proceedings of the Tropical Cyclone Symposium.

Brisbane 1956, Australian Bureau of Meteorology, P.O. Box 1289K,
Melbourne, Victoria 3001.

Bureau of Meteorology, 1973, Proceedings of the Regional Cyclone Seminar, Brisbane.
Bureau of Meteorology PO Box 1289K Melbourne, Vic., 3001, Australia.

Bureau of Meteorology, 1976, Symposium on the impact of tropical cyclones on oil and
mineral development in north-west Australia.
Bureau of Meteorology PO Box 1289K Melbourne, Vic., 3001, Australia.

Bureau of Meteorology, 1978, The Australian tropical cyclone forecasting Manual
1978, Bureau of Meteorology PO Box 1289K Melbourne, Vic., 3001, Australia.

Bureau of Meteorology, 1979, International conference on tropical cyclones, Perth.
Bureau of Meteorology PO Box 1289K Melbourne, Vic., 3001, Australia.

Chen, S.A. & Frank W.M. 1993, 'A numerical study of the genesis of extratropical
convective mesovortices. Part I: Evolution and dynamics',
J Atmos. Sci., vol.50, pp. 2401-2406.

Chou, S-H., Atlas, R.M., Shie, C-L. & Ardizzone, J. 1995, Estimates of surface
humidity and Latent heat fluxes over oceans from SSM/I data,
Mon. Wea. Rev., vol. 123, pp. 2405-2425.

Das P.K. 1986, *Monsoons*, Report No WMO - No.613. World Meteorological
Organisation, Geneva Switzerland.

Davidson, N.E., McAvaney, B.J., 1981, The ANMRC tropical analysis scheme. *Asut
Met. Mag.*

Davidson, N.E., Hendon, H.H. 1989, Downstream development in the Southern
Hemisphere monsoon during FGGE/WMONEX.

Mon Wea. Rev., vol. 117, pp. 1458-1470.

Davidson, N.E., Holland, G.J. 1987, A diagnostic analysis of two intense monsoon depressions over Australia. *Mon. Wea. Rev.*, vol 115, pp 380-392

Davidson, N.E., McBride, J.L., & McAvaney, B.J. 1983, The onset of the Australian monsoon during winter MONEX: Synoptic aspects.
Mon. Wea. Rev., vol. 111, pp 496-516.

Davidson, N.E., Holland G.J., Mc Bride J.L. & Keenan T.D. 1990, 'On the formation of AMEX tropical cyclones Irma and Jason',
Mon. Wea. Rev., vol. 118, pp. 1981-2000.

Davidson, N.E., Puri, K., 2001, Operational numerical prediction in the tropics: Status, problems and prospects. International Workshop on the dynamics and forecasting of tropical weather systems, Darwin 22 - 26 January 2001.

Davidson, N.E., Weber, H.C., 2000, The BMRC high resolution tropical cyclone prediction system: TC-LAPS. *Mon. Wea. Rev.*, vol128, pp 1245-1265.

Drosowsky, W. & Chambers, L. 1998, Near global sea surface temperatures anomalies as predictors of Australian seasonal rainfall.
BMRC Research Report No. 65. Bureau of Meteorology, Australia

Dvorak, V.F. 1972, *A technique for the analysis and forecasting of tropical cyclone intensities from satellite pictures*. NOAA Technical Memorandum NESS 36, U.S. Department of Commerce, National Oceanic and Atmospheric Administration, National Earth Satellite Service, Washington, D.C. 20233, 15pp.

Dvorak, V.F. 1975, 'Tropical cyclone intensity analysis and forecasting from satellite imagery', *Mon Wea. Rev.*, vol. 103, pp.420-430.

- Dvorak, V.F. 1984, *Tropical cyclone intensity analysis using satellite data*, NOAA Technical Report NESDIS 11 U.S. Dept. of Commerce, Washington, DC 47pp.
- Elsberry, R.L. (Ed) 1995, *Global Perspectives on Tropical Cyclones*, Report No.TCP-38. World Meteorological Organisation. Geneva Switzerland.
- Emanuel, K.A. 1993, 'The physics of tropical cyclogenesis over the eastern Pacific', in *Tropical Cyclone Disasters*, eds Lighthill J., Zheming Z., Holland G.J. & Emanuel Peking University Press Beijing, pp.136-142.
- Evans, J.L., & Allen, R.J. 1992, El Niño/ Southern Oscillation modification to the structure of the monsoon and tropical activity in the Australian region. *Intl. J. Climatology*, vol. 12, pp 611-623.
- Feng, M., Meyers, G., Wijffels, S., 2001, Interannual upper ocean variability in the tropical Indian Ocean. *Geophysical Research Letters*, vol 28 (21), pp 4151-4154
- Foster, I.J. 1987, 'The development of tropical cyclones in the north-west of Australia'. Ph.D Thesis, School of Environmental and Life Sciences, Murdoch University
- Foster, I.J. & Lyons, T.J. 1984, 'Tropical cyclogenesis: a comparative study of two depressions in the northwest of Australia', *Quart J.R. Met. Soc.* vol. 110, pp. 105-119.
- Foster, I.J. & Lyons, T.J. 1988, 'Development of tropical cyclones in the northwest of Australia', *Quart J.R. Met. Soc.* vol. 114, pp. 1187-1199.
- Frank, W.M. 1982, 'Large scale characteristics of tropical cyclones', *Mon. Wea. Rev.*, vol. 110, pp. 572-586.
- Frank, W.M. 1987, 'Tropical Cyclone Formation', in *A Global View of Tropical*

Cyclones. Office of Naval Research, Arlington, VA 22217, pp.53-90.

Gentry, R.C., Rodgers, E., Steranka, J. and Shenk, W.E. 1980. Predicting tropical cyclone intensity using satellite measured equivalent blackbody temperature of cloud tops. *Mon. Wea. Rev.*, vol. 108 pp445-455.

Gray, W.M., 1968, 'Global view of the origin of tropical disturbances and storms', *Mon Wea Rev.*, vol. 96, pp. 669-700.

Gray, W.M., 1975, Tropical cyclone genesis. *Dept. of Atmos. Sci. paper No. 232*, Colorado State University, Fort Collins CO, USA, 121 pp.

Gray, W.M. 1979, 'Hurricanes: their formation, structure and likely role in the tropical circulation' in *Supplement to Meteorology over the tropical oceans*, ed. B Shaw, Roy. Met. Soc. James Glaisher House, Grenville place, Bracknell, Berkshire RG 12 1BX pp.155-218

Gray, W.M. 1984, 'Atlantic seasonal hurricane frequency. Part I: El Nino and 30mb QBO influences', *Mon Wea. Rev.*, vol.112, pp. 1649-1668.

Gray, W.M. 1988, 'Environmental influences on tropical cyclones', *Aust. Met. Mag.*, vol. 36, pp. 127-139.

Guinn, T.A. & Schubert W.H. 1993, 'Hurricane spiral bands', *J. Atmos Sci.*, vol. 50, pp. 3380-3408.

Hasternath, S. & Lamb P.J. 1979a, *Climatic Atlas of the Indian Ocean, Part I: Surface Climate and Atmospheric Circulation*, The University of Wisconsin Press. 114 North Murray Street, Madison, Wisconsin 53715. ISBN 0-299-07814-0.

Hasternath, S. & Lamb, P.J. 1979b, *Climatic Atlas of the Indian Ocean, Part II: The Oceanic Heat Budget*. The University of Wisconsin Press. 114 North Murray

Street, Madison, Wisconsin 53715. ISBN 0-299-07814-0.

Hastings, P.A. 1990, Southern oscillation influences on tropical cyclone activity in the Australian/ Southwest Pacific region.

Intl. J. Climatology, vol. 10, pp 291-298.

He, S.W. & Yang, Z.F. 1981, 'The relationship between the intensity of the summer southwest monsoon over the northwest Pacific and circulation patterns of the southern hemisphere', *Scientia Atmospherica Sinica*. vol. 5, pp. 50-59.

Hendon, H.H., & Liebmann, B. 1990, The intraseasonal (30-50 day) oscillation of the Australian summer monsoon. *J. Atmos. Sci.*, vol 47, pp 2909-2923.

Holland, G.J. 1983, *Tropical cyclones in the Australian/Southwest Pacific region*, Atmospheric Science Paper No. 363 Dept Atmospheric Science, Colorado State University, Fort Collins Co. pp264

Holland, G.J. 1984a, 'On the Climatology and Structure of Tropical Cyclones in the Australian/southwest Pacific Region: I Data and Tropical Storms', *Aust. Meteorol. Mag.*, vol. 32 pp. 1 - 16.

Holland, G.J. 1984b, 'On the Climatology and Structure of Tropical Cyclones in the Australian/southwest Pacific Region: II Hurricanes', *Aust. Meteorol. Mag.*, vol. 32 pp. 17 - 32.

Holland, G.J. 1984c, 'On the Climatology and Structure of Tropical Cyclones in the Australian/southwest Pacific Region: III Major hurricanes', *Aust. Meteorol. Mag.*, vol. 32 pp. 33 - 46.

Holland, G.J. 1987, Interannual variability of the Australian summer monsoon at Darwin: 1952-82. *Mon. Wea. Rev.*, vol 114, pp594-604

Johnson, R.H., & Houze, R.A. 1987, Precipitation cloud systems of the Asian

- monsoon. In *Monsoon Meteorology*, Chang C.-P & Krishnamutri, T.N., Eds)
- Keenan, T.D., Brody, L.R. 1988, Synoptic scale modulation of convection during the Australian summer monsoon. *Mon. Wea. Rev.*, vol. 116, 71-85.
- Latham, R.(ed) 1958, Marco Polo - the travels. *Penguin Books*, Harmondsworth. Pp. xx. English translation of “*Divisament don Monde*” (Description of the world, 1289).
- Lau, K.M., Nakazawa, T. & Sui CH., 1991, ‘Observations of cloud cluster hierarchies over the tropical western Pacific’, *J. Geophys. Res.*, vol. 96, pp. 3197-3208.
- Liebmann, B., Hendon, H.H. & Glick J.D. 1994, ‘The relationship between tropical cyclones of the western Pacific and Indian Oceans and the Julian-Madden oscillation’, *J. Meteor. Soc. Japan*, vol. , pp. 401-412.
- Lopez, L., Raymond, D. & Emanuel K. 1993, ‘Preliminary results from TEXMEX: The development of tropical storm Guillermo’, *Preprints, 20th conf. Hurr. Trop. Meteor.*, San Antonio, TX, Amer. Meteor. Soc., Boston, MA 02108, 114-117.
- Love, G. 1985a, *The role of the general circulation in western Pacific tropical cyclone genesis*, Atmos. Sci. Paper No.340, Colorado State University, Ft. Collins 80523, 215pp.
- Love, G. 1985b, ‘Cross-equatorial influence of winter hemisphere subtropical cold surges’, *Mon. Wea. Rev.*, vol. 113, pp. 1487-1498.
- Lunney, P.A. 1988, *Environmental and convective influences on tropical cyclone development vs non-development*, Atmos. Sci. Paper No.436, Colorado State University, Ft. Collins 80523, 105pp.

- Madden, R.A. 1986. Seasonal variation of the 40-50 day oscillation in the tropics.
J. Atmos. Sci., vol 43, pp3138-3158.
- Madden, R.A., Julian, P.R. 1971. 'Detection of a 40-50 day oscillation in the zonal wind in the tropical Pacific'. *J. Atmos. Sci.*, 28, 702-708.
- Madden, R.A., Julian, P.R. 1972. 'Description of global-scale circulation cells in the tropics with a 40-50 day period'. *J. Atmos. Sci.*, 29, 1109-1123.
- Manton, M.J. & McBride J.L. 1992, 'Recent research on the Australian Monsoon',
J Met Soc Japan, vol. 70, pp. 275 - 285.
- Matsumoto, Y., & Meyers, G. 1998, Forced Rossby waves in the southern tropical Indian Ocean. *J. Geophys. Res.*, vol. 103(C12), 27 589- 27 602.
- McBride, J.L. 1981, 'Observational analysis of tropical cyclone formation: Part 2, Basic description of the data sets'.
J. Atmos Sci., vol. 38, pp. 1132-1131.
- McBride, J.L. 1983, Satellite observations of the Southern Hemisphere monsoon during winter MONEX. *Tellus*, vol. 35A, 189-197.
- McBride, J.L. 1986, Tropical cyclones in the Southern Hemisphere summer monsoon.
Second International Conference on Southern Hemisphere Meteorology.
Amer. Meteor. Soc., Boston, MA. 358-364.
- McBride, J.L. 1995, 'Tropical Cyclone Formation', in *Global Perspectives on Tropical Cyclones*. Report No. TCP-38. World Meteor. Organisation, Geneva, Switzerland, Section 3.1 - 3.6.3.
- McBride, J.L., & Gray, W.M. 1980, Mass divergence in tropical weather systems. Part I: diurnal variation. *Quart. J. Roy. Meteor. Soc.*, vol. 106, pp. 501-516.

- McBride, J.L. & Keenan T.D. 1982, 'Climatology of tropical cyclone genesis in the Australian region', *J. Climat.*, vol. 2, pp. 13-33.
- McBride, J.L. & Zehr, R.M. 1981, 'Observational analysis of tropical cyclone formation: Part 2, Comparison of non developing and developing systems', *J. Atmos Sci.*, vol. 38, pp. 1132-1151
- Meehl, G.A. 1987. The annual cycle and interannual variability in the tropical Pacific and Indian Ocean Regions. *Mon. Wea. Rev.*, vol 115, pp27-50.
- Meyers, G. 1996, Variation of Indonesian throughflow and the El Niño- Southern Oscillation. *J. Geophys. Res.*, vol. 101(C5), pp 12 255-12 263.
- Milton, J.D. 1978, 'Tropical cyclones affecting Western Australia: A synoptic climatology'. Ph.D thesis, University of Western Australia
- Neumann, C.J. 1993, 'Global Overview', in *Global Guide to Tropical Cyclone Forecasting*. World Meteor. Organisation, Geneva, Switzerland, pp. 1.1 - 1.56.
- Nicholls, N. 1979, 'A possible method for predicting seasonal tropical cyclone activity in the Australian region', *Mon Wea Rev.*, vol. 107, pp. 1221-1224.
- Nicholls, N. 1984, 'The Southern Oscillation, sea-surface temperature, and interannual fluctuations in Australian tropical cyclone activity', *J. Climatol.*, vol. 4, pp. 661-670.
- Nicholls, N. 1985, 'Predictability of interannual variations of Australian seasonal tropical cyclone activity', *Mon Wea. Rev.*, vol. 113, pp. 1144-1149.
- Nicholls, N. 1989, Sea surface temperatures and Australian winter rainfall. *J. Climate*, vol. 2, pp. 965-973.

- Nicholls, N. 1992, 'Recent performance of a method for forecasting Australian seasonal tropical cyclone activity', *Aust Meteor. Mag.*, vol. 21, pp. 105-110.
- Nicholls, N., Landsea C. & Gill J. 1998, 'Recent trends in Australian Region Tropical Cyclone Activity', *Meteorol. Atmos Phys.*, vol. 65, pp. 197-205.
- Palmen, E. 1948, 'On the formation and structure of the tropical hurricane', *J Phys. Oceanogr.*, vol. 11 pp. 153-175.
- Palmen, E. 1956, 'A review of knowledge on the formation and development of tropical cyclones', in *Proc Trop. Cyc. Symp.* Brisbane 1956, Australian Bureau of Meteorology, P.O. Box 1289K, Melbourne, Victoria 3001 Australia, pp.213-232.
- Pearce, A.F. & Phillips B.F. 1988, 'ENSO events, the Leeuwin Current, and larval recruitment of the western rock lobster', *J. Cons. Int. Explor. Mer*, vol. 45, pp. 13-21.
- Prata, A.J., Lynch, M.J., Hille, R. and Van Burgel, J.L. 1986. Observations of tropical cyclones in Western Australia using combined TOVS and AVHRR radiances. *Technical Proceedings of the Third International TOVS study Conference*, Madison, Wisconsin pp222-254.
- Puri, K., Davidson, N.E., Leslie, L.M., and Logan, L.W., 1992, The BMRC tropical limited area model. *Aust. Met. Mag.* Vol. 40, pp 81-104
- Puri, K., Deitachmayer, G., Mills, G., Davidson, N.E., Bowen, R., Logan, L., and Leslie, L.M., 1998, The new BMRC limited area prediction system, LAPS. *Aust. Met. Mag.*, vol 47, 203-223.
- Ramage, C.S. 1968, 'Role of the tropical maritime continent in the atmospheric circulation', *Mon. Wea. Rev.*, vol. 96, pp. 365-370.

- Ramage C.S. 1971, *Monsoon Meteorology*, Academic Press New York xxpp
- Ramage, C.S. 1995, *Forecasters Guide to Tropical Meteorology*, AWS/TR 95/001.
Air Weather Service 102 West Losey Street, Scott Airforce Base,
Illinois 62225-5026. 392pp.
- Rao, A.S., Behera, S.K., Masumoto, Y., Yamagata, T., 2002, Interannual variability in the subsurface Indian Ocean with special emphasis on the Indian Ocean dipole. *Deep-Sea Research-II*, vol 49, pp 1549-1572.
- Revell, C.G., & Goulter, S.W. 1986a, South pacific tropical cyclones and the Southern Oscillation. *Mon. Wea. Rev.* vol. 114, pp. 1138-1145.
- Revell, C.G., & Goulter, S.W. 1986b, lagged relations between the Southern Oscillation and numbers of tropical cyclones in the South Pacific region. *Mon. Wea. Rev.* vol. 114, pp. 2669-2670.
- Revelle, C.G. 1981, *Tropical cyclones in the Southwest Pacific November 1969 to April 1979*, Misc. Pub. 170 New Zealand Met. Service, Wellington NZ.
- Riehl, H. 1954, *Tropical Meteorology*, McGraw-Hill, New York 392pp.
- Riehl, H. 1979, *Climate and Weather in the Tropics*. Academic Press, 611pp.
- Ritchie, E.A. 1993, 'Contributions by mesoscale convective systems to the formation of tropical cyclones', *Preprints, 20th conf. Hurr. Trop. Meteor.*, San Antonio, TX, Amer. Meteor. Soc., Boston, MA 02108, 409-412.
- Ritchie, E.A., Holland G.J. & Lander M. 1993, 'Contributions by mesoscale convective systems to movement and formation of topical cyclones', in *Tropical Cyclone Disasters*, eds. J. Lighthill, Z. Zhemín, G.J. Holland & Emanuel, Peking University Press Beijing, pp. 286-289.

- Ruprecht, E., and Gray W.M. 1976a, Analysis of satellite-observed cloud clusters.
Part I: Thermal, moisture and precipitation. *Tellus*, vol. 28, pp 414-426.
- Ruprecht, E., and Gray W.M. 1976b, Analysis of satellite-observed cloud clusters.
Part II: Wind and dynamic fields. *Tellus*, vol. 28, pp 391-413.
- Saji, N.H., Goswami, B.N., Vinayachandran, P.N., & Yamagata, T. 1999,
A dipole mode of the Indian Ocean. *Nature*, vol. 401, pp.360-363.
- Seaman, R., Bourke, W., Steinle, P., Embery, G., Naughton, M., & Rikus, I. 1995,
Evolution of the Bureau of Meteorology's Global Assimilation and Prediction
system. Part 1: analysis and initialisation. *Aust Met. Mag.*, vol. 44, pp1-18.
- Shapiro, L.J. 1987, 'Month-to-month variability of the Atlantic tropical circulation
and its relationship to tropical cyclone formation',
Mon. Wea. Rev., vol. 115, pp. 2598-2614.
- Shewchuck J.D., Wier R.C. 1980, An evaluation of the Dvorak technique for
estimating tropical cyclone intensity from satellite imagery. NOCC/JTWC
80-2, USNOCC, JTWC, Comnavmarinas, Box 17, FPO San Fransisco,
CA 96630, 25pp.
- Simpson, J., Ritchie, E., Holland, G.J., Halverson, J. & Stewart, S. 1997,
Mesoscale interactions in tropical cyclone genesis,
Mon. Wea. Rev., vol. 125, pp. 2643-2661.
- Steranka, J., Rodgers E.B. & Gentry R.C. 1986, 'The relationship between satellite
measured convective bursts and tropical cyclone intensification',
Mon Wea. Rev., vol. 114, pp. 1539-1546.
- Suomi, V.E., 1983, McIDAS IIIa modern interactive data access and analysis system,
J. Climatol. And Appl. Meteorol. vol., 22, pp766-778.

- Suppiah, R. 1993. ENSO phenomenon and 30-50 day variability in the Australian summer monsoon rainfall. *Int. J. Climatol.*, vol. 13, pp837-851.
- Tapp, R.G., & Barrel, S.L. 1984, The North-West Australian Cloud Band: Climatology, characteristics and factors associated with development. *J. Climatol.*, vol. 4, pp. 411-424.
- Tropical Cyclone Study Group 1982, *Development and movement of tropical cyclones in the north west of Australia*, Report Number 3. Murdoch Uni. Perth Western Australia. pp 116,
- Toole, J.M. 1987, 'Problems of interbasin exchanges and marginal-sea overflows', *Bull. Amer. Met. Soc.*, vol. 68. pp. 136-140.
- Van Burgel, J.L. 1999, The study of tropical cyclones using satellite microwave data MSc Thesis, Curtin University of Technology.
- Velasco, I., Fritsch, J.M., 1987, Mesoscale convective complexes in the Americas. *J. Geophys. Res.*, vol. 92. Pp. 9592-9613
- Veldon, C.S., Olander, T.L., and Zehr, R.M.1998. Development of an objective scheme to estimate tropical cyclone intensity from digital geostationary satellite imagery. *Weather and Forecasting*, 13 pp172-186
- Wang, Y. 1999, *A triply-nested movable mesh tropical cyclone model with explicit cloud microphysics - (TCM3)*, BMRC Research Report No. 74. Bureau of Meteorology PO Box 1289K Melbourne, Vic., 3001, Australia.
- Wentz, F.J., Song Ye., 1997a, *Cloud water algorithms for SSM/I and AMSR*. RSS Tech. Report 063097-C Available online at <http://www.ssmi.com>
- Wentz, F.J., Song Ye., 1997b, *Rain algorithms for SSM/I and AMSR*. RSS Tech. Report 063097-R Available online at <http://www.ssmi.com>

- Wentz, F.J., Song Ye., 1997c, *Vapor algorithms for SSM/I and AMSR*.
RSS Tech. Report 063097-V Available online at <http://www.ssmi.com>
- Wentz, F.J., Song Ye., 1997d, *Wind algorithms for SSM/I and AMSR*.
RSS Tech. Report 063097-W Available online at <http://www.ssmi.com>
- Williams, M., Houze, R.A. Jr. 1987, 'Satellite-observed characteristics of winter monsoon cloud clusters'. *Mon. Wea. Rev.*, 115, 505-519
- Zehr, R.M, 1976, *Tropical Disturbance Intensification*. Atmospheric Science Paper No. 259 Dept Atmospheric Sciences, Colorado State university, Fort Collins, Colorado. December 1976.
- Zehr, R.M. 1992, *Tropical cyclogenesis in the western North Pacific*,
NOAA Technical Report NESDIS 61 U.S. Dept Commerce, Washington D.C..
- Zehr, R.M. 1999, Improving the quantitative assessment of vertical wind shear on tropical cyclone intensity change. *23rd Conference on Hurricanes and Tropical Meteorology*, Jan 1999, Dallas, TX. Amer. Meteor. Soc., Boston, MA
- Zehr, R.M. 2000, Tropical cyclone research using large infrared images data sets. *Preprints of the 24th Conference on Hurricanes and Tropical Meteorology & 10th Conference on Interaction of the sea and atmosphere*, 29 May - 2 June 2000, Ft. Lauderdale, FL by the Amer. Meteor. Soc., Boston, MA.

11.0 APPENDICES

11.1 Meteorological terms used in this document

CISK	<u>C</u> onditional <u>I</u> nstability of the <u>S</u> econd <u>K</u> ind.
Core Region:	The region within 200 km of the cyclone centre.
ENSO	El Niño/ Southern Oscillation. Briefly, the El Niño is an event in the pacific Ocean where the warmest water which is normally in the west migrates to the middle or east of the pacific Ocean causing major changes in the climate patterns of the area. There is some correspondence between El Niño and changes in climate in many parts of the world, particularly in tropical regions. The Southern Oscillation (described below) is a quantification of the El Niño process.
Hurricane:	A tropical cyclone in which the maximum winds are 34ms^{-1} (68 knots) or greater.
Inner Circulation:	The region within 300 km of the cyclone centre.
Intensification:	Three modes; Intensity change, size change and strengthening.
Intensity	A measure of the maximum wind speed of the system. If there is no maximum wind data then by the central pressure.
IOD	Indian Ocean Dipole. An ENSO like feature occurring in the Indian Ocean.
Major Hurricane:	A tropical cyclone in which the maximum winds are

46ms⁻¹ (87 knots) or greater, or the central pressure is less than 980 hPa

Madden -Julian Oscillation (MJO)

A long wave feature found moving slowly eastwards along the Equator. As originally described, it has a frequency of 40 - 50 days.

Monsoonal Depression (MD):

A cyclone (low pressure system) on the monsoon trough.

Monsoonal Trough (MT):

The trough of low pressure into which the monsoon converges.

Outer Circulation: The region 300-800 km from the cyclone centre.

Size: defined as the axis-symmetric extent of the galeforce winds, or by the outer closed isobar. }

SOI: Southern Oscillation Index. This is calculated by subtracting the monthly mean pressure at Darwin from the monthly mean pressure at Tahiti and then normalising by the standard deviation of the Tahiti minus Darwin series. This also known as the Troupe Index of the southern Oscillation.

Strength: Defined by the average relative angular momentum of the low level inner circulation.

Tropical cyclone (TC):

A non-frontal synoptic scale, cyclonic rotational low pressure

system of tropical origin, in which the 10 minute mean winds are at least 17.5 ms^{-1} (34 knots).

Tropical Disturbance (TD):

A synoptic scale weather system of tropical origin which may or may not be detectable as a wind field perturbation.

Tropical Storm (TS): A tropical cyclone in which the maximum winds are in the range $17 - 33 \text{ ms}^{-1}$ (34- 67knots). {H83}

Typhoon: See Hurricane.

Appendix 11.2 Comparison of terms used in different cyclone basins

Cyclone Basin	Australia /SE Asia 90-142E	Australia / SW Pacific Ocean >142E	Western North Pacific	Eastern North Pacific	North Atlantic	North Indian Ocean	Southwest Indian Ocean <90E
Terminology	(10 minute av)	(10 minute av)	(10 minute av)	(1 minute av)	(1 minute av)	(10 minute av)	(10 minute av)
Mean winds exceeding 115 Knots	Severe Tropical Cyclone	Hurricane	Typhoon	Hurricane	Hurricane		Very Intense Tropical Cyclone
Mean winds between 90-114 knots	Severe Tropical Cyclone	Hurricane	Typhoon	Hurricane	Hurricane		Intense Tropical Cyclone
Mean winds between 64-89 knots	Severe Tropical Cyclone	Hurricane	Typhoon	Hurricane	Hurricane	Severe Cyclonic Storm with Hurricane core	Tropical Cyclone
Mean winds between 48-63 knots	Tropical Cyclone	Tropical Cyclone	Severe Tropical Storm	Hurricane	Tropical Storm	Severe Cyclonic Storm	Severe Tropical Storm
Mean winds between 34-47 knots	Tropical Cyclone	Tropical Cyclone	Tropical Storm	Tropical Storm	Tropical Storm	Cyclonic Storm	Moderate Tropical Storm
Winds less than 34 knots (closed circulation)	Tropical Depression	Tropical Depression	Tropical Depression	Tropical Depression	Tropical Depression	Tropical Depression	Tropical Depression
Winds less than 34 knots (open circulation)	Tropical Disturbance	Tropical Disturbance					Tropical Disturbance

11.3 Contents of the Computer Data disk attached to this thesis.

The Computer data disk (CD) attached to this thesis contains a copy of the data used to analyse the case studies. It also contains a digital copy of this thesis, which was written using Word Perfect 2000. Finally, there are some utilities which will enable the reader to manipulate the raw data.

The directory structure of the CD is as follows. For each of the three case studies the directory structure is the same. The naming of the three data directories suggest the case study and name. For case studies one, two, and three, they are, c_1_tim, c_2_elaine, and c_3_isobel

- case_study
 - proc_img Processed image files
 - proc_img_jpg Processed image files converted to .jpg
 - proc_prog Computer model data extracted
 - proc_prog_calc proc_prog files imported to Excel sheets
 - raw_img The satellite imagery as downloaded
 - raw_prog The computer model data as downloaded
 - satpix Satellite imagery as scanned
 - sst Scanned sea surface temperature files

- Thesis
 - data Data used in the thesis
 - diags Diagrams used in the thesis
 - text The thesis!
 - pdf_text The thesis converted to a .pdf document

- Utilities
 - Some programs for viewing the raw data

Within each directory are the files used for this thesis. The directories starting with “raw” contain the data as downloaded from the original source. The directories starting with “proc” contain the processed files.

In most cases the files names are self explanatory. For the DMSP data, the filenames are in the form of date and satellite number with the extension being the type of data extracted. An example is 94032011.alw, where 94 is the year, 03 the month, 20 the day of the month, and 11 being the DMSP satellite number. The “alw” is for files containing information on liquid water. Other extensions used are “ara” for rainfall, “aws” for wind speed, and “awv” for water vapour. These files are stored in the proc_img file. For the convenience of importing the files into the word processor, the files were converted to .jpg files. These files are stored in the proc_img_jpg directories.

The computer model data as downloaded from the Bureau of Meteorology is stored in the raw_prog directory.

The data extracted from the files in the raw_prog directory was deposited in the proc_prog directory. The file names follow the same convention as for the satellite imagery. That is, the filename is the date and the extension containing the type of data held by the file. Even in this format the data is not particularly easy to manipulate and so was imported into Excel spreadsheets. The data in this form is stored in proc_prog_calc.

Imagery from the GMS satellite is stored in the satpix directory.

The last data source is the SST which was scanned from maps produced by the Bureau of Meteorology.